The effect of blood loss anemia on heart function and energy imbalance after acute myocardial infarction

Inaugural-Dissertation

zur Erlangung des Doktorgrades
der Mathematisch-Naturwissenschaftlichen Fakultät
der Heinrich-Heine-Universität Düsseldorf

vorgelegt von

Vithya Yogathasan
aus Nettetal

Düsseldorf, Juli 2025

aus der Klinik für Kardiologie, Pneumologie und Angiologie
der Heinrich-Heine-Universität Düsseldorf
Klinikdirektor: Univ.-Prof. Dr. med. Malte Kelm

Gedruckt mit der Genehmigung der
Mathematisch-Naturwissenschaftlichen Fakultät der
Heinrich-Heine-Universität Düsseldorf

Berichterstatter:

1. Prof. Dr. Dr. med. Christian Jung

2. Prof. Dr. rer. nat. Axel Gödecke

Tag der mündlichen Prüfung: 19.11.2025

Eidesstattliche Versicherung

Ich versichere an Eides Statt, dass die Dissertation von mir selbstständig und ohne unzulässige fremde Hilfe unter Beachtung der „Grundsätze zur Sicherung guter wissenschaftlicher Praxis an der Heinrich-Heine-Universität Düsseldorf“ erstellt worden ist.

Die aufgeführten Versuche wurden selbständig durchgeführt. Mit Ausnahme der folgenden Versuche und Ergebnisse, welche von Dritten bzw. in Kooperation mit Dritten erstellt wurden:

- Die IR-Operationen und Millar Katheter Messungen wurden von Stefanie Becher durchgeführt.
- Die Aufnahmen und Analysen der Echokardiographie wurde in Zusammenarbeit mit Dr. Patricia Wischmann erstellt.
- Die Proteomanalyse und Auswertung wurde von Biogenity und DTU Proteomics durchgeführt.
- Die CMRI Aufnahmen und Analyse wurden von Prof. Dr. Ulrich Flögel durchgeführt

Diese Dissertation wurde weder in gleicher noch in ähnlicher Form in einem anderen Prüfungsverfahren vorgelegt. Außerdem erkläre ich, dass ich bisher noch keine weiteren akademischen Grade erworben oder zu erwerben versucht habe.

Düsseldorf, den 30.07.2025

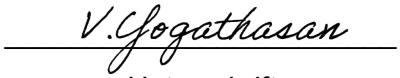

Unterschrift

Parts of this dissertation were already published in a scientific journal or presented on scientific conferences:

Posters:

03.04.2024 – 06.04.2024

90. DGK-Jahrestagung in Mannheim, Germany

Acute anemia is associated with left ventricular energy imbalance after myocardial infarction

Ramesh Chennupati, **Vithya Yogathasan**, Isabella Solga, Patricia Wischmann, Sarah Piel, Norbert Gerdes, Ulrich Flögel, Christian Jung, Malte Kelm

03.04.2024 – 06.04.2024

90. DGK-Jahrestagung in Mannheim, Germany

Dysfunctional RBCs in anemia mitigate the hypertension in RBC eNOS deficient mice

Vithya Yogathasan, Patricia Wischmann, Isabella Solga, Norbert Gerdes, Malte Kelm, Christian Jung, Ramesh Chennupati

26.06.2024 – 28.06.2024

1st European ImmunoMetabolism Conference: Metabolism Meets Immunology, Comwell Køge Strand, Køge, Denmark

Acute anemia is associated with left ventricular energy imbalance after myocardial infarction

Vithya Yogathasan, Ramesh Chennupati, Isabella Solga, Elric Zweck, Patricia Wischmann, Stefanie Becher, Sarah Piel, Norbert Gerdes, Ulrich Flögel, Malte Kelm, Christian Jung

Abstract

Background: Anemia is frequently observed in patients with cardiovascular diseases (CVD) such as acute and chronic coronary syndromes as well as heart failure. Anemia alone or in combination with other morbid conditions leads to poor prognosis in acute myocardial infarction (AMI). Previous studies on anemic mouse models and patient data demonstrated that anemia is associated with an unchanged infarct size but with an increased mortality. The effect of anemia on energy metabolism in the left ventricle (LV) after AMI has not been investigated.
Anemia is associated by red blood cell (RBC) dysfunction. Under physiological function RBCs express functionally active endothelial nitric oxide synthase (eNOS), which contributes to the regulation of blood pressure (BP) independently of endothelial-derived eNOS. Moreover, RBC-derived eNOS has been shown to exert cardioprotective effects during AMI. We hypothesise that energy imbalance in anemia contributes to LV dysfunction in AMI leading to worse prognosis and that RBC eNOS deficiency worsens vascular and cardiac function in anemia.

Aims and Methods: This study's first aim is to assess the energy metabolism in anemia after AMI in the LV. For this purpose, cardiac function and cardiac energetics were assessed using echocardiography and cardiac magnetic resonance imaging (CMRI) in anemic and non-anemic mice with and without AMI. Next, unbiased proteomic analysis was performed in isolated LV tissues from anemic and non-anemic mice with and without AMI. To identify the regional differences in the proteome profiles of LV tissues after AMI, proteomic profiles of remote (non-infarcted area) and ischemic region (infarcted area) were compared between anemic and non-anemic mice. To attain details on oxidative phosphorylation (OXPHOS) changes, respirometry analysis was performed in LV tissues of anemic and non-anemic mice with and without AMI in the ischemic and remote region. Biochemical assays were used to evaluate redox enzymes in LV tissues from anemic and non-anemic mice, both with and without AMI, to investigate the redox state of LV tissues following anemia. Next, to evaluate the potential role of reactive oxygen species (ROS) in mediating LV dysfunction in anemia, respirometry analysis was performed in N-acetyl cysteine (NAC) supplemented anemic and non-anemic mice after AMI. Finally, to assess the potential role of anemic RBCs in mediating LV dysfunction in anemia, RBCs were incubated with wild type mice hearts in an ex vivo Langendorff system. These hearts were subjected to global ischemia and reperfused for 60 min after which high resolution respirometry analysis was performed.
Furthermore, the second aim of this study is to assess the effects of anemia on RBC eNOS in vascular and cardiac function. In this study, we examined the functional consequences of RBC-specific eNOS deletion on hemodynamics and cardiac performance in the context of blood loss-induced anemia. Anemia was induced in RBC-specific eNOS knockout (KO) mice and their corresponding control littermates. Hemodynamic parameters were assessed using

invasive Millar catheterization. Vascular function was evaluated both *in vivo*, via flow-mediated dilation (FMD), and *ex vivo*, using wire myography of isolated aortic rings. To investigate the role of RBC-derived eNOS following AMI, mice were subjected to ischemia-reperfusion (I/R) surgery. Cardiac function was monitored *in vivo* by transthoracic echocardiography, and myocardial injury was quantified by 2,3,5-triphenyltetrazolium chloride (TTC) staining to determine infarct size.

Results: Echocardiography data demonstrated an adapted cardiac function in anemic mice without AMI, evidenced by increased end-systolic volume (ESV), ejection fraction (EF), stroke volume (SV) and cardiac output (CO). After AMI induction anemic mice showed decreased EF and increased ESV compare to non-anemic mice. Assessment of heart function using cardiac magnetic resonance imaging (CMRI) at baseline, 3 days of anemia and 24 h after AMI demonstrated that anemia was associated with an unchanged PCr/ATP ratio at base line and 3 days after anemia. After AMI induction, no changes in PCr/ATP and Pi/ATP were observed in the remote region of anemic mice compared to non-anemic mice. In the ischemic region, PCr/ATP ratio was significantly reduced, and Pi/ATP ratio was significantly increased 24 h post-AMI in anemic mice compared to non-anemic mice. The fractional shortening, an indicator for contractile function, at base line, 3 days after anemia in the remote region was unchanged in anemic and non-anemic mice. Interestingly, the fractional shortening was significantly decreased in the ischemic region of anemic mice compared to non-anemic mice 24 h post-AMI. Proteomic analysis of LV tissues revealed that energy metabolism and mitochondria related proteins were less affected in the remote region of anemic mice after AMI. However, compensatory increase in mitochondrial respiration related proteins was observed in the ischemic region of anemic mice compared to non-anemic mice. Functional high resolution respirometry analysis of isolated LV tissues revealed that respiratory control ratio (RCR) $Coupling_{FNS}$, an indicative of OXPHOS efficiency, was unchanged in the remote region of anemic and non-anemic mice. In the ischemic region of anemic mice RCR $Coupling_{FNS}$ was significantly decreased compared to non-anemic mice. Oxidative stress was increased in LVs of anemic mice compared to non-anemic mice without AMI, indicated by decreased redox enzyme, namely superoxide dismutase (SOD), activity and reduced glutathione concentration. Additionally, a tendency towards increased ROS promoting enzyme, myeloperoxidase (MPO), activity was observed in anemic mice compared to non-anemic mice without AMI. After AMI, oxidative stress was increased in the remote region of anemic mice compared to non-anemic mice, as glutathione concentration was decreased. Furthermore, MPO activity was significantly increased in the remote region of anemic mice compared to non-anemic mice 24 h post-AMI. Similarly, in the ischemic region of anemic mice 24 h post-AMI, oxidative stress promoting MPO activity was significantly higher. Anemic mice treated with NAC, showed unchanged RCR

Coupling$_{FNS}$ in the remote region of anemic and non-anemic mice in high-resolution respirometry analysis. Interestingly, RCR Coupling$_{FNS}$ was preserved in the ischemic region of NAC treated anemic mice compared to non-anemic mice 24 h post-AMI. Anemic patient's RBCs, which were incubated for 40 min with wild type mice hearts *ex vivo* using a Langendorff system, did not affect mitochondrial respiration in LVs subjected to global I/R.

The functional analysis of RBC eNOS deficiency on cardio vascular function under anemic condition revealed the following observations: *In vivo* vascular function assessment of FMD showed that RBC-eNOS-KO mice maintained FMD responses under both baseline and anemic conditions. Similarly, *ex vivo* assessment of endothelium-dependent relaxation (EDR) in isolated aortic rings using wire myography demonstrated preserved EDR in anemic RBC-eNOS-KO mice. Blood pressure measurements using a Millar catheter showed that both systolic and diastolic BP were significantly elevated in non-anemic RBC-eNOS-KO mice, while BP remained unchanged in anemic RBC-eNOS-KO mice compared to controls. Echocardiographic analysis conducted at baseline, 3 days post-anemia induction, and 24 h after AMI demonstrated preserved cardiac function across all mice groups. However, infarct size analysis using TTC staining revealed a significantly increased infarct area in anemic RBC-eNOS-KO mice compared to anemic controls, consistent with prior observations under non-anemic conditions.

Conclusion: Taken together, findings of this study suggest that increased oxidative stress, evidenced by elevated MPO activity, in anemia impairs regional mitochondrial respiration and ATP availability in LVs. This results in altered cardiac energetic state and fractional shortening in the ischemic region after AMI. Anemic mice supplemented with NAC showed improved mitochondrial respiration in the ischemic region 24 h post-AMI. Therefore, NAC might be a potential therapeutic option to reverse altered energy imbalance in anemia after AMI.

Reduction in RBC number in anemia mitigates the increase in blood pressure caused by the deletion of eNOS in RBCs. Despite of unchanged heart function, RBC eNOS deficiency results in increased infarct size in anemia.

Zusammenfassung

Hintergrund: Anämie tritt häufig bei Patienten mit kardiovaskulären Erkrankungen (CVD) wie akuten und chronischen Koronarsyndromen sowie Herzinsuffizienz auf. Anämie, allein oder in Kombination mit anderen Komorbiditäten, führt zu einer ungünstigen Prognose beim akuten Myokardinfarkt (AMI). Frühere Studien an anämischen Mausmodellen und Patientendaten zeigten, dass Anämie mit einer unveränderten Infarktgröße, jedoch mit einer erhöhten Mortalität assoziiert ist. Der Einfluss von Anämie auf den Energiestoffwechsel im linken Ventrikel (LV) nach AMI wurde bisher nicht untersucht.

Anämie ist mit einer Dysfunktion der roten Blutkörperchen (RBCs) assoziiert. Unter physiologischen Bedingungen exprimieren RBCs funktionell aktive endotheliale Stickstoffmonoxid-Synthasen (eNOS), die unabhängig vom endothelialen eNOS zur Regulation des Blutdrucks beiträgt. Darüber hinaus wurde gezeigt, dass RBC eNOS während eines AMI kardioprotektiv ist. Wir vermuten, dass ein Energieungleichgewicht bei Anämie zur LV-Dysfunktion nach AMI beiträgt und damit zu einer schlechteren Prognose führt. Zudem vermuten wir, dass Anämie die Funktion von RBC-eNOS im Gefäßsystem und im Herzen verändert.

Ziele und Methoden: Das erste Ziel dieser Studie ist die Untersuchung des Energiestoffwechsels bei Anämie nach AMI im LV. Zu diesem Zweck wurden die Herzfunktion und die kardiale Energetik mittels Echokardiographie und kardialer Magnetresonanztomographie (CMRI) bei anämischen und nicht-anämischen Mäusen mit und ohne AMI gemessen. Anschließend wurde eine unvoreingenommene proteomische Analyse an isolierten LV-Geweben von anämischen und nicht-anämischen Mäusen mit und ohne AMI durchgeführt. Um regionale Unterschiede in den Proteomprofilen der LV-Gewebe nach AMI zu identifizieren, wurde die Proteomanalyse in der remote (nicht-infarktbetroffenen) und ischämischen (infarktbetroffenen) Region des LV-Gewebes durchgeführt. Zur genaueren Analyse der Veränderungen der oxidativen Phosphorylierung (OXPHOS) wurde eine Respirometrie-Analyse in den ischämischen und remote Regionen der LV-Gewebe von anämischen und nicht-anämischen Mäusen mit und ohne AMI durchgeführt. Biochemische Assays dienten der Bestimmung redoxaktiver Enzyme in den LV-Geweben, um den Redoxstatus in Anämie zu untersuchen. Zur Beurteilung der möglichen Rolle reaktiver Sauerstoffspezies (ROS) bei der LV-Dysfunktion in Anämie wurden zusätzlich Respirometrie-Messungen in LVs von N-Acetylcystein (NAC) behandelten anämischen und nicht-anämischen Mäusen nach AMI durchgeführt. Schließlich wurden zur Untersuchung der möglichen Rolle von RBCs bei der Beeinträchtigung der LV-Funktion in Anämie RBCs *ex vivo* mit Herzen von Wildtypmäusen im Langendorff-System inkubiert. Diese Herzen wurden einer globalen

Ischämie und Reperfusion unterzogen und anschließend mittels hochauflösender Respirometrie analysiert.

Das zweite Ziel der Studie war die Untersuchung des Einflusses von Anämie auf die RBC eNOS Funktion in Bezug auf Gefäß- und Herzfunktion. Hierzu wurden die funktionellen Konsequenzen einer RBC-spezifischen eNOS-Deletion auf die Hämodynamik und Herzleistung im Kontext einer blutverlustinduzierten Anämie analysiert. Anämie wurde in RBC eNOS Knockout (KO) Mäusen und deren Kontrollgruppen induziert. Die hämodynamischen Parameter wurden mittels invasiver Millar-Katheterisierung bestimmt. Die Gefäßfunktion wurde sowohl *in vivo* mittels flussvermittelter Dilatation (FMD) als auch *ex vivo* mittels Wiremyographie isolierter Gefäße untersucht. Zur Bewertung der Rolle von RBC eNOS nach AMI wurden Mäuse einer Ischämie-Reperfusions (I/R) Operation unterzogen. Die Herzfunktion wurde *in vivo* durch transthorakale Echokardiographie überwacht und die Infarktgröße mittels TTC-Färbung bestimmt.

Ergebnisse: Echokardiographische Daten zeigten eine adaptive Herzfunktion bei anämischen Mäusen ohne AMI, erkennbar an Veränderungen von endsystolischem Volumen (ESV), Ejektionsfraktion (EF), Schlagvolumen (SV) und Herzzeitvolumen (CO). CMRI-Messungen im basalem Zustand, nach 3 Tagen Anämie sowie 24 h nach AMI zeigten, dass das PCr/ATP-Verhältnis in der Ruhephase und nach 3 Tagen Anämie unverändert blieb. Nach AMI wurden in der remote Region weder Veränderungen im PCr/ATP- noch im Pi/ATP-Verhältnis bei anämischen und nicht-anämischen Mäusen festgestellt. In der ischämischen Region war das PCr/ATP-Verhältnis jedoch signifikant reduziert und das Pi/ATP-Verhältnis signifikant erhöht bei anämischen Mäusen im Vergleich zu nicht-anämischen 24 h nach AMI. Die fraktionelle Verkürzung, ein Maß für die Kontraktilität, war im basalem Zustand, nach 3 Tagen Anämie sowie in der remote Region unverändert zwischen beiden Gruppen, jedoch signifikant vermindert in der ischämischen Region bei anämischen Mäusen im Vergleich zu nicht-anämischen. Die Proteomanalyse zeigte, dass Proteine des Energiestoffwechsels und mitochondriale Proteine in der remote Region anämischer Mäuse nach AMI weniger stark betroffen waren. In der ischämischen Region wurde jedoch ein kompensatorischer Anstieg von mitochondrialen Proteinen bei anämischen Mäusen festgestellt. Die hochauflösende Respirometrie von isolierten LV-Geweben ergab, dass der Respiratorische Kontrollquotient (RCR $\text{Coupling}_{\text{FNS}}$), ein Maß für die OXPHOS-Effizienz, in der remote Region zwischen den Gruppen unverändert war, jedoch in der ischämischen Region bei anämischen Mäusen signifikant verringert war. Der oxidative Stress war bei anämischen Mäusen ohne AMI erhöht, was sich in reduzierter Aktivität von Redoxenzymen (z. B. Superoxiddismutase, SOD) und verringerten Glutathion Konzentration äußerte. Außerdem zeigte sich eine Tendenz zur erhöhten Aktivität des ROS-fördernden Enzyms Myeloperoxidase (MPO) in Anämie. Nach AMI

war der oxidative Stress in der remote Region von anämischen Mäusen im Vergleich zu nicht-anämischen erhöht, erkennbar an verminderter Glutathion Konzentration und signifikant erhöhter MPO-Aktivität. In der ischämischen Region war die MPO-Aktivität 24 h nach AMI ebenfalls signifikant erhöht bei anämischen Mäusen. Anämische Mäuse, die mit NAC behandelt wurden, zeigten einen unveränderten RCR $Coupling_{FNS}$ in der remote Region und einen normalisierten RCR $Coupling_{FNS}$ in der ischämischen Region im Vergleich zu nicht-anämischen Mäusen. RBCs von anämischen Patienten, die *ex vivo* 40 Minuten lang mit Wildtypherzen im Langendorff-System inkubiert wurden, beeinträchtigten die mitochondriale Atmung unter globaler I/R nicht.

Die funktionelle Analyse der RBC-eNOS-Defizienz bei Anämie ergab Folgendes: *In vivo* zeigte sich, dass FMD-Reaktionen bei RBC-eNOS-KO-Mäusen unter Basal- und Anämiebedingungen erhalten blieben. *Ex vivo* war die endothelabhängige Relaxation (EDR) in isolierten Aortenringen ebenfalls bei anämischen RBC-eNOS-KO-Mäusen erhalten. Blutdruckmessungen zeigten, dass sowohl systolischer als auch diastolischer Blutdruck bei nicht-anämischen RBC-eNOS-KO-Mäusen signifikant erhöht war, jedoch bei anämischen RBC-eNOS-KO-Mäusen im Vergleich zu Kontrollmäusen unverändert blieb. Echokardiographische Untersuchungen zu verschiedenen Zeitpunkten zeigten eine erhaltene Herzfunktion in allen Gruppen. Die TTC-Färbung ergab jedoch eine signifikant größere Infarktgröße bei anämischen RBC-eNOS-KO-Mäusen im Vergleich zu anämischen Kontrollen, entsprechend früheren Beobachtungen unter nicht-anämischen Bedingungen.

Fazit: Zusammenfassend deuten die Ergebnisse dieser Studie darauf hin, dass erhöhter oxidativer Stress bei Anämie, nachweisbar durch erhöhte MPO-Aktivität, die mitochondriale Atmung und ATP-Verfügbarkeit in regionalen Myokardarealen beeinträchtigt, was zu einer gestörten Energetik und reduzierter fraktioneller Verkürzung in der ischämischen Region nach AMI führt. NAC-Behandlung in Anämie führte zu einer Erhaltung der mitochondrialen Atmung in der ischämischen Region. Somit spiegelt NAC eine potenzielle therapeutische Option zur Behandlung des gestörten Energiemetabolismus bei Anämie nach AMI wider. Die reduzierte Erythrozytenzahl bei Anämie kompensiert den Blutdruckanstieg, der durch die Deletion von eNOS in RBCs verursacht wird. Trotz erhaltener Herzfunktion führt der eNOS-Mangel in RBCs zu einer vergrößerten Infarktgröße bei Anämie.

Table of content

List of Figures

List of tables

List of abbreviations

$^1O_2$	Singlet oxygen
4-HNE	4-Hydroxynonenal
AODS	Antioxidant defence system
Acetyl-CoA	Acetyl coenzyme A
ADP	Adenosine diphosphate
AMI	Acute myocardial infarction
Arl2	ARF Like GTPase 2
Armc10	Armadillo Repeat Containing 10
ATP	Adenosine triphosphate
Bcl2l13	BCL2-like 13
BNip3	Bcl-2 interacting protein 3
BSA	Bovine serum albumin
CAA	Chloroacetic Acid
CAD	Coronary artery disease
Ca^{2+}	Calcium ion
CAT	Catalase
CETF	Electron-transferring flavoprotein Complex
CI	Complex I
CII	Complex II
CIII	Complex III
CIV	Complex IV
CM	Cardiomyocyte
CMRI	Cardiac magnetic resonance imaging
CO_2	Carbon dioxide
CPEO	Chronic progressive external ophthalmoplegia

CS	Citrate synthase
CV	Complex V
CV	Coefficient of variation
CVD	Cardiovascular diseases
CVS	Cardiovascular system
DTT	Dithiothreitol
Drp1	Dynamin-Related Protein 1
EDV	End-diastolic volume
EF	Ejection fraction
EGTA	Ethyleneglycol bis(2-aminoethyl ether)
eNOS	Endothelial nitric oxide synthase
ESV	End-systolic volume
EPO	Erythropoietin
ETS	Electron transport system
FAO	Fatty acid oxidation
FCCP	Carbonyl-cyanide p-(trifluoromethoxy) phenylhydrazone
FAD	Flavin adenine dinucleotide
Fis1	Mitochondrial fission 1 protein
FKBP8	FKBP Prolyl Isomerase 8
GP_x	Glutathione peroxidase
GR	Glutathione reductase
GSH	Reduced glutathione
GST	Glutathione s-transferase
GTP	Guanosine triphosphate
H_2O_2	Hydrogen peroxide
HAA	Hospital acquired anemia

Hb	Haemoglobin
Hct	Haematocrit
HEPES	4-(2-hydroxyethyl)-1-piperazineethanesulfonic acid
HOCl	Hypochlorous acid
HR	Heartrate
IDA	Iron deficiency anemia
I/R	Ischemia reperfusion
IMS	Intermembrane space
iNOS	Inducible nitric oxide synthase
i.p.	Intraperitoneal
KH2PO4	Potassium dihydrogen phosphate
K-MES	2-(N-Morpholino)ethanesulfonic acid potassium salt
Kyat3	Kynurenine aminotransferase 3
LANUV	Landesamt für Natur, Umwelt- und Verbraucherschutz
LAD	Left anterior descending
LV	Left ventricle
MCU	Mitochondrial Ca2+ uniporter
MCV	Mean corpuscular volume
$MgCl_2$	Magnesium chloride
MI	Myocardial infarction
MELAS	Mitochondrial myopathy, encephalopathy, lactic acidosis and stroke-like episodes
MFN1	Mitofusin 1
MFN2	Mitofusin 2
MM	Mitochondrial matrix
MMP	Mitochondrial membrane potential
MPO	Myeloperoxidase

MS	Mass spectrometry
Mtch2	Mitochondrial carrier homolog 2
Mtfp1	Mitochondrial Fission Process 1
Mul1	Mitochondrial E3 ubiquitin protein ligase 1
NAC	N-acetyl cysteine
NAD	Nicotinamide adenine dinucleotide
Ndufb6	NADH ubiquinone oxidoreductase subunit B6
Ndufs7	NADH ubiquinone oxidoreductase core subunit S7
Nipsnap2	Nipsnap Homolog 2
nNOS	Neuronal nitric oxide synthase
NO	Nitric oxide
NOS	Nitric oxide synthase
Nox	NADPH-oxidases
NSTEMI	Non-ST-segment elevation myocardial infarction
O_2	Oxygen
OAA	Oxaloacetic acid
OPA1	Optic atrophy 1
OPA3	Optic atrophy 3
Optn	Optineurin
OXPHOS	Oxidative phosphorylation
Park7	Parkinsonism Associated Deglycase
PBS	Phosphate buffered saline
PCr	Phosphocreatine
Phb2	Prohibitin 2
Pi	Phosphate
PMD	Primary mitochondrial disease

PFC	Perfluorocarbons
RBC	Red blood cell
RCR	Respiratory control ratio
ROS	Reactive oxygen species
Sdhaf2	Succinate dehydrogenase complex assembly factor 2
Slc25a46	Solute carrier family 25 member 46
SMD	Secondary mitochondrial disease
SOD	Superoxide dismutase
STEMI	ST-segment elevation myocardial infarction
SV	Stroke volume
TCA	Tricarboxylic acid
TCEP	Tris(2-carboxyethyl)phosphine
TFA	Trifluoroacetic acid
Txnrd2	Thioredoxin reductase 2
Uqcr10	Ubiquinol-cytochrome c reductase complex
UV	Ultraviolet
WHO	World Health Organization
WT	Wild type
XO	Xanthine oxidase
$\cdot O_2^-$	Superoxide anion
·OH	Hydroxyl radical

1 Introduction

1.1 Heart function and dysfunction

The circulatory system supplies oxygen and nutrients to the entire body and is composed of a network of blood vessels and the heart. The heart is a muscular organ, which pumps the blood through the body. It is divided into four chambers: right atrium, right ventricle, left ventricle and left atrium (Figure 1) [1]. Deoxygenated blood enters the right atrium via the coronary sinus, after which the blood flows into the right ventricle through the tricuspid valve. The right ventricle pumps the deoxygenated blood into the pulmonary artery, where it is distributed to the lungs. Blood is oxygenated in the lungs and collected in four pulmonary veins, which pass the blood to the left atrium. Oxygen-rich blood in the left atrium enters via mitral valve the left ventricle, which contracts and enables the distribution of the blood to the entire body through the aortic valve [1, 2].

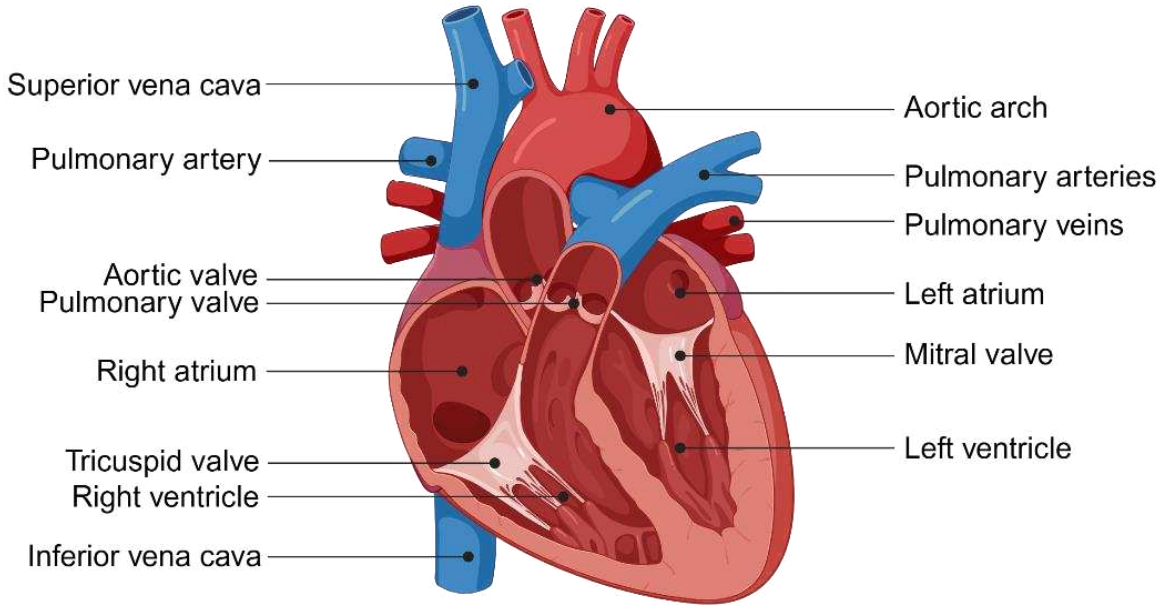

Figure 1: Anatomy of the heart. The blood flow through the four chambers, namely left atrium, left ventricle, right atrium, right ventricle, is a controlled process aided by different valves as depicted, which enable blood flow in one direction. Illustration adapted and created in BioRender, based on Jean-Francis.B. (2020) The physiology of Heart.

As the left ventricle (LV) supplies blood and therefore oxygen and nutrients to all organs, its functionality is of immense importance. The assessment of LV function plays a significant role in the evaluation and prognosis of different cardiovascular diseases (CVD)s, such as coronary artery disease (CAD) [3, 4], myocardial infarction [5], coronary bypass surgery [6, 7], malignant ventricular arrhythmias [8-10], and chronic valvular regurgitation [11, 12]. Therefore, LV functionality is measured for the prediction of cardiac mortality and morbidity [13]. Early diagnosis of LV dysfunction enables early treatment, preventing the progression of CVDs, such

as heart failure [14, 15]. In clinical setting, LV dysfunction is characterized by abnormal LV parameters, such as heart rate, ejection fraction, cardiac output, and stroke volume, which can be assessed using non-invasive methods such as echocardiography and magnetic resonance imaging (MRI).

Various mechanisms trigger the development of LV dysfunction. LV hypertrophy, a disease in which individuals show increased LV mass and thus thickened myocardial wall, may evolve into LV dysfunction [16]. Critically ill patients often develop LV dysfunction as a result of inflammation and endotoxins resulted from sepsis [17]. Other cardiometabolic conditions, such as CAD, tachycardia, hypertension and severe metabolic disorders can cause LV dysfunction independently [17, 18].

1.2 Acute myocardial infarction

The leading cause of death and disability worldwide is acute myocardial infarction (AMI), affecting 3 million people annually [19]. It is the most severe manifestation of CAD [20], and categorized into non-ST-segment elevation myocardial infarction (NSTEMI) and ST-segment elevation myocardial infarction (STEMI) [21-23]. NSTEMI can result from coronary artery narrowing, transient occlusion or microembolization of thrombus, whereas STEMI is caused by complete and prolonged occlusion of a coronary blood vessel [24]. Rupture of vulnerable atherosclerotic plaques are the most common cause of blood vessel occlusion, causing 70% of fatal AMI cases [19]. After rupture, macrophages and monocytes are recruited, which initiate inflammatory responses resulting in thrombus formation and platelet aggregation. This process leads to the occlusion or narrowing of coronary vessels, which in turn results in the restriction of oxygen and nutrients supply to myocardial cells due to decreased or inhibited blood flow, damaging myocardial cells. Prolonged occlusion leads to the necrosis of these cells [25]. Modifiable risk factors, such as smoking, dyslipidemia, diabetes mellitus, hypertension and obesity [26], and non-modifiable risk factors, such as age, sex and family history, play a crucial role in the narrowing of coronary vessels and impairment of the blood flow [19]. Affected individuals show symptoms such as radiating pain from the chest, oppressive pain, nausea and/or vomiting, sweating, and absence of chest-wall tenderness on palpation [27]. Over the years, treatment of AMI improved, reducing the mortality rate [28-31]. The most effective therapy in AMI is early reperfusion, as it limits infarct size and saves viable cardiomyocytes (CMs), improving AMI outcome [32, 33], however, till date AMI remains the leading cause of death worldwide. The number of patients hospitalised after AMI with one or more comorbidities is increasing [34]. Several studies have shown, that in combination with other comorbidities, AMI outcome is worsened, by increasing mortality rate and prolonging hospital stays. The most frequent comorbidities in these patients are hypertension, diabetes mellitus, chronic kidney disease, anemia and chronic obstructive pulmonary disease [35, 36]. These comorbidities alter

both the inflammatory, metabolic and energetic state of the heart, leading to a worsened prognosis.

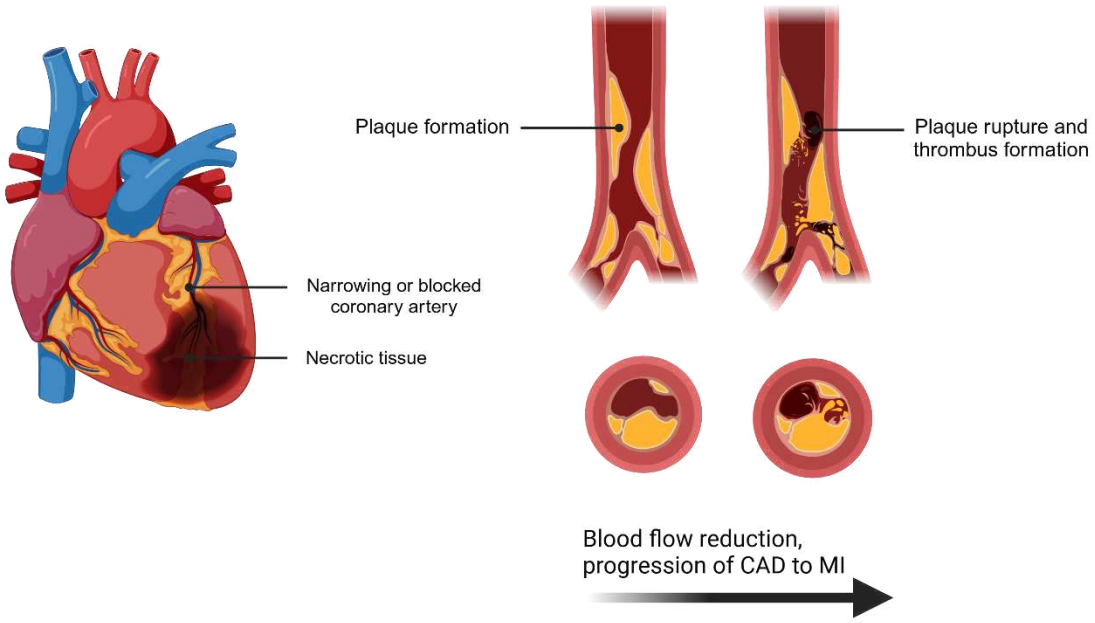

Figure 2: Progression of CAD to myocardial infarction (MI). Narrowing of coronary artery results from atherosclerotic plaque formation in blood vessels. Rupture of atherosclerotic plaques induce thrombus formation, leading to the blockage of vessels and ultimately to MI. Illustration based on © IHH Healthcare Singapore and created in BioRender.

1.2.1 Cardiac metabolism and energy sources

Approximately 60-70% of generated ATP is consumed by the heart for its contraction [37-39]. Therefore, ATP synthesis- and ATP turnover rate in the heart is increased depending on its energy demand [37, 40]. As energy cannot be sufficiently stored in CMs, tight coupling of ATP synthesis and heart contraction is integral [41, 42]. Oxidative phosphorylation (OXPHOS) fuels the synthesis of more than 95% of ATP in the heart. During the process of glycolysis the remaining 5% of ATP are generated [37, 43]. In order to gain energy continuously, cardiac mitochondria utilize different substrates to synthesize ATP, which are carbohydrates, fatty acids, amino acids and ketone bodies [41, 44]. Among these substrates, the majority of ATP in the heart is generated from fatty acids (60-90%) [43]. ATP has a high molecular weight, restricting it to diffuse through the mitochondrial membrane. For the usage of ATP in the cytosol, the high energy phosphate bond in ATP is transferred to creatine. This reaction is catalysed by mitochondrial creatine kinase and results in the phosphorylation of creatine to phosphocreatine (PCr). PCr's molecular weight is lower compared to the molecular weight of

ATP, enabling its diffusion through the mitochondrial membrane. In the cytosol, the high-energy phosphate bond is transferred to ADP, generating ATP [45].

Due to high energy demand in the heart, mitochondrial number is increased in cardiac cells [46]. Approximately 1/3rd of the CM volume is occupied by mitochondria [47]. To ensure regulated ATP synthesis in the heart, mitochondrial fusion and fission is tightly regulated [48], as CMs are not able to readily divide in homeostasis [49].

1.3 Mitochondria

The heart requires a substantial amount of energy in the form of ATP, which is produced by mitochondria. Mitochondria are known as the powerhouse of the cell, which comes from their primary function in generating metabolic energy in nearly all eukaryotic cells. The characteristic structure of mitochondria includes a double phospholipid bilayer, the inner- and outer membrane, which are separated by the intermembrane space. The inner membrane forms so called “cristae”, in which the complexes of the electron transport system (ETS) are embedded. The mitochondrial matrix (MM) contains mitochondrial DNA (mtDNA), which encode for 13 distinct mitochondrial proteins, including the subunits of the ETS complexes. Approximately, 95% of the mitochondrial proteins are encoded by nuclear DNA [50]. Apart from their crucial role in energy metabolism, mitochondria have been identified to participate in the regulation of phospholipid and heme synthesis, Ca^{2+} homeostasis and apoptosis [51, 52]. The regulation of energy production is mediated in mitochondria through Ca^{2+} signalling. Cytosolic Ca^{2+} concentration increases when high energy levels are required [53]. Ca^{2+} influx in the MM is fuelled by the increase in cytosolic Ca^{2+}, which enter MM through the mitochondrial Ca^{2} uniporter (MCU). High Ca^{2+} concentration in MM activates pyruvate, α-ketoglutarate and nicotinamide adenine dinucleotide (NAD)-isocitrate dehydrogenases, increasing co-substrate synthesis for the ETS [54, 55]. In addition, mitochondria are known to thrive reactive oxygen species (ROS) generation, containing at least 10 known sites capable of ROS formation [56].

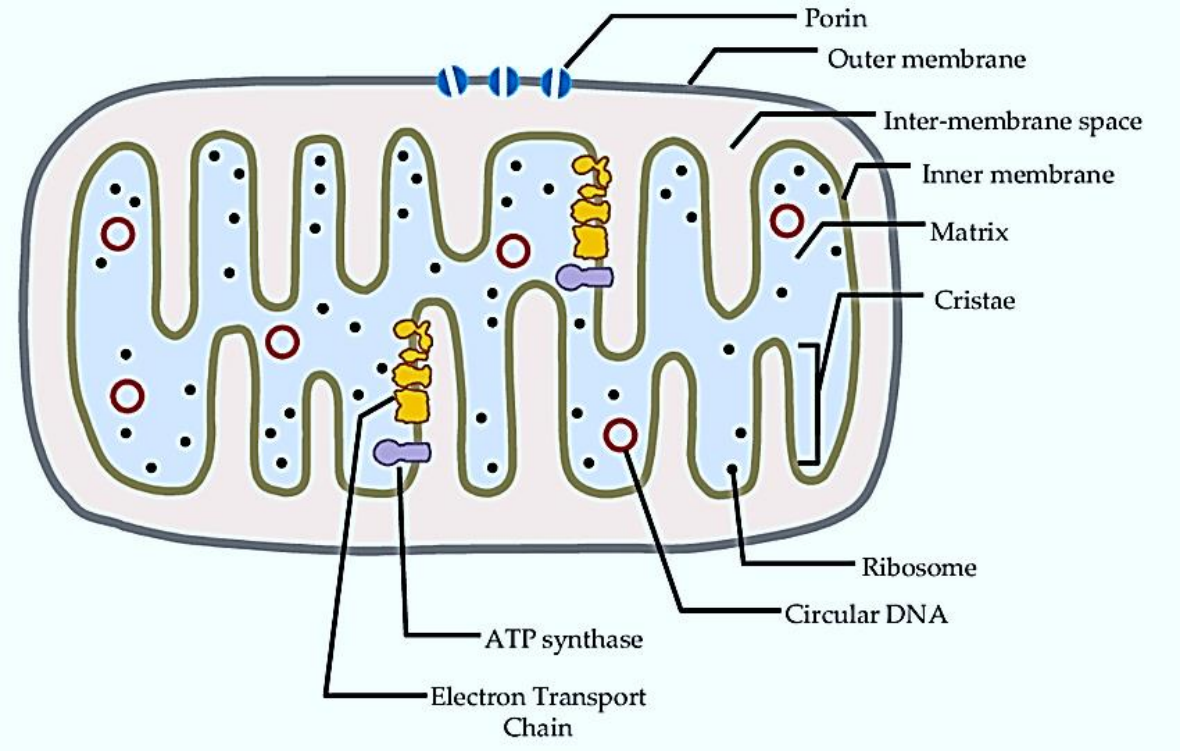

Figure 3: Mitochondrial morphology. Mitochondria consist of double lipid bilayers, the outer and inner membrane, which are separated by the intermembrane space. The inner membrane forms cristae, which embeds electron transport system complexes. The mitochondrial matrix contains mtDNA and ribosomes. Adapted from Yusoff et al [57].

Mitochondrial morphology is dynamic and regulated by the processes of mitochondrial fusion and fission [58]. Mitochondrial fusion describes the process of conjoining two mitochondria, which is mediated by different proteins, namely mitofusin (MFN) 1, MFN2 and optic atrophy 1 (OPA1) [59, 60]. Deficiency of these proteins results in mitochondrial fragmentation [61, 62]. Fission of mitochondria is the process of segregating one mitochondria into two, regulated through the interplay of several proteins, such as dynamin-related protein 1 (Drp1) and mitochondrial fission 1 protein (Fis1) [63, 64]. Impairment of mitochondrial fission triggers hyperfused mitochondrial structure [65]. To ensure mitochondrial quality, damaged mitochondria are removed via mitophagy [66]. Mitophagy, the controlled removal of mitochondria, plays a pivotal role in inflammation, metabolic adaptations, cellular reprogramming and redox homeostasis [67, 68]. In AMI, mitochondrial fission has been reported to be upregulated, leading to worse prognosis [69]. Piamsiri et al. demonstrated that chronic mitochondrial dynamic-targeted therapy in rats, that underwent AMI surgery, improved cardiac function [70], highlighting the pivotal role of mitochondrial dynamics in AMI.

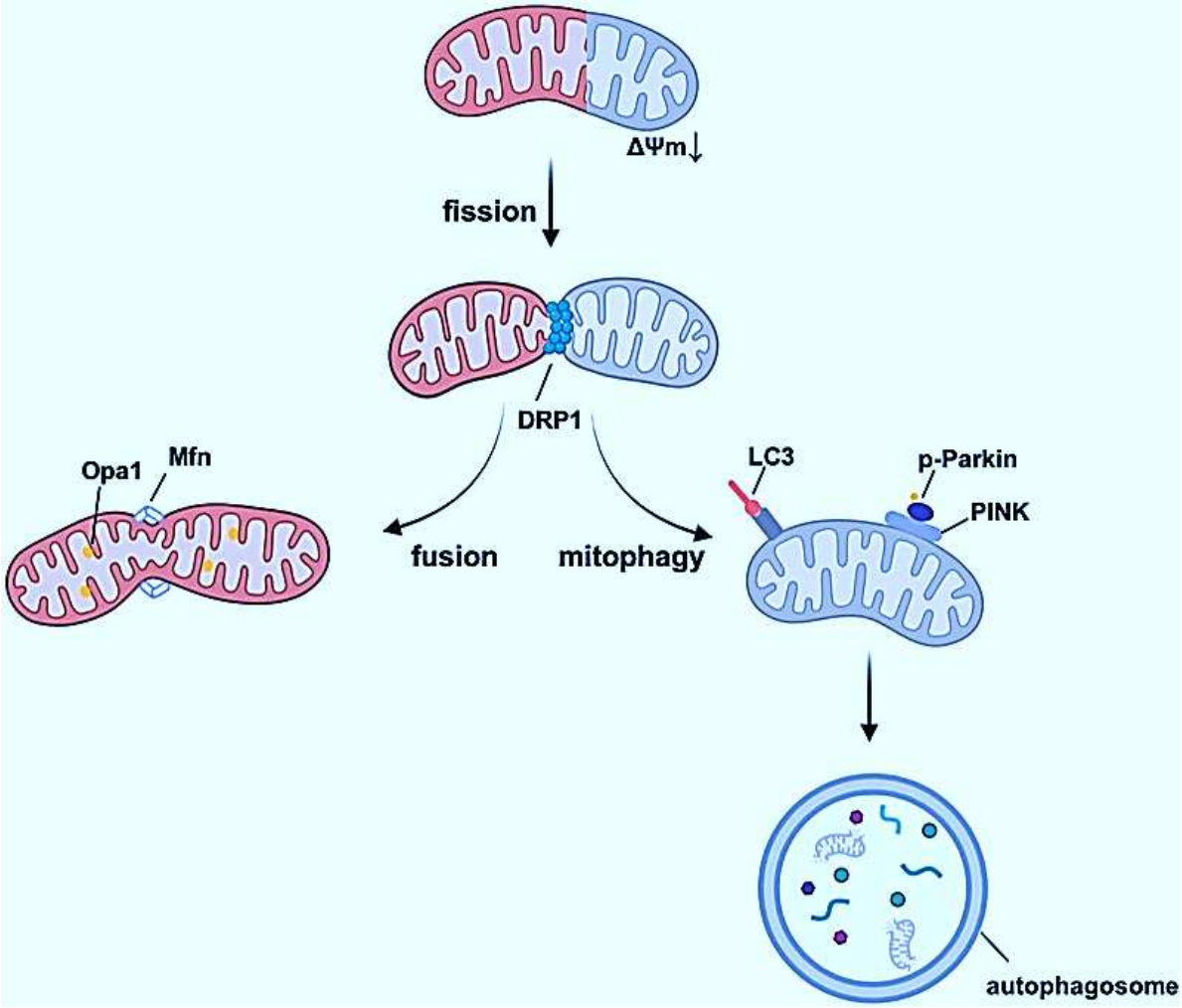

Figure 4: Mitochondrial dynamics. Mitochondrial fission separates damaged mitochondria from healthy mitochondria. Through mitophagy damaged mitochondria are degraded. Mitochondrial fusion conjoins two healthy mitochondria and maintain physiological mitochondria function. Adapted from Yang et al. [71].

1.4 Energy metabolism

Adenosine triphosphate (ATP), the main source of energy for life, is the energy currency utilized in the myocardium to pump blood throughout the body. ATP is an organic molecule consisting of a ribose sugar, a nitrogenous base and three bonded phosphate groups [72]. ATP is mainly generated in mitochondria through a process called OXPHOS. The synthesis of ATP is driven by the metabolism of carbohydrates, fats and proteins. Glucose is catabolized by three subsequent processes: glycolysis, tricarboxylic acid (TCA) cycle and OXPHOS [73]. Glycolysis is an anaerobic ATP source, which occurs in the cell's cytoplasm. Glucose conversion during glycolysis is catalysed by different enzymes, resulting in two molecules of ATP and two molecules of pyruvate [74]. When oxygen is present, pyruvate dehydrogenase converts pyruvate to acetyl-CoA, which then enters the TCA cycle. The TCA cycle, also known as Krebs cycle, is a closed loop consisting of various enzymes that convert acetyl-CoA [75]. One TCA cycle generates three molecules of $NADH_2$, one molecule of $FADH_2$ and one

molecule of GTP [76]. The last step of aerobic respiration is the ETS in combination with chemiosmosis, which together portray the OXPHOS. OXPHOS creates the largest amount of ATP, compared to glycolysis. At the ETS, electrons are transferred through protein complexes, anchored in the inner mitochondrial membrane (Figure 5) [77]. NADH-ubiquinone oxidoreductase or complex I (CI) oxidizes $NADH_2$ enabling the transfer of two electrons through flavinmononucleotide (FMN) and Fe-S clusters to Coenzyme Q. This leads to the release of redox energy, which is utilized to transport four hydrogen ions through CI into the intermembrane space, increasing the proton gradient (Figure 5) [77, 78]. The next complex of the ETS is complex II (CII) or succinate dehydrogenase, which is another entry point into the ETS. CII oxidizes succinate, an intermediate of the TCA cycle, to fumarate. In this process, two electrons are transferred from FAD over Fe-S to Coenzyme Q, generating $FADH_2$ (Figure 5). Electron-transferring flavoprotein complex (CETF) is an additional complex, which feeds electrons from flavoenzymes into the ETS by transferring electrons to Coenzyme Q. This complex is especially important in fatty acid oxidation [79]. The transferred electrons on Coenzyme Q are then transported to complex III (CIII), which is also known as cytochrome c reductase. There the electrons are passed through the Q-Cycle, pumping four hydrogen ions into the intermembrane space (IMS), contributing to the electrochemical gradient (Figure 5) [77]. The electrons are then transferred via the mobile electron carrier Cytochrome C to complex IV (CIV) also known as cytochrome c oxidase. Cytochrome C is then oxidized by CIV and the electrons are transferred to the final electron acceptor of the ETS, oxygen, which is then reduced to water (Figure 5). This process pumps two hydrogen ions from the mitochondrial matrix into the IMS per conversion, further increasing the electrochemical gradient [77]. Complex V (CV) or ATP synthase uses this electrochemical gradient to synthesize ATP by phosphorylating ADP (Figure 5) [80].

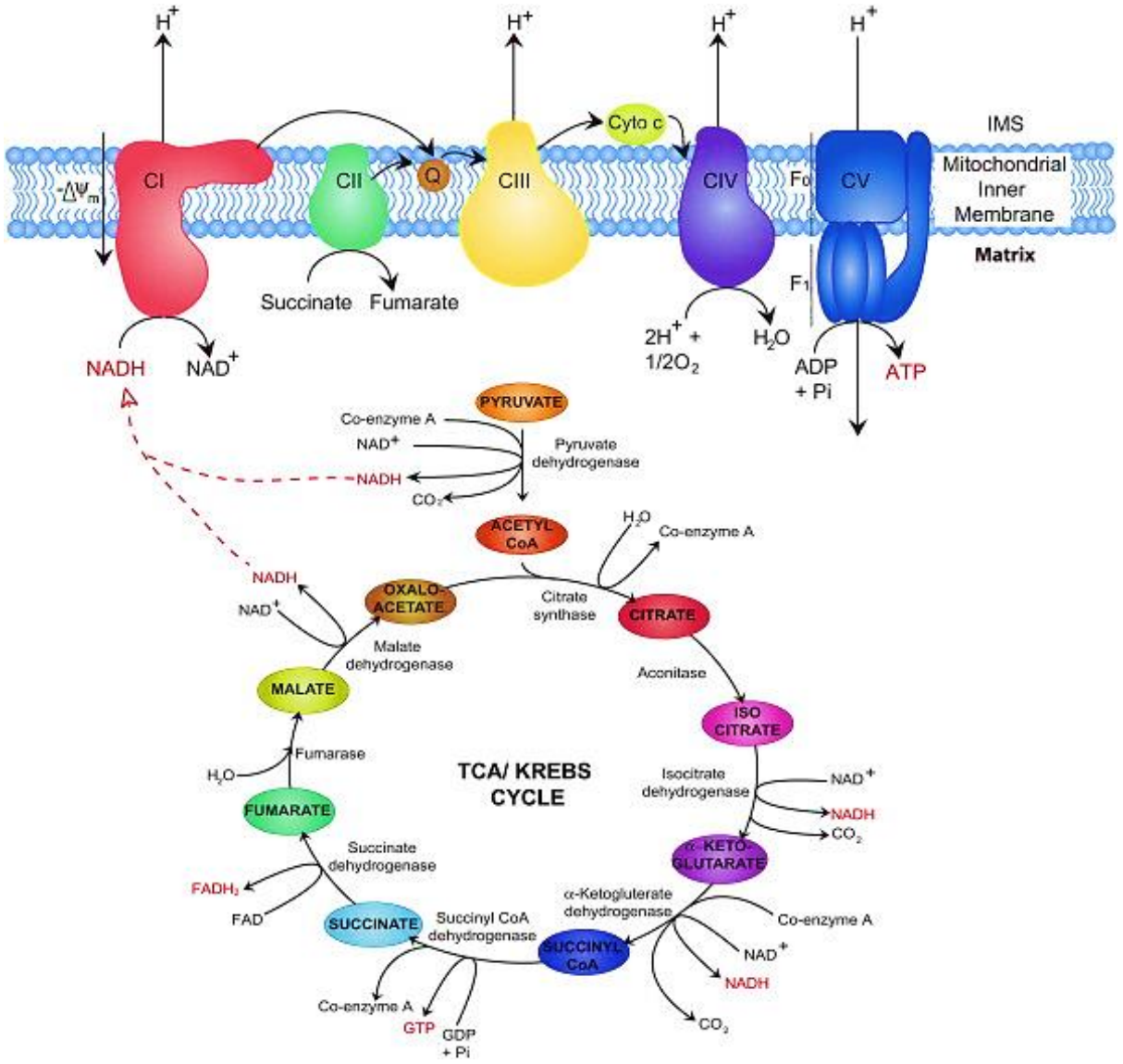

Figure 5: Energy metabolism via TCA/Krebs cycle and ETS. TCA cycle generates cofactors, namely NADH, GTP and $FADH_2$, which fuel ETS through proton gradient in the IMS. ATP synthase uses the proton gradient to phosphorylate ADP to ATP. Adapted from Osellame et al. [53].

1.4.1 Substrate sources for ETS

Substrate sources of the ETS include various molecules, such as carbohydrates, fatty acids, and proteins, which provide electrons through metabolic pathways like glycolysis, the TCA cycle, and fatty acid oxidation. Fatty acid oxidation (FAO) plays a pivotal role in the heart by providing ATP using OXPHOS as the primary metabolic pathway, ensuring continuous energy production for myocardial function. FAO or mitochondrial beta-oxidation utilizes fatty acids as substrate to produce ATP, mainly in skeletal muscle, heart and kidneys [81]. Fatty acids transport proteins, e.g. CD36 and fatty-acid-binding proteins are required to transport fatty acids between extra- and intracellular membranes [82]. Within the cytosol fatty acids are transformed into fatty acyl-CoA, catalysed by acyl CoA synthetase. Carnitine palmitoyltransferase I (CPT1) catalyzes the conversion of fatty acyl-CoA to fatty acyl-carnitine

on the outer mitochondrial membrane [83]. Fatty acyl-carnitine is transported through the inner mitochondrial membrane via carnitine/acylcarnitine translocase. In the mitochondrial matrix, CPT2 converts fatty acyl-carnitine back to fatty acyl-CoA, which is then cleaved into acetyl coenzyme A (acetyl-CoA) [83]. Acetyl CoA enters the TCA cycle, generating cofactors for ETS as described previously.

FAO generated end product acetyl-CoA is predominantly the source for ketone body synthesis in the liver. When the body is deprived of nutrients, acetone levels in the blood increases. D-β-hydroxybutyrate is converted into acetoacetate which reacts with an ester-CoA and succinyl-CoA and enters the TCA cycle [44].

1.5 Mitochondrial dysfunction in pathologies

Efficient regulation of mitochondrial function is fundamental for life. Disorders and alterations in mitochondrial function, morphology or number lead to the development of metabolic, cardiac, neurodegenerative, immune, and neoplastic diseases [84-86]. Repair mechanisms for DNA mutations are less efficient in mitochondria, as mtDNA is in close proximity to ETS, which generates ROS. This results in increased mutation rate in mtDNA [87]. Thus, mitochondrial function is prone to errors, leading to various pathological conditions [71, 88, 89].

Primary mitochondrial diseases (PMD), e.g., Leigh syndrome, mitochondrial myopathy, encephalopathy, lactic acidosis and stroke-like episodes (MELAS), and chronic progressive external ophthalmoplegia (CPEO), result from inherited mitochondrial dysfunction due to mtDNA mutations [90-93]. PMD prevalence increases with aging and has been proven to worsen clinical outcome [94]. In addition to PMD, secondary mitochondrial diseases (SMD) exist, which originate from mutations in genes not directly related to OXPHOS. SMD are characterized by the impairment of mitochondrial function regulating pathways and ROS contributing factors [93, 95, 96]. These factors are common in different disease states, such as neurodevelopmental and neurodegeneration diseases, diabetes and cancer [96, 97].

One of the major sources of ROS is OXPHOS in mitochondria [98, 99]. Mitochondrial respiration promotes superoxide anion ($\cdot O_2^-$) production, especially at the sites of CI and CIII [100, 101]. Several CVDs, such as atherosclerosis, cardiac hypertrophy, heart failure and degenerative aortic valve diseases, are associated with mitochondrial dysfunction through increased mitochondrial oxidative stress [102]. A breakthrough in the area of dysfunctional mitochondria in AMI was achieved by elucidating that mitochondrial ROS induces ischemia reperfusion (I/R) injury in the heart [71] through TCA cycle intermediate succinate accumulation [103]. Re-oxidation of accumulated succinate is catalysed by succinate dehydrogenase, leading to reversed electron transport and ROS formation [103].

1.6 ROS and antioxidant defence system in CVD

ROS are oxygen-containing molecules that possess one or more unpaired electrons. ROS include radicals, such as superoxide anion and hydroxyl radical (•OH), and non-radical molecules like hydrogen peroxide (H_2O_2), singlet oxygen ($^1O_2$), which are all generated by partial reduction of oxygen [104, 105]. Physiological levels of ROS are generated during mitochondrial respiration and inflammation in the cells [105]. Excessive ROS formation is triggered by diseases, UV radiation, long-term stress conditions, intense physical exercise, improper diet and use of stimulants [105, 106]. Cellular responses to xenobiotics, cytochrome p450, xanthine oxidase (XO), the endoplasmic reticulum, peroxidases, and cyclooxygenases also generate ROS [104, 107, 108]. The role of ROS has been described in physiological functions, such as cell proliferation, differentiation, migration, apoptosis and necrosis [109-112]. In low levels ROS are integral for redox homeostasis, cell signalling and to govern important transcription factors [111, 113]. However, enhanced ROS generation results in redox imbalance, tissue injury, altered permeability and protein expression [104, 114-117]. Due to their unpaired electrons, ROS are highly reactive, damaging DNA, RNA, lipids and proteins [118-120]. The counterpart of ROS is the antioxidant defence system (AODS) [121, 122]. AODS includes a variety of antioxidants to maintain redox balance [121]. Enzymatic antioxidants, namely thioredoxin, peroxidases, superoxide dismutase (SOD), catalase (CAT), glutathione reductase (GR), glutathione peroxidase (GPx), glutathione s-transferase (GST) [121, 123, 124], and non-enzymatic antioxidants, such as reduced glutathione (GSH), vitamin E, C, A, lycopene, and beta-carotene scavenge oxyradicals [125], reducing tissue injury [126].

Elevated ROS levels in the vasculature contribute to endothelial dysfunction and cardiac inflammation, resulting in the development of CVDs. [104, 116, 127]. In CMs, ROS generation is increased through NADPH-oxidases (Nox) activity, an important class of enzymes for host defense, cellular signalling and regulation of gene expression [98, 128, 129]. Overexpressed Nox2 and Nox4 have been associated with ROS induced oxidative stress in CVDs, causing cardiac dysfunction [128, 130, 131]. Excessive ROS can trigger progression of CAD and AMI by oxidizing LDL, which enhances atherosclerotic plaque formation [113, 132]. The process of reperfusion after ischemia is associated with increased ROS levels [133-135]. This effect and enhanced Ca^{2+} levels after ischemia are speculated to contribute to the opening of mitochondrial permeability transition pore (mPTP), leading to necrosis [136-140]. Elevated ROS levels also play a crucial role in distinct types of anemia [141-143]. A previous study using an iron-deficient mouse model demonstrated that iron deficiency anemia leads to higher oxidative stress in red blood cells (RBCs), through increased hemoglobin (Hb) autooxidation [143]. Another study highlighted the link between oxidative stress and the progression of autoimmune hemolytic anemia in a mouse model [144]. Our working group has shown that chronic anemia induces endothelial dysfunction, which is accompanied by excessive ROS

levels [127]. Our study also revealed that acute anemia is associated with elevated oxidative stress in RBCs and loss of their cardioprotective properties following global ischemia. However, the underlying molecular mechanisms remain poorly understood [145].

1.7 RBCs and their function

RBCs or erythrocytes are the most abundant cell type in the blood, having the important function to transport gases and nutrients throughout the body [146, 147]. Hematopoietic stem cell differentiation, a process called erythropoiesis, generate RBCs. The precursor of RBCs are proerythroblasts, which are the first derived cells from multipotent hematopoietic stem cells. These cells undergo various cell divisions, in which the cells anucleate, and differentiate into reticulocytes. Reticulocytes enter the circulation and mature within one day into RBCs [148]. Matured RBCs have a unique biconcave shape, enabling reversible elastic deformation via a high surface-to-volume ratio. RBCs membrane flexibility allows the passing of RBCs through the smallest capillaries, to transport oxygen and carbon dioxide [149]. The most abundant protein in RBCs is Hb, a heme containing tetramer, consisting of two α-subunits and two β-subunits, with each of them having the ability to bind one oxygen molecule [150]. Having a high affinity for oxygen and low affinity for carbon dioxide in arterial circulation and vice versa in venous circulation, Hb functions as a two-way respiratory carrier [151].

Apart from their gas-transport function, RBCs have been identified to play an important role in vascular redox regulation [152, 153]. Through autooxidation, Hb can oxidize to methaemoglobin (metHb), which impairs the oxygen carrying capacity in elevated levels [154]. As a source for ROS, metHb has the potential to generate peroxide resulting in ROS mediated tissue damage [155]. As they are at risk of producing high levels of ROS, RBCs have a robust antioxidant defence system, consisting of enzymatic and non-enzymatic molecules [153, 156].

1.8 RBCs and NO synthases in CVDs

RBCs are additionally known for their vascular tone modulation through nitric oxide (NO) regulation [157]. Through hemolysis, Hb is released into the plasma. Free plasma Hb is capable of scavenging NO, 600-fold times faster than RBC Hb. Increased NO scavenging disrupts NO homeostasis, eventually resulting in vasoconstriction, decreased blood flow, platelet activation, increased endothelin-1 (ET-1) expression, and end-organ injury [158]. In addition to NO regulation by free Hb, RBCs have been shown to possess NO-synthases (NOS) and thus contribute to NO synthesis [157]. Our previous study demonstrated that similarly to endothelial cell (EC) eNOS, RBC eNOS regulate NO metabolites and blood pressure. In the same study, we showed that RBC eNOS deficiency after AMI led to increased infarct size [157].

All three isoforms of NOS, which are neuronal NOS, inducible NOS and endothelial NOS, synthesize NO and L-citrulline by oxidizing its substrate L-arginine in the presence of oxygen [159]. Neuronal NOS (nNOS) is primarily expressed in central and peripheral neurons, in which they regulate neurotransmission and neuromodulation [160]. Inducible NOS (iNOS) expression is induced by pro-inflammatory cytokines and bacterial lipopolysaccharide in different cell types and is pivotal for inflammatory responses [161-163]. Endothelial NOS (eNOS) is mainly expressed in endothelial cells, but is also found in other cells, such as RBCs and CMs. eNOS is crucial for the maintenance of the vascular tone and consequently for blood pressure regulation [164]. As NO is a crucial modulator for maintenance of the vascular function, physiological NOS function is pivotal for the cardiovascular system. For the physiological NOS function, dimerization of the enzyme, the presence of its substrate L-arginine and its cofactors nicotinamide adenine dinucleotide phosphate (NADPH), flavin adenine dinucleotide (FAD), flavin mononucleotide (FMN) and (6R)-5,6,7,8-tetrahydro-l-biopterin (BH4) are required [165].

Impairment in the function of NOS, particularly eNOS, has been associated with the development of CVDs, such as atherosclerosis, arterial hypertension, cardiac hypertrophy and heart failure [166-168]. The mechanism driving eNOS dysfunction is eNOS uncoupling, which decreases NO synthesis and generates ROS formation, resulting in endothelial dysfunction [169]. Our previous study observed elevated eNOS expression under anemic conditions to mediate circulatory compensation in anemia [170].

1.9 Anemia

Anemia is a condition described as a decrease in the amount of RBCs, Hb or hematocrit (Hct) [171], leading to the impairment of oxygen carrying capacity in the blood [172]. The World Health Organization (WHO) defines anemia as Hb level <13.5 in men, <12.0 in women and <11.0 in children [173]. About 2 billion people worldwide are affected, of which women and children are the majority. Anemic individuals typically show symptoms such as fatigue, reduced cognitive function, lethargy and tiredness [171, 174].

Based on the mean corpuscular volume (MCV), anemia can be classified in three distinct subgroups: microcytic, normocytic and macrocytic anemia. Each of the subgroups contain various anemia types (Table 1).

Table 1: Anemia categorization based on MCV. Anemia can be categorized into three distinct subgroups by MCV: micro- normo- and macrocytic anemia. The subtypes of each group and their causes are listed [171].

	Subtypes	Causes
Microcytic anemia (MCV <80 fl)	Iron deficiency anemia (IDA)	Iron deficiency
	Anemia of chronic disease	Inflammation
	Thalassemias	DNA mutations
	Sideroblastic anemia	Alcohol consumption, heavy metal poisoning
Normocytic anemia (MCV 80-100 fl)	Blood loss anemia	Blood loss
	Aplastic anemia	Autoimmune disorders
	Hemolytic anemia	Defective RBCs and or production
	Anemia of inflammation	Erythropoietin (EPO) disorders
Macrocytic anemia (MCV >100 fl)	Megaloblastic anemia	Vitamin B12 deficiency, folate deficiency
	Non-megaloblastic anemia	Alcohol consumption, liver disease

The two factors driving anemia development are reduced RBC production and increased RBC destruction. Reduced RBC production mainly originates from genetical disorders, nutritional deficiencies or inflammation, whereas increased RBC destruction results from blood-loss or hemolysis [175]. Depending on the severity and type of anemia, different treatments are provided, which are iron, vitamin B12 and folic acid supplementation, erythropoietin and immunosuppressants medication, blood transfusion and stem cell transplant [171].

Many patients develop anemia during hospitalization as a result of frequent blood withdrawal for diagnostic tests [176], with the most patients manifesting moderate or severe anemia [177]. This type of blood-loss anemia is known as hospital acquired anemia (HAA) and affects approximately 40-74% of hospitalized patients [177-179]. HAA has been associated with increased mortality and worsened health status in patients with CAD [180], such as AMI [181-183]. Anemia has been identified as an independent predictor for poor outcomes in several disease states [184-186], by increased risk of bleeding, thromboembolic events, arrhythmias and hypertension [152].

Anemia is associated with RBC dysfunction, although the cause of RBC dysfunction varies between different types of anemia. RBC dysfunction may result from genetical disorders, e.g.

in sickle cell anemia and thalassemia, impairment of cytoskeletal proteins or redox imbalance [152].

1.9.1 Anemia in CVDs

Anemia has been described as an independent risk factor for the development of CVD [187]. In a pioneer study, a cohort of 14,410 subjects without CVD at baseline were examined in a follow-up trial, in which anemic patients had an increased risk of CVD [188]. Several other studies have proven that anemia serves as a predictor for CVD pathogenesis [186, 189, 190]. Evident anemia in chronic heart failure, LV hypertrophy, chronic kidney disease, diabetes mellitus and acute coronary syndrome patients lead to an increased mortality rate [188, 191-193].

Decreased oxygen transport to tissues aggravates progression of CVDs in anemia [194]. By elevating cardiac output, via higher preload, heart rate and stroke volume, LV hypertrophy or arterial hypertrophy may occur [195-198]. These anemia associated wall-thickening effects can be manifested severely in combination with other comorbidities [199]. Apart from the impaired oxygen supply, anemic conditions result in redox imbalance and disturbed NO homeostasis. Increased ROS levels and decreased NO levels contribute to endothelial dysfunction in anemia [127], which is associated with the pathogenesis of atherosclerosis [200].

1.9.2 Anemia in AMI

One of the risk factors identified in AMI is anemia [201, 202], which has been associated with adverse outcomes in AMI patients [203], by increasing the risk of death and prolonging the hospital stay [202, 204]. The prevalence of anemia in AMI patients varies among studies [201, 205, 206]. Anemic conditions further deteriorate AMI outcome, due to increasing the existing oxygen demand, impairing vascular healing, decreasing NO bioavailability, and pathological ventricular remodelling [170, 207-209]. Due to which, anemic AMI patients often experience cardiovascular complications such as thromboembolic events, augmented bleeding, hypertension and arrhythmias [210-213]. Furthermore, we demonstrated that RBCs from anemic AMI patients lose their cardioprotective properties in an *ex vivo* isolated mouse heart model [145], highlighting the importance of RBCs in AMI. This study proved that anemic RBCs are dysfunctional, characterized by decreased NO levels, which lead to the impairment of heart function post ischemia [145].

2 Aim of the study

Anemia has been identified as an independent risk factor for CVD in many clinical studies, which demonstrated worsened outcome by increased mortality and morbidity [186, 189, 190]. Our previous study showed that anemia aggravates endothelial dysfunction after AMI [214]. Similarly, heart function has been shown to be impaired in different studies, which demonstrated increased heart failure and arrhythmias in anemic patients after AMI [203, 215]. However, the underlying mechanism of how anemia affects heart function after AMI remains unknown. AMI is known to exhibit impaired energy metabolism, resulting in inefficient ATP production. Cardiac energy metabolism in anemia after AMI is not very well understood. RBC eNOS is known to be cardioprotective and deficiency leads to increased infarct size. The effects of anemia on RBC eNOS deficiency and associated consequences on cardiovascular system have not been investigated.

This thesis aimed to investigate two hypotheses. Firstly, we hypothesize that anemia impairs energy metabolism in the LV after AMI due to increased oxidative stress, resulting in LV dysfunction (Figure 6). For this purpose, LV function and cardiac energetics are assessed in anemic and non-anemic mice before and after AMI induction using echocardiography and cardiac magnetic resonance imaging (CMRI). Unbiased proteomic analysis is performed to explore the alterations in protein expression in LV tissues of anemic and non-anemic mice with and without AMI. Next, deep proteomic analysis is performed to identify differentially regulated proteins that are related to energy metabolism and mitochondrial proteins. Next, respirometry analyses are performed in anemic and non-anemic mice after AMI, to investigate potential changes in mitochondrial respiration in anemia after AMI. To assess the role of ROS, LV tissues of N-acetyl cysteine (NAC) treated anemic and non-anemic mice after AMI are measured using high resolution respirometry. To gain insights into the antioxidant capacity and oxidative stress state of LV tissues from anemic and non-anemic mice with and without AMI, biochemical assays and western blotting are performed. Pathological alterations in mitochondrial content and expression of ETS complexes are analysed in anemic and non-anemic mice after AMI, with and without ROS scavenging. Finally, the potential role of anemic RBCs in mediating LV dysfunction is investigated by incubating anemic patients' RBCs with hearts, which were then subjected to global ischemia and reperfusion in a Langendorff apparatus. The respiration of the LVs isolated from these hearts are then analysed using high resolution respirometry

In addition, this thesis also aimed to elucidate the role of RBC eNOS in anemia on vascular and heart function with and without AMI. We hypothesize that eNOS deficiency in RBCs under anemic conditions worsen heart- and vascular function after AMI (Figure 6). To test our hypothesis, a RBC-eNOS-KO mouse model is used, in which anemia is induced. Heart function

is assessed by using Millar catheter measurements in anemic RBC-eNOS-KO and non-anemic RBC-eNOS-KO mice. Moreover, vascular function is analysed in the same mouse groups by *ex vivo* wire myography and *in vivo* flow-mediated dilation (FMD) measurements. Furthermore, AMI is induced in anemic and non-anemic RBC-eNOS-KO mice, after which heart function is measured using echocardiography. Finally, infarct sizes are assessed using Triphenyl Tetrazolium Chloride (TTC) staining, in anemic and non-anemic RBC-eNOS-KO mice hearts after AMI.

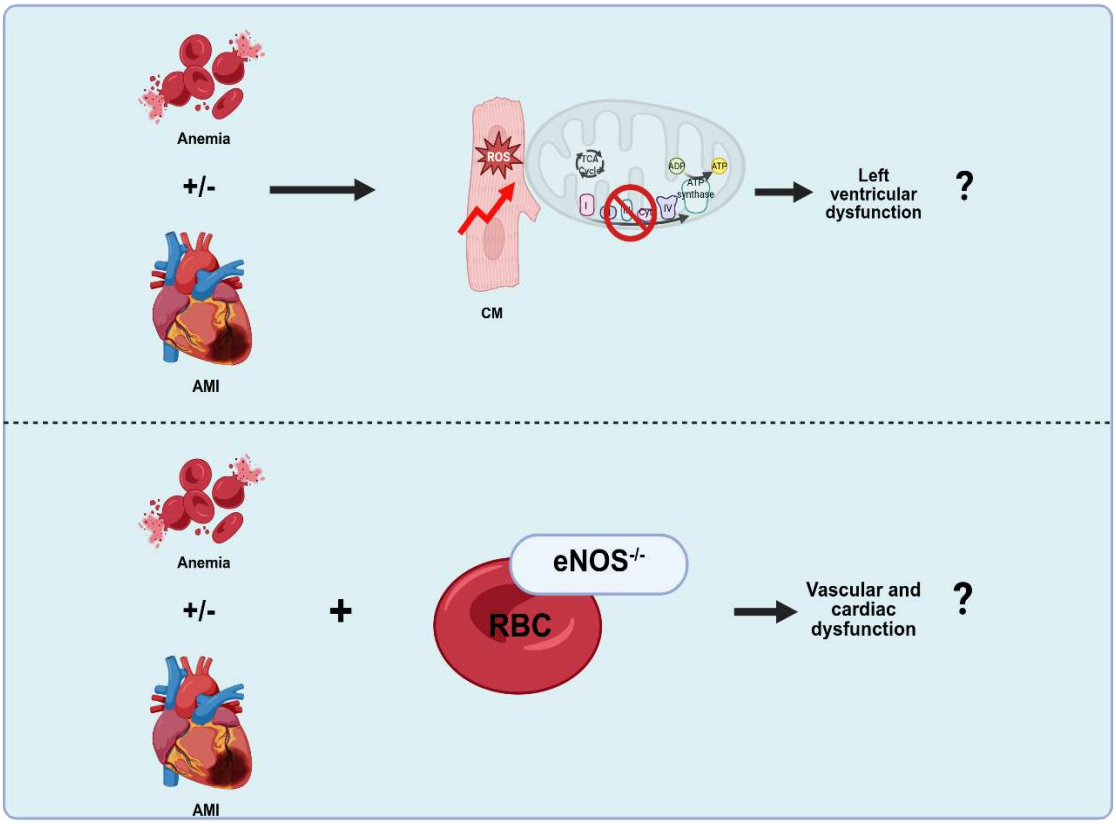

Figure 6: Hypotheses of this study. Presence of anemia with and without AMI increases oxidative stress in CMs, resulting in impaired energy metabolism, ultimately leading to LV dysfunction. RBC eNOS deficiency worsen the cardiac function after AMI. Created in BioRender.

3 Material and Methods

To evaluate the role of anemia after AMI in LV dysfunction and associated signalling pathways and to investigate the effect of RBC eNOS in anemia with and without AMI on LV and vascular function, this thesis used mouse models and a variety of methods and techniques, which are presented in the below paragraphs.

3.1 Mouse studies

Experiments and procedures in the context of this work were approved and performed in accordance with the guidelines of LANUV (Landesamt für Natur, Umwelt- und Verbraucherschutz Nordrhein-Westfalen, Germany). All mice were treated according to the European Convention for the protection of Vertebrate Animals used for Experimental and other Scientific Purposes (Council of Europe Treaty Series No. 123). To generate RBC-specific nitric oxide synthase knockout mice (RBC-eNOS-KO), homozygous $eNOS^{flox/flox}$ mice were crossed with erythrocyte-specific Hbb-Cre^{pos} mice (C57BL/6-Tg(Hbb-Cre)12Kpe/J; MGI: J:89725;) [156]. The approved permits for the animal experiments are 84-02.04. 2020.A073 and O47/90. The C57Bl/6J (wild type, WT) mice were obtained from Janvier Labs (Saint-Berthevin Cedex, France). All mice were housed in standard cages (constant room temperature and humidity, 12 h light/dark cycles) and were fed standard pellet chow and tap water *ad libitum*.

3.2 Anemia induction

To induce anemia, C57Bl/6J mice (10–12-week-old) were divided into two groups, a control (n=10) group without anemia, which will be termed as “non-anemic” in this thesis. The second group was induced with anemia, which will be termed as “anemic” in this thesis [214]. Additionally, anemia was induced in RBC-eNOS-KO mice (n=10) and in RBC eNOS control mice (n=10). To induce anemia, a repetitive mild blood withdrawal (by <20 g/l changes in Hb) from the facial vein was performed daily for three days. At the end of the third day, mice with Hb levels < 10 g/l were considered for experiments.

3.3 Supplementation of NAC

NAC is a widely accepted ROS scavenger, which is a synthetic precursor of glutathione [216]. To evaluate the potential role of ROS in LV dysfunction, both anemic and non-anemic mice were supplemented with NAC. For NAC supplementation C57Bl/6J mice were divided into anemic and non-anemic groups. Both groups were treated with 1% NAC through drinking water for four weeks [214].

3.4 Blood collection

Peripheral blood samples were collected from patients diagnosed with CAD, with and without anemia, using EDTA-coated tubes. Anemia was defined based on the WHO criteria: Hb concentrations below 13.0 g/dL in adult males and below 12.0 g/dL in adult females. All participants provided written informed consent prior to inclusion in the study. Patient recruitment was conducted through the Department of Cardiology, Pulmonology, and Angiology at Düsseldorf University. Blood sample collection was approved by the ethics committee of Düsseldorf University Hospital under the reference numbers 5481R, 2018-14, and 2018-47.

3.5 Ischemia reperfusion surgery

To induce AMI in mice, to mimic human MI, I/R surgeries were performed in anemic, non-anemic, anemic RBC-eNOS-KO and control mice one day after anemia induction [214]. To induce ischemia, mice were injected with buprenorphine (0.1 mg/kg body weight, Temgesic©; Indivior Europe, Dublin, Ireland) subcutaneously. Using an inhalation chamber consisting of 3% isoflurane, mice were anesthetized for 30 min. Afterwards the mice were intubated, for which an indwelling venous cannula (Vasofix Safety Kanüle 20 G 1,1x25 mm, B. Braun, Melsungen, Germany) was used. Once the mice were intubated, they were placed on a heated surgery table with a rectal probe, allowing the monitoring of the body temperature throughout the surgery. To check heart function during surgery an ECG (Powerlab 8/35, Software: LabChart, ADInstruments, Sydney, Australia) was utilized. Furthermore, the mice received eye ointment (Bepanthen Augensalbe, Bayer, Leverkusen, Germany) to prevent drying out of the eyes. The mice were ventilated at a tidal volume of 0.2–0.25 mL, and a respiratory rate of 140 breaths per minute and constantly anesthetized (2% isoflurane and 40% oxygenated air) using a rodent ventilator (MiniVent Type 845, Hugo Sachs, March-Hugstetten, Germany). After a left lateral thoracotomy between the third and fourth rib, the pericardium was dissected, and a 7–0 surgical suture was cautiously passed underneath the left anterior descending (LAD) artery at a position 1 mm from the tip of the left auricle. The LAD was occluded leading to ischemia for 45 min and a short silicone role was placed into the suture loop to facilitate its reopening. The positioning of the suture was adjusted to its right position by blanching of the apex and characteristic changes in the electrocardiogram (ST-segment elevation). Afterwards, the ligation was removed, which lead to the reperfusion of the heart. Using a 4-0 silk thread (Ethicon) the opened ribs were closed. Furthermore, the skin was stitched by using a 5-0 prolene thread (Ethicon). The suture was disinfected carefully and mice were extubated. Mice were caged with a heating lamp. For 24 h post I/R the mice received buprenorphine (0.5 mg/kg BW) s.c. every 8 h until euthanasia.

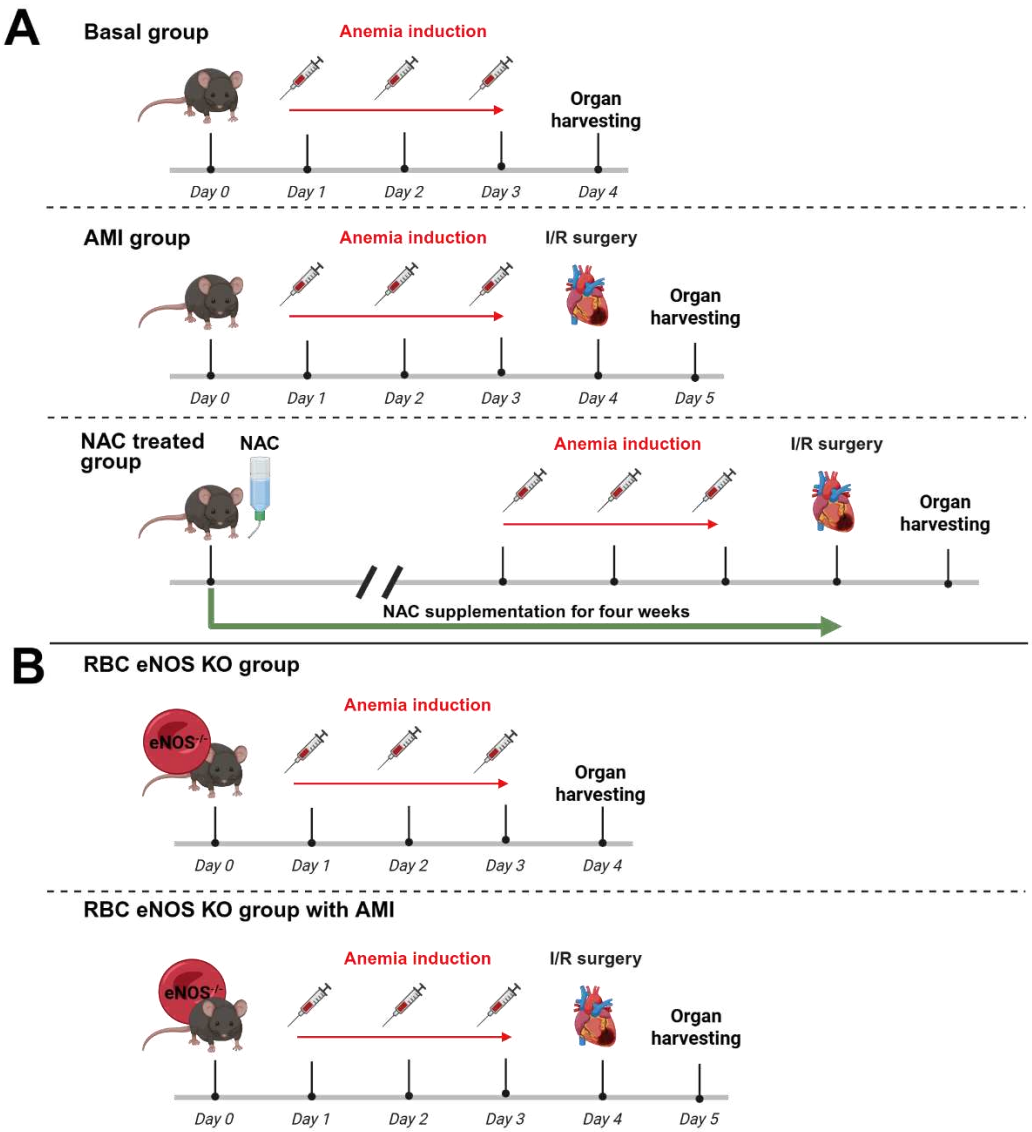

Figure 7: Schematic representation of the experimental groups. (A) C57BL/6J mice were separated into two groups, and in one of these groups anemia was induced for three consecutive days. To generate anemic and non-anemic mice with AMI, C57BL/6J mice were separated into two groups, and in one group anemia was induced. On the fourth day I/R surgery was performed in both anemic and non-anemic mice. Another set of mice was also separated into two groups. Both groups were supplemented with NAC (1%) for four weeks before experimental procedures. In one of these groups, anemia was induced in the last days of the four-week time period. On the last day I/R surgery was performed in both groups. (B) Anemia was induced for three consecutive days in RBC-eNOS-KO mice and control mice. In a different set of anemic RBC-eNOS-KO and RBC eNOS control mice, I/R surgery was performed on the fourth day. This study used in total 14 different mouse groups: anemic- and non-anemic mice, anemic and non-anemic mice with AMI, NAC-treated anemic and non-anemic mice with AMI, anemic and non-anemic RBC-eNOS-KO mice, anemic and non-anemic RBC eNOS control mice, anemic and non-anemic RBC-eNOS-KO mice with AMI and anemic and non-anemic RBC eNOS control mice with AMI. Created in BioRender.

3.6 Echocardiography

To assess cardiac parameters, echocardiography measurements were performed in anemic and non-anemic mice before and after induction of AMI. For this purpose, Fujifilm VisualSonics Vevo 3100 Ultra High Frequency Imaging Platform (18–38 MHz linear array micro scan transducer; VisualSonics, Toronto, Canada) was used. Firstly, mice were anesthetized by placing them in an oxygen enriched induction chamber, consisting of 2.5-3 % isoflurane. After a brief time period, the anesthetized mice were placed on a heated table with integrated components, which allowed the monitoring of electrocardiogram, respiratory rate, heart rate and body temperature. Mice were continuously anesthetized using an isoflurane (1.5-2 %) mask. The fur on the chest of the mice was removed using a chemical hair remover, enabling enhanced cardiac imaging. After applying preheated Aquasonic 100 Gel (Parker Laboratories, Fairfield, United States), cardiac imaging in the parasternal long-axis was conducted. Different cardiac function parameters such as LV chamber volume in end-diastole (EDV) and end-systole (ESV), stroke volume (SV), ejection fraction (EF), cardiac output (CO) and heart rate (HR) were assessed using the B-Mode in Vevo LV-Trace function and strain. Echocardiography data was analysed using Vevo Lab software (Visual Sonics, Fujifilm, Japan).

3.7 CMRI

Cardiac function and cardiac energetics were assessed using CMRI, based on fluorine-19 (^{19}F) [217]. ^{19}F MRI is non-invasive and allows *in vivo* usage as it gives low background signal for cardiac imaging.

^{19}F was imaged using perfluorocarbons (PFC), which are highly stable and non-toxic. For the preparation of the PFC emulsion, purified egg lecithin (E 80 S, 4% wt/wt, Lipoid, Ludwigshafen, Germany) was dissolved in an isotonic phosphate buffer containing 10 mmol/L phosphate and 150 mmol/L NaCl with a pH of 7.4, by magnetic stirring for 30 min. Next, the prepared lecithin was mixed with rhodamine dihexadeconic phosphatidylethanolamine (Molecular Probes, Leiden, the Netherlands) and dissolved in absolute ethanol. Afterwards, the resulting solvent was removed under lowered pressure at 37°C and evaporated with vacuum. The emerged lipid film was hydrated by gentle stirring and dispersion after adding isotonic phosphate buffer. Perfluoro-15-crown-5 ether (10% wt/wt, Fluorochem Ltd, Glossop, UK) was added to the mixture, which was then dispersed with a high-performance disperser (T18 basic ULTRA TURRAX, IKA Werke GmbH & Co KG, Staufen, Germany) at 14000 rpm for 2 min at room temperature. Using a high-pressure homogenizer (APV Gaulin Micron Laboratory 40, APV, Unna, Germany), the emulsion was homogenized for 10 cycles with a pressure of 70 MPa. The resulting nanoemulsion was finally filtered using a sterile 0.22 µm sterile filter (Millex-GS, Millipore, Ireland) and stored at 6°C until further use.

The instrument utilized for MRI was a Bruker DRX 9.4-T wide-bore (89-mm) nuclear MR spectrometer (Bruker, Rheinstetten, Germany), which conducts at frequencies of 400.13 MHz for 1H and 376.46 MHz for 19F measurements. Images were taken using a Bruker microimaging unit (Mini 0.5) with an actively shielded 57-mm gradient set, which were acquired from a 30-mm birdcage resonator tunable to 1H and 19F.

To perform CMRI analyses, mice were first anesthetized using 1.5 % isoflurane, while being kept at 37°C. By using an ECG- and respiratory-triggered fast-gradient-echo cine sequence (field of view [FOV], 30×30 mm^2; matrix, 128×128; slice thickness, 1 mm) ^1H images of mice hearts were attained. CMRI measurements were performed in collaboration with Prof. Dr. Ulrich Flögel.

3.8 Organ harvesting

Anemic and non-anemic mice with and without AMI were anesthetized by intraperitoneal (i.p.) injection with ketamine (Ketaset®; Zoetis, Parsippany-Troy Hills Township, United States) (100 mg/kg body weight) and xylazine (Rompun®; Serumwerk Bernburg, Bernburg, Germany) (10 mg/kg body weight). After ensuring the efficiency of the anesthesia, mice were fixed with tape on surgery tables. Euthanasia was induced by cardiac puncture using a 1 ml syringe, after which hearts were perfused with phosphate buffered saline (PBS), to reduce the amount of RBCs. The hearts were then isolated and the ischemic (infarct) and remote (non-infarct) regions of the LVs were separated using a light microscope. Samples were snap frozen and stored at -80°C until further use.

3.9 Proteomic analysis

To assess the proteome of LV tissues, LVs were isolated from anemic and non-anemic mice with and without AMI induction. LV tissues of mice that underwent AMI induction, were further separated in remote and ischemic region. Tissues were snap frozen and analyzed in the proteomic facility Biogenity ApS (Denmark). The sample preparation, mass spectrometry (MS) analysis and data analysis were performed by the Biogenity and DTU Proteomics.

3.9.1 Sample preparation for proteomic analysis

Tissues were prepared according to the protocol of Kulak et al. [218]. Briefly, tissues were lysed using a lysis buffer (6 M Guanidinium Hydrochloride, 10 mM TCEP, 40 mM CAA, 50 mM HEPES pH 8.5), and afterwards incubated at 95°C for 5 min. Next, the samples were processed using a tissue lyser for 1 min going from 3 to 30 Hz, which was repeated one more time. Then, the samples were sonicated at 4°C for 5x 60 seconds on and 30 seconds off in a Bioruptor Pico sonication water bath (Diagenode). Afterwards, protein concentration was measured using BCA, and 200 µg of the samples were further used for digestion. Next the samples were diluted with acetonitrile (1:3 ratio) and 50 mM HEPES pH 8.5, LysC (MS grade,

Wako) was added in a 1:50 (enzyme to protein) ratio. Samples were then incubated at 37°C for 4 h. After another 1:10 dilution with acetonitrile, 50 mM HEPES pH 8.5, trypsin (MS grade, Sigma) was added in a 1:100 (enzyme to protein) ratio and samples were incubated at 37°C overnight. Enzyme activity was terminated by adding 2% trifluoroacetic acid (TFA) to achieve a final concentration of 1%. Before further processing, peptides were desalted using a SOLAμ SPE plate (HRP, Thermo). For each sample, the filters were pre-activated with 200 µl of 100% methanol (HPLC grade, Sigma), followed by 200 µl of 80% acetonitrile containing 0.1% formic acid. The filters were then equilibrated twice with 200 µl of 1% TFA and 3% acetonitrile. Samples were loaded onto the filters by centrifugation at 1500 rpm. The filters were washed twice with 200 µl of 0.1% formic acid, and the peptides were eluted into clean 1.5 ml Eppendorf tubes using 40% acetonitrile with 0.1% formic acid. The eluted peptides were concentrated using an Eppendorf SpeedVac and reconstituted in 50 mM HEPES buffer (pH 8.5).

Using 16plex tags (Thermo), part of the digested sample was isolated for TMT labeling. Afterwards, TFA was added to reduce the acetonitrile concentration to <5% and to acidify the sample. Before MS analysis, peptides were fractioned with an offline ThermoFisher Ultimate3000 liquid chromatography system using high pH fractionation (5 mM Ammonium Bicarbonate, pH 10) at a flowrate of 5 µl/min. An amount of 15 µg of peptides were divided using a 120 min gradient (5% to 35% acetonitrile), during which fractions were collected every 130 seconds. The resulting 60 fractions were combined into 30 final fractions, acidified to a pH below 2 using 1% TFA, and loaded onto EvoSep StageTips following the manufacturer's protocol.

3.9.2 Mass spectrometry analysis

Firstly, the peptides pre-set "30 samples per day" program on the EvoSep One instrument was used for each fraction. After elution over a 44 min gradient, the peptides were analysed using an Orbitrap EclipseTM TribridTM instrument (Thermo Fisher Scientific) with FAIMS ProTM Interface (Thermo Fisher Scientific) switched between coefficient of variations (CVs) of -50 V and -70 V with cycle times of 2 s and 1.5 s respectively. Next, at a resolution of 120000, whole MS spectra were measured with normalized AGC target set to 100% or maximum injection time of 50 ms and a scan range of 375–1500 m/z. For MS2 analysis, MS1 precursors with an intensity of >5×103 and charge state of 2-7 were selected. Then dynamic exclusion was configured to 120 seconds, with the exclusion list shared between CV values, and Advanced Peak Determination was turned off. The precursor fit threshold was set at 70% with a fit window of 0.7 m/z for MS2. Afterwards, selected precursors for MS2 were separated in the quadrupole using a 0.7 m/z isolation window. Ion collection was conducted to a maximum injection time of 35 ms, with a normalized AGC target set to 300%. Fragmentation was carried out using HCD normalized collision energy of 30%, and MS2 spectra were acquired in the ion trap at a rapid

scan rate. Next, the MS2 spectra were analyzed using RTS with the UniProt Mus musculus protein database, with trypsin specified as the enzyme. Static modifications included TMTpro labeling on lysine (K) and the peptide N-terminus, as well as carbamidomethylation on cysteine (C). Oxidation of methionine (M) was set as a variable modification. Thereafter, maximum number of missed cleavages was set to 1, with maximum 2 variable modification, FDR filtering was enabled, and the maximum search time was limited to 35 ms. After scoring thresholds were defined as 1 Xcorr, 0 dCn, and a 5 ppm precursor tolerance, the "use as trigger only" option was disabled, while close-out was enabled, with a maximum of 4 peptides per protein. Precursors were afterwards filtered with isobaric tag loss exclusion for TMT and a precursor mass exclusion range of ±25 ppm.

Next, precursors identified by RTS were separated for an MS3 scan using the quadrupole with a 2 m/z isolation window. Ions were then collected with a maximum injection time of 86 ms and a normalized AGC target of 300%. After deactivating Turbo TMT, the number of dependent scans was set to 10. The isolated precursors were then fragmented again using HCD with a normalized collision energy of 50%, and MS3 spectra were acquired in the Orbitrap at a resolution of 50,000 with a scan range of 100–500 m/z. Consistency of MS performance was verified by analyzing a complex cell lysate quality control standard.

3.9.3 Data analysis

Biogenity contributed to the data analysis, including generating figures, tables, and reports. Using Proteome Discoverer 2.4 (Thermo Fisher Scientific), raw data files were processed. TMT reporter ion quantitation was enabled during both the processing and consensus workflows, and spectra were matched against the UniProt Mus musculus database, encompassing both reviewed and unreviewed proteins. Dynamic modifications were specified as oxidation (M) and acetylation on protein N-termini, while static modifications contained cysteine carbamidomethylation (on C residues) and TMT 16-plex labeling (on peptide N-termini and K residues). Results were filtered to achieve a 1% FDR, and protein quantitation was performed using the Minora Feature Detector. Data filtering enabled that only proteins with at least 2 unique peptides were included in the downstream analysis.

3.10 High resolution respirometry

To assess mitochondrial respiration in LV tissues of anemic and non-anemic mice with and without AMI, and with and without NAC supplementation, high resolution respirometry was performed using a high resolution oxygraph (Oroboros-O2k, Oroboros Instruments, Innsbruck, Austria). Measurements were performed at 37°C, with the chamber filled with 2 ml MiRO5 buffer (0.5 mM EGTA, 3 mM $MgCl_2$ x 6 H_2O, 60 mM lactobionic acid, 20 mM taurine, 10 mM KH_2PO_4, 20 mM HEPES, 110 mM sucrose and 1 g/l of BSA (pH 7.1)) [219]. The stirrer speed was set at 750 rpm, and the instrumental background corrections and air calibration were

performed according to the manufacturer's instructions. Every 2 seconds the respiration was measured. Respiratory values were corrected for the oxygen solubility factor of MiRO5 (0.92), and the chamber was reoxygenated when O_2 concentration fell below 150 µM.

LVs were collected as described above and separated into ischemic and remote region. The tissue was immediately put in BIOPS buffer (0 mM Ca-EGTA buffer, 0.1 µM free calcium, 20 mM imidazole, 20 mM taurine, 50 mM K-MES, 0.5 mM DTT, 6.56 mM MgCl2, 5.77 mM ATP, 15 mM phosphocreatine, pH 7.1) on ice. Muscle fibre bundles were mechanically separated gently by using forceps while on ice and in BIOPS buffer. The muscle fibres were then transferred into a permeabilization solution containing 50 µg/mL saponin and incubated for 30 min on ice on a horizontal shaker. Afterwards the samples were washed twice for 10 min with MiRO5 buffer. The samples were weighed and placed into the respirometry chambers. Respiration was corrected for sample weight and expressed as (nmol O_2/ (s x mg)).

The respiratory parameters were assessed using a Substrate-Uncoupler-Inhibitor-Titration (SUIT) protocol [219]. The CI substrates malate (2 mM), the fatty acid octanoyl-carnitine (1 mM) were used to assess FAO pathway in the LEAK state (**[F]$_L$**). Afterwards, ADP (2.5 mM) was added to assess (F) oxidation mediated OXPHOS capacity (**[F]$_P$**). Convergent fatty acid- and NADH-linked (N) OXPHOS capacity was measured by subsequently adding glutamate (10 mM) (**[FN]$_P$**). Afterwards $FADH_2$-related substrate succinate (S) (20 mM) was injected to additionally assess contribution of CII-linked respiration to maximal OXPHOS capacity (**[FNS]$_P$**). Next, cytochrome C (0.01 mM) was injected as a quality control for the tissue preparation. Subsequently, oligomycin (0.005 mM), which inhibits ATP synthase, was injected to measure respiration independent of ADP phosphorylation. Respiration measured after oligomycin injection is referred as "LEAK" state, as this respiration is a compensation for the leakage of protons across the inner mitochondrial membrane (**[FNS]$_L$**). Next, maximal uncoupled respiration, driven by convergent electron input to the ETS, was assessed as next step through the precise titration (1 mM) of the protonophore carbonyl-cyanide p-(trifluoromethoxy) phenylhydrazone (FCCP) until the maximal level of respiration was achieved (**[FNS]$_E$**). FCCP dissipates the mitochondrial membrane potential (MMP) and stimulates electron flux along the respiratory system. Afterwards, rotenone (0.001 mM), an inhibitor of CI, was injected to assess CII linked ETS. Finally, Antimycin A (0.005 mM) was added, which inhibits CIII to measure residual respiration, also referred to as non-mitochondrial respiration. All respiratory values were corrected for the non-mitochondrial respiration.

Before statistical analysis, the increase in respiration in response to cytochrome c was calculated as measure of preserved integrity of the outer mitochondrial membrane. A high increase in respiration after cytochrome C injection (> 40 %) indicates a damaged

mitochondrial membrane. High resolution respirometry experiments with an increase over 40 % in response to cytochrome C injection were excluded from further analysis.

In addition to evaluation of the absolute respirometry values (pmol O2 / (s× mg)) described above, the following respiratory control ratios (RCR) were calculated. RCR $Coupling_{FNS}$ is a measure, which describes how well electron transport is coupled to ATP synthesis, which was calculated by dividing $\mathbf{[FNS]}_L$ by $\mathbf{[FNS]}_P$. RCR $Uncoupling_{FNS}$ was calculated by dividing $\mathbf{[FNS]}_L$ by $\mathbf{[FNS]}_E$, to assess efficiency of electron transport.

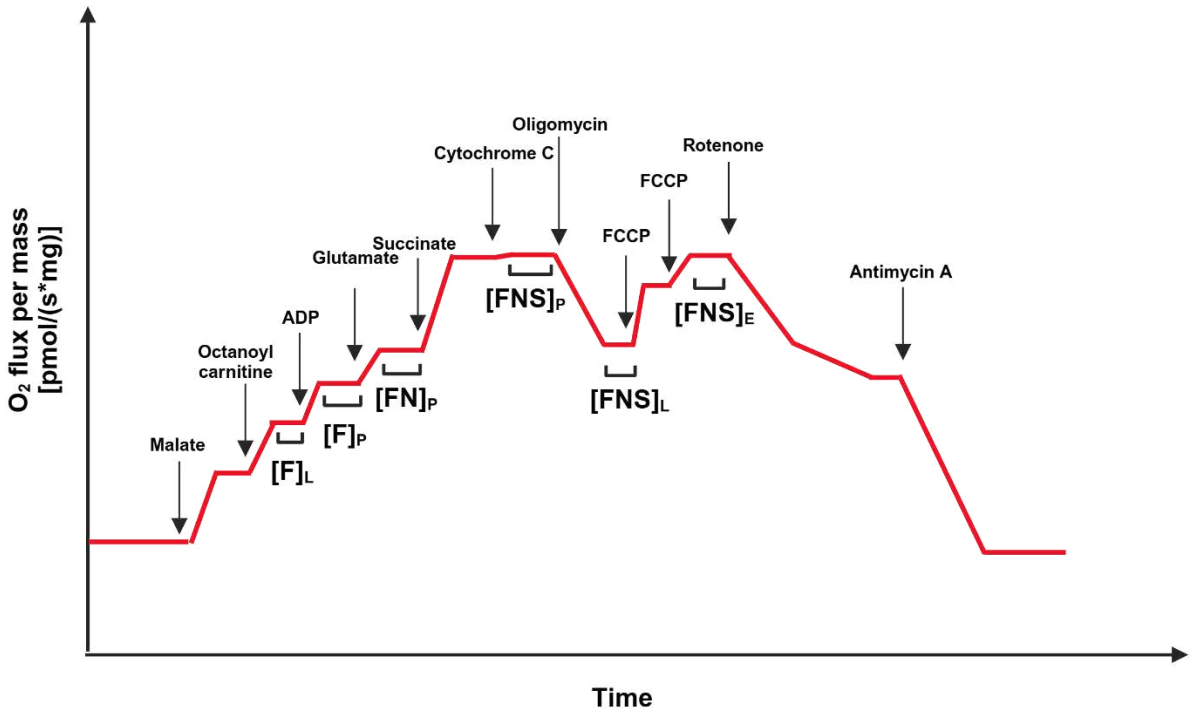

Figure 8: Representative illustration of O_2 consumption measured using high resolution respirometry using a standard SUIT protocol. Subsequent injections of SUIT reagents enable the assessment of (F) fatty acid oxidation pathway, (N) NADPH linked respiration and (S) succinate linked respiration indicated as O_2 consumption (O_2 flux per mass). E: electron transport system capacity, P: oxidative phosphorylation capacity, L: LEAK. Created in BioRender.

3.11 Protein concentration measurements

In this study, prior to different type of experiments such as biochemical assays and western blotting, protein concentration was measured using DC protein Assay kit (Bio-Rad), which is based on the BCA method. Following the manufacturers protocol, the protein concentrations of the samples were measured and calculated. Briefly, 5 µl of the samples and standards were added to a 96 well plate. A volume of 25 µl reaction solution A was added to each sample and standard. Next 200µl of DCTM Protein Reagent B was added to each well and the plate was incubated at room temperature for 10 min in the dark. The OD of the samples were then measured using Microplate Reader FLUOstar® Omega at a wavelength of 740 nm. Based on

the standard concentrations, linear regression curve was generated and protein concentration was determined based on linear regression equation.

3.12 Citrate synthase activity

Mitochondrial content is frequently analysed by determining citrate synthase (CS) activity. Mitochondrial content analysis could provide crucial information about the ETS, specifically in cardiac setting. CS is an enzyme of the TCA cycle, which catalyses the condensation of oxaloacetate and acetyl coenzyme A to citrate [220]. CS activity was measured using a commercially available kit from Sigma and used according to the company's instructions. Briefly, tissues were lysed in PBS (pH 7.4) with proteinase and phosphatase inhibitor, using RETSCH MM400 mixing mill (3x1 min, 20 Hz). Tissues were then sonicated for 10 min and centrifuged at 16000 g for 10 min at 4°C. The supernatant was collected and the pellet was discarded. Protein concentration of these samples were then measured using the DC protein Assay Kit as described before. Samples were diluted to a final concentration of 0.5 mg/ml for CS activity measurements. The following samples were prepared prior to the assay: positive control (45 µl 1x Assaybuffer + 5 µl CS aliquot), mastermix (9520 µl 1x Assaybuffer + 140 µl 30 mM Acetyl CoA + 140 µl 10 mM DTNB), oxaloacetate (OAA) (1 mg 10 mM OAA + 769 ml 1x Assaybuffer) and controlmix (368 µl 1x Assaybuffer+ 4 µl 30 mM Acetyl CoA + 4 µl 10 mM DTNB). Samples (50 µl) and positive control (2 µl) were added to a 96-well plate, after which 140 µl mastermix was added to each sample. Baseline absorbance at a wavelength of 412 nm for 3 min (1 cycle per minute) in kinetic mode was measured. Afterwards, OAA (10 µl) was added to each well and the absorbance was measured in kinetic mode for 10 min at 412 nm. Based on the slope of each linear curve CS activity was calculated.

3.13 Western Blot

To investigate ETS complex expression in anemia, western blotting was performed in LV tissues of anemic and non-anemic mice after AMI (ischemic region) [127]. Briefly, LV of anemic and non-anemic mice post-AMI were lysed with radioimmunoprecipitation assay (RIPA) buffer and homogenized with RETSCH MM400 mixing mill (3x1 min, 20 Hz), followed by a 10 min sonication. After centrifugation at 10000 g for 15 min at 4°C, the supernatant was stored. Protein concentration of the samples were measured using the DC protein assay kit, as described previously. Samples were diluted with H_2O, after which 4 µl lithium dodecyl sulfate (LDS) and 2 µl sample reducing agent (SRA) were added to each sample, with a final protein concentration of 1 µg/µl. Samples (20 µl) and Spectra™ Multicolor Broad Range Protein Ladder (5 µl) were carefully pipetted into 4-12 % bis-tris gradient gel chambers. The gel electrophoresis was performed at 80 -130 Volt (V). After running the gel, the separated proteins were transferred to a 0.2 µm nitrocellulose membrane by wet blotting at 40 V for 90 min in transfer buffer (pH 8.3, Tris Base 25 mM, Glycine 192 mM). Afterwards, the membrane was

rinsed in water and incubated for 5 min in a staining solution, which was diluted in washing buffer. Total protein staining was detected at 700 nm on the Odyssey® Fc Imaging System. The staining was removed by incubating the membrane with Revert™ Destaining Solution. To block non-specific binding sites, the membrane was blocked with blocking agent for 60 min at room temperature. The membrane was then washed three times with TBS-T for 10 minutes on a shaker at 4°C, followed by overnight incubation with the primary antibody for ETS complexes detection (Total OXPHOS Rodent WB Antibody Cocktail, ab110413). The next day, the membrane was washed three times for 15 min with TBS-T on a shaker. The membrane was then incubated with the corresponding secondary antibody (IRDye® 680RD Goat anti-Rabbit IgG Secondary Antibody, IRDye® 800CW Goat anti-Mouse IgG Secondary Antibody, LICOR) for 60 min at room temperature and light-protected on a shaker. Lastly, the target proteins were detected with the Odyssey® Fc Imaging System.

3.14 Reactive oxygen species: Biochemical Assays

3.14.1 SOD Colorimetric Activity Kit

This biochemical assay principle is based on the generation of superoxide by xanthine oxidase after substrate supplementation. The substrate reacts with xanthine oxidase resulting in the development of yellow colour which is calorimetrically measured. The higher the SOD concentration in the sample, the lower the xanthine oxidase product, which results in lowered colour intensity.

Ischemic and remote LV tissues of anemic and non-anemic mice 24 h post-AMI as well as LV tissues of non-anemic and anemic mice without AMI were lysed with ice cold PBS buffer using the RETSCHMM40 mixing mill. After 10 min sonication and centrifugation at 1500 g for 10 min at 4°C, the supernatant was collected. SOD colorimetric assay was performed following the company's instructions (ThermoFisher scientific, EIASODC). Shortly, the samples were diluted 1:4 in assay buffer. For the preparation of the standards, the SOD standard was reconstituted with assay buffer (250 µl). Afterwards, a serial dilution was prepared according to the company's protocol. Prior to the measurement, xanthine oxidase and the substrate was prepared. Next, standards and samples (50 µg in well) were pipetted in a 96-well plate, in which the xanthine oxidase and substrate was added subsequently. The plate was then incubated for 20 min at room temperature. Next, using the microplate reader OMEGA the absorbance of the samples at 450 nm wavelength was measured. Linear regression fit was performed and based on that, SOD concentration in samples were calculated.

3.14.2 Catalase Colorimetric Activity Kit

Catalase biochemical assay principle is based on the ROS scavenging property of catalase, which converts H_2O_2 to oxygen and water. Horseradishperoxidase (HRP) reacts with the

substrate when H_2O_2 is present, turning the colourless substrate into pink-coloured product. Catalase concentration is proportional to less intense coloured samples.

LV tissues from non-anemic and anemic mice with (ischemic and remote region) and without AMI were homogenized using RETSCH MM40 mixingmill in 1x Assaybuffer, followed by a 10 min sonication and a centrifugation step at 10000 g for 15 min at 4°C. The supernatant was further used for the catalase colorimetric assay. The assay was conducted according to the company's instructions (ThermoFisher scientific, EIACATC). Samples were diluted using 1x Assaybuffer to a final concentration of 2 µg/µl. Standard serial dilution was prepared by adding 10 µl catalase standard to 190µl 1x Assaybuffer (5 U/ml). Standards were prepared according to the protocol. HRP solution was prepared by mixing 50x HRP (50 µl) concentrate with 1x Assaybuffer (2.45 ml). Afterwards, samples and standards (25 µl) were added to a 96-well plate. Hydrogen peroxide reagent (25 µl) was added to each sample and standard well, followed by an incubation for 30 min at room temperature. Next, substrate (25 µl) and 1x HRP (25 µl) solution were added to each well successively. After a 15 min incubation time, the absorbance at a wavelength of 560 nm was measured. Finally, linear regression-based curve fitting was used to calculate catalase concentration in the sample.

3.14.3 Glutathione Colorimetric Detection Kit

Glutathione biochemical assay principle is based on the reaction of the free thiol group of glutathione and the substrate. This reaction results in a colour change.

Tissues from the same experimental groups as mentioned before were used for this assay and were lysed as described before. Protein concentration of the samples were measured as mentioned before. After adding 1 volume of 5% 5-sulfo-salicylic acid dehydrate (SSA), the samples were thoroughly mixed and centrifuged at 14000 g for 10 min at 4°C. The supernatant was collected and used for the further analysis. By adding 1.5 volumes of 1x Assay buffer the samples were diluted, reducing the SSA concentration to 1%. Further dilution using sample diluent was performed, generating samples with a final protein concentration of 1 µg/µl. The glutathione colorimetric detection assay was performed according to the manufacturers protocol (ThermoFisher scientific, EIAGSHC). A standard serial dilution was prepared according to the company's protocol. Afterwards, colorimetric detection reagent and reaction mixture were prepared. Next, samples (50 µl) were added to a 96-well plate, in which colorimetric detection reagent (25 µl) was added. After adding reaction mixture (25 µl) to the wells, the plate was carefully mixed by tapping the sides. Once the plate was incubated for 20 min, the absorbance at 405 nm was read. A linear regression curve was generated from the standards, and the sample concentrations were calculated.

3.14.4 Myeloperoxidase

Myeloperoxidase (MPO) activity kit is based on the reaction between hypochlorus acid (HOCl) and taurine, forming taurine chloramine, which in turn reacts with the chromophore TNB. This reaction results in the generation of the colourless DTNB.

LV tissues from anemic and non-anemic mice with AMI (ischemic and remote region) and without AMI were lysed using MPO Assay Buffer. Homogenization was performed with RETSCH MM40 mixingmill, followed by a 10 min sonication. The samples were afterwards centrifuged at 13000 g for 10 min at 4°C. The supernatant was collected and used for further analysis. All samples were diluted to a concentration of 1 µg/µl. The assay was performed according to the company's instructions (Sigma Aldrich, MAK068). First, samples (50 µl) were added to a 96-well plate. A mastermix with 20% MPO substrate was prepared. Afterwards, the mastermix was added to each sample well and the plate was incubated for 60 min protected from light. Stop mix (2 µl) was added to each sample well and incubated for 10 min. Next, TNB Reagent/Standard (50 µl) was added to each sample well, and different volumes of the same reagent were pipetted into Assay Buffer containing standard wells. Finally, the absorbance at 412 nm was read and MPO activity was calculated with linear regression fit.

3.14.5 ROS detection using westernblot

To investigate ROS production in anemia, 4-Hydroxynonenal (4-HNE) western blotting was performed in LV tissues of anemic and non-anemic mice after AMI (ischemic region). 4-HNE is a product of lipid peroxidation, which is known to be used to quantify ROS. The westernblotting was performed as described before (3.133.13) using primary antibody against 4-HNE (ab46545).

3.15 RBC transfer experiments

In this study we further aimed to evaluate the potential role of anemic RBCs on the mitochondrial respiration of LVs. For this purpose, RBCs from anemic and non-anemic CAD patients were isolated by centrifuging the whole blood at 800 g for 10 min at 4°C. Subsequently, plasma and buffy coat were removed and RBC pellet was washed four times with 2 ml PBS at 800 g for 10 min at 4°C. Afterwards, hearts from wildtype mice were incubated for 40 min with the isolated RBCs in the Langendorff apparatus [221]. After global ischemia (40 min) and reperfusion (60 min), the hearts were collected and the respiration was measured using high resolution respirometry.

The isolated perfused heart is an *ex vivo* method to examine LV function. This method was used in order to characterize the effect of anemic patient's RBCs on LV energy metabolism post ischemia. C57BL/6J mice were anesthetized with i.p. injection of ketamin and xylazin (volume according to body weight). After injecting heparin i.p. (1000 IU/mouse; Rotexmedica,

Trittau, Germany), hearts were carefully isolated and placed in cold KHB buffer. The hearts were then prepared by excising the excess fat. A part of the ascending aortae was left to cannulate the heart into the Langendorff apparatus. After mounting the hearts into the Langendorff apparatus the hearts were perfused retrogradely at a constant pressure of 100 mmHg with modified gassed (5% CO_2 in O_2) Krebs-Heinseleit buffer (KHB) containing 118 mM NaCl, 4.7 mM KCl, 0.8 mM $MgSO_4$, 25mM $NaHCO_3$, 1.2 mM KH_2PO_4, 5 mM glucose, 110 mM Napyruvate, and 2.5 mM $CaCl_2$ at 37°C. To monitor the isometric LV developed pressure, its positive and negative first derivate and the LV end-diastolic pressure a water filled balloon, connected to a pressure transducer, was inserted into the LV. An ultrasound flow probe, positioned upstream the cannulated heart, allowed the recording of the coronary flow. Through adjusting the water volume inside the balloon, the LVDEP was set between 5 to 15 mm Hg. A pacer was used to set a constant heart rate of 600 bpm, according to the physiological murine heart rate. The hearts were the perfused for 20 min during the preliminary phase. Afterwards a 20 seconds global ischemia was induced by restricting the perfusion. During a 5 min reperfusion period a few criteria were examined. Hearts were excluded from the analysis when they did not fulfill following criteria: (1) coronary flow >4 mL/min, (2) LV developed pressure <50 mm Hg, or (3) a coronary flow reserve revealed by a transient ischemia <70% of the baseline flow. Global ischemia was induced by restricting the perfusion for 40 min. During the first minute of ischemia isolated anemic and non-anemic CAD patient's RBCs (40% Hct) were loaded onto the cannulated heart via a side arm using a syringe driver set to 0,4 mL/min. After ischemia the cannulated heart was reperfused for 1 h. The heart was then further processed as following in order to assess respirometry function parameters. The hearts were kept in BIOPS buffer and processed as described before (3.10).

3.16 Hemodynamics assessment using a Millar catheter

In order to assess hemodynamic parameters, Millar catheter experiments were conducted in anemic and non-anemic RBC eNOS deficient mice and their respective control mice. Prior to the measurement, mice were given Temgesic (0.05mg/kg) subcutaneously 30 min before intubation. After anesthetizing the mice with 3.5% isoflurane, mice were ventilated at 140 times/min of respiratory rate. For the preparation, isoflurane was decreased to 2% after successful anesthesia. Before preparing the catheter, the catheter was calibrated using the IOX software v.2.10.0 (EMKA technologies, Paris, France). For the preparation of the catheter skin at the centre of the neck was removed carefully. After removing the muscles up to the trachea, the carotid artery was separated from the vagus nerve. 5/0 sutures were placed underneath the carotid artery and tied to an irreversible knot, which was followed by the clamping of the artery. A hole was cut in the artery, in which a 1.4 F Millar pressure-conductance catheter (SPR-839, Millar Instruments, Houston, TX, USA) was placed. The clamp was removed and the measurement was performed with the IOX program. Different

parameters such as systolic blood pressure (SBP), diastolic blood pressure (DBP), heart rate (HR), left ventricle developed pressure (DP), maximal rate of rise of left ventricular pressure (dP/dt_{max}), minimum rate of left ventricular pressure drop (dP/dt_{min}) and mean arterial pressure were assessed. The recorded pressure values were analysed using IOX software. Systemic vascular resistance (SVR) will be calculated according to the following formula: SVR ≅ MAP (mean arterial pressure) / CO (cardiac output). To evaluate left ventricular end-diastolic developed pressure (LVEDP), developed pressure (DP), maximum rate of pressure increase (dP/dt_{max}) and maximum rate of pressure decrease (dP/dt_{min}), the Millar catheter was advanced into the left ventricle (LV) of the heart.

3.17 Flow-mediated dilation assessment

FMD responses in anemic and non-anemic RBC-eNOS-KO and control mice were assessed using the Vevo 2100 high-resolution ultrasound scanner using a 30–70 MHz linear transducer (Visual Sonics Inc., Toronto, Canada) [222]. Briefly, mice were anesthetized with isoflurane (5% induction, 2% maintenance). Mice were then placed on a heated examination table, which enabled the maintenance of the body temperature and furthermore enabled the monitoring of the heart function with ECG electrodes. Using a chemical hair remover, the fur on the hindlimb was shaved and covered in pre-warmed ultrasound gel. The transducer was placed using a stereotactic holder and adjusted manually to visualise the femoral artery. A vascular occluder (8 mm diameter, Harvard Apparatus, Boston, MA, USA) was placed around the lower limb. Baseline images of the vessel were firstly recorded, for which the cuff was inflated to 200 mmHg, and pressure was kept constant for 5 min (Druckkalibriergerät KAL 84, Halstrup Walcher, Kirchzarten, Germany); then the cuff was released to assess FMD. The upstream diameter of the vessel was determined every 30 s both during inflation and deflation of the cuff. Changes in vessel diameter were quantified as the percentage of baseline (%) = [diameter (max)/diameter (baseline)] × 100.

3.18 Wire Myography

To assess the effect of anemia on eNOS deficiency in RBCs on the vascular tone, wire myograph experiments were conducted. For this purpose, thoracic aortas from euthanized anemic and non-anemic RBC-eNOS-KO and their respective control mice were dissected free from perivascular adipose tissue. The aortas were cut in 2 mm size aortic rings and mounted in a wire-myograph system (Danish Myotechnology, Aarhus, Denmark), containing KHB (118 mM NaCl, 4.7 mM KCl, 0.8 mM MgSO4, 25 mM NaHCO3, 1.2 mM KH2PO4, 5 mM glucose, 110 mM Sodium pyruvate, and 2.5 mM CaCl2). Aortic rings were gradually distended to 1 gr force or 9.8 mN, which is equal to a physiological wall tension of 100 mmHg. For a time period of 45 min the aortic segments were allowed to normalize. Every 15 min during this time, buffer was aspirated, fresh buffer was added and the segments were adjusted to 9.8 mN force. Prior

to the experiment, endothelial integrity was checked by assessing relaxation responses to acetylcholine (ACH) (10 µM) in phenylephrine (PHE) (10 µM) pre-contracted arteries. The aortic segments were pre-contracted and segments which showed less than 80 % relaxation responses were excluded. Afterwards, aortic segments were incubated with indomethacin (10 µM), which inhibits cyclooxygenase enzymes enabling the NO-dependent relaxation measurements. Initially, contraction was induced by adding increasing concentrations of PHE (0.001-10 µM) successively to the aortic segments. Following PHE concentration-response-curve (CRC), ACH CRC was generated by adding increasing concentration of ACH (1 nM-10 µM) consecutively, which displays the relaxation responses. The same protocol for PHE and ACH CRC was conducted, after incubating the aortic segments with indomethacin and L-NG-nitro arginine methyl ester (L-NAME), a NOS inhibitor. After generating ACH CRC, increasing concentrations of NO donor sodium nitroprusside (SNP) (10 nM-10 µM) was added to the segments, measuring the relaxing effects of SNP.

3.19 Triphenyl tetrazolium chloride (TTC) staining

Anemic and non-anemic RBC-eNOS-KO and control mice 24 h post-AMI were anesthetized by i.p. injection of 100 mg/kg ketamine (Ketanest®) and 10 mg/kg xylazine (Rompun®) and anticoagulated with heparin (1000 IU i.p.). Mice were sacrificed with heart puncture and hearts were then rapidly transferred to isotonic 0.9 % saline solution (Fresenius Kabi, Bad Homburg, Germany) supplemented with 1 ml heparin (5000 IU) (B. Braun). Fat and otiose tissue was removed and a short part of the ascendant aorta was left to cannulate the heart. Afterwards, the heart was cannulated and rinsed through the short part of the ascendant aorta with 0.9% saline solution. After the blood was removed from the heart, the remaining thread from the I/R surgery was removed and replaced with a 7-0 silk thread (Eticon). Evans blue dye (1 mL of a 1% solution) was injected into the aorta and coronary arteries for visualization of the ischemic area at risk (AAR) from the non-ischemic zone. The heart was rinsed with 0.9% saline, until remaining dye was removed. The tissue was afterwards wrapped in a plastic wrap and stored for 1 h at −20°C, followed by serial sectioning (1mm) along the long axis. The sections were weighed and incubated in 1% 2,3,5-triphenyltetrazolium chloride (TTC) solution for 5-7 min at 37°C, during which viable cells convert TTC into a red dye. This enabled the distinction of viable and non-viable myocardium within the risk zone. Pictures of each slices were taken using camera attached to a microscope (Leica DM6B). Infarct area (INF, white), viable areas affected (red) or unaffected (blue) by I/R surgery and area at risk (AAR, white + red) were measured, based on the slice weight, with a computer assisted planimetry software (Diskus Viewer, Technisches Büro Hilgers, Königswinter, Germany).

3.20 Data analysis and statistics

Statistical analyses for the proteomics data were conducted using R (© The R Foundation) programming environment. High resolution respirometry data was analysed using DatLab8 Software (© 2025 Oroboros Instruments GmbH). GraphpadPrism 6.01 program was used to analyse data. Two groups are compared using student t-Test. Multiple groups/conditions will be compared using one-way ANOVA or 2-way ANOVA. A p-value of <0.05 was considered statistically significant. Additional significance levels were stated as $*p \leq 0.05$, $**p \leq 0.01$, $***p \leq 0.001$, and $****p \leq 0.0001$. P-values exceeding 0.100 were not considered in this study and were excluded from the graphs.

4 Results

This study primarily aimed to investigate the effect of anemia on LV function after AMI, with a focus on energy metabolism. Additionally, given the cardioprotective role of functional eNOS in RBCs after AMI, this study assessed the impact of RBC-derived eNOS on vascular and cardiac function in anemia, with and without AMI

4.1 Blood loss anemia is associated with LV energy imbalance after AMI

We first aimed to assess the effect of anemia after AMI on LV energy metabolism and resulting dysfunction. For this purpose, we assessed the LV function, LV energetics, LV proteomics, LV respirometry analyses, LV redox state and LV respiration and compared the data between anemic and non-anemic mice before and/or after AMI. In the following paragraph the results of this part will be presented.

4.1.1 Cardiac function in anemia before and after AMI using echocardiography

Anemia is known to compensatory increase cardiac function evidenced by increased SV and cardiac stress [223]. In MI, anemia causes a worsened prognosis [207], however cardiac energy metabolism in anemia after AMI and its effect on heart function has not been studied yet. Heart function was assessed using echocardiography before and 24 h post-AMI. The measurements revealed no significant differences in HR or EDV between anemic and non-anemic mice before and after AMI induction (Figure 9 A, C). The ESV representing the ventricular volume at the end of systole, was significantly increased in anemic mice before and after AMI compared to their respective control groups (Figure 9 B). Prior to AMI induction, EF was significantly elevated in anemic mice compared to their controls, whereas following AMI EF was diminished in anemic mice compared to non-anemic mice after AMI (Figure 9 D). Additionally, EF was significantly reduced both in anemic and non-anemic mice after AMI compared to their controls without AMI (Figure 9 D). SV was significantly increased in anemic mice compared to control mice (Figure 9 E). After AMI, SV was significantly decreased in anemic and non-anemic mice compared to the respective control group of mice without AMI (Figure 9 E). The CO, which is the amount of blood pumped per minute, was significantly higher in anemic mice compared to their control mice (Figure 9 F). After AMI, CO was significantly reduced in both anemic and non-anemic groups compared their respective group of mice without AMI (Figure 9 F). Nevertheless, no significant differences in CO were observed between anemic and non-anemic mice after AMI (Figure 9 F). These findings suggest that anemia induces a compensatory increase in LV function, which is subsequently impaired following AMI.

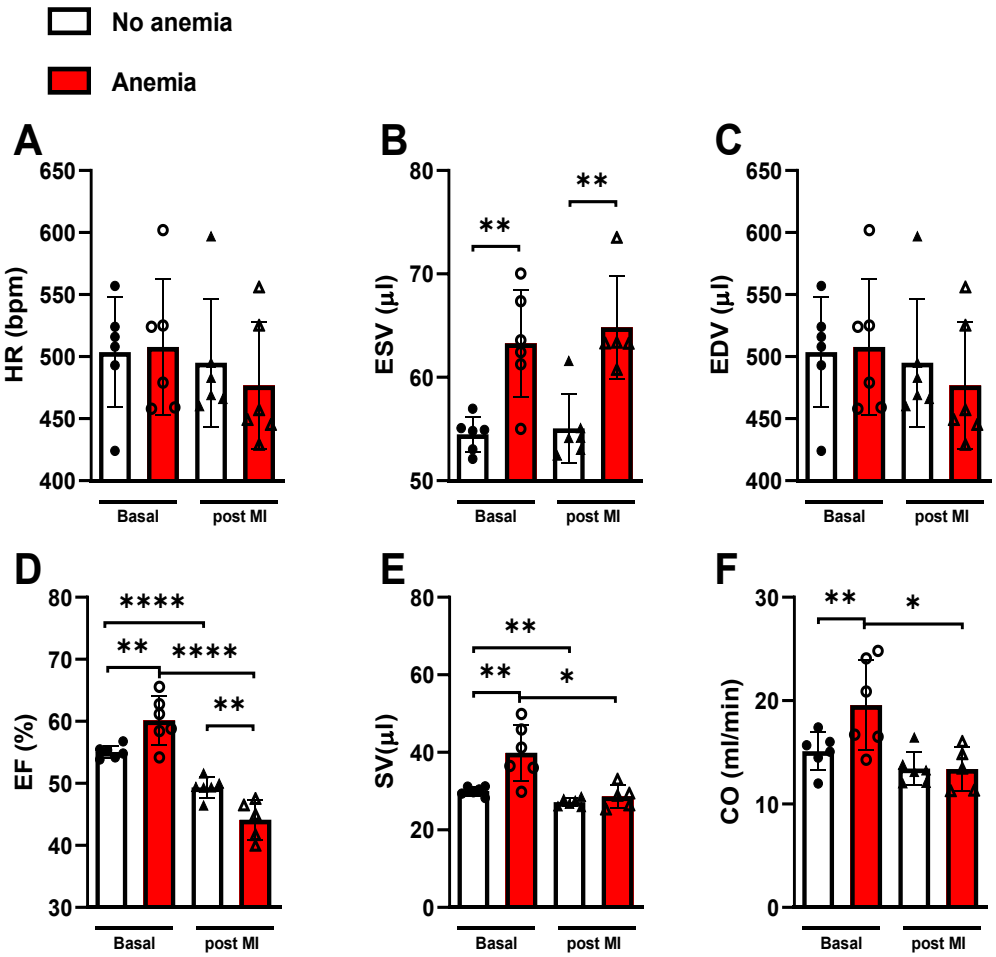

Figure 9: Altered cardiac function in anemic mice after AMI. Cardiac function was assessed using echocardiography in anemic (red bars) and non-anemic mice (white bars) before (circles) and 24 h post-AMI induction (triangles). Following cardiac parameters were assessed: A) Heartrate (HR), B) End-systolic volume (ESV), C) End-diastolic volume (EDV), D) Ejection fraction (EF), E) Stroke volume (SV), and F) Cardiac output (CO). Values are shown as the means ± SEM. *p≤0.05, **p ≤ 0.01, ****p≤0.0001. Student t-test was used to compare between two groups.

4.1.2 Altered cardiac energetics and fractional shortening in anemia after AMI

Mitochondrial respiration and ATP accessibility are critical for CM energy supply and overall heart function. To evaluate ATP availability and usage, CMRI measurements *in vivo* were performed in anemic and non-anemic mice, before, after induction of anemia and 24 h post-AMI. The Pi/ATP ratio, an indicator for ATP hydrolysis, remained unchanged in mice after anemia induction compared to non-anemic mice (Figure 10 A, C). Similar results were observed in the remote region of anemic mice compared to non-anemic mice 24 h post-AMI (Figure 10 C). Interestingly, Pi/ATP ratio was significantly increased in the ischemic region of anemic mice compared to non-anemic mice 24 h post-AMI (Figure 10 A). The resynthesis of ATP, assessed via the PCr/ATP ratio, remained unchanged in anemic mice compared to non-anemic mice (Figure 10 B, D). Similarly, PCr/ATP ratio was not significantly differed between anemic mice compared to non-anemic mice in the remote region 24 h post-AMI (Figure 10 D).

In the ischemic region of anemic mice 24 h post-AMI, the PCr/ATP ratio was significantly reduced compared to non-anemic mice 24 h post-AMI (Figure 10 B). In conclusion, these results show decreased regional ATP availability in the ischemic region of anemic mice after AMI compared to their non-anemic controls.

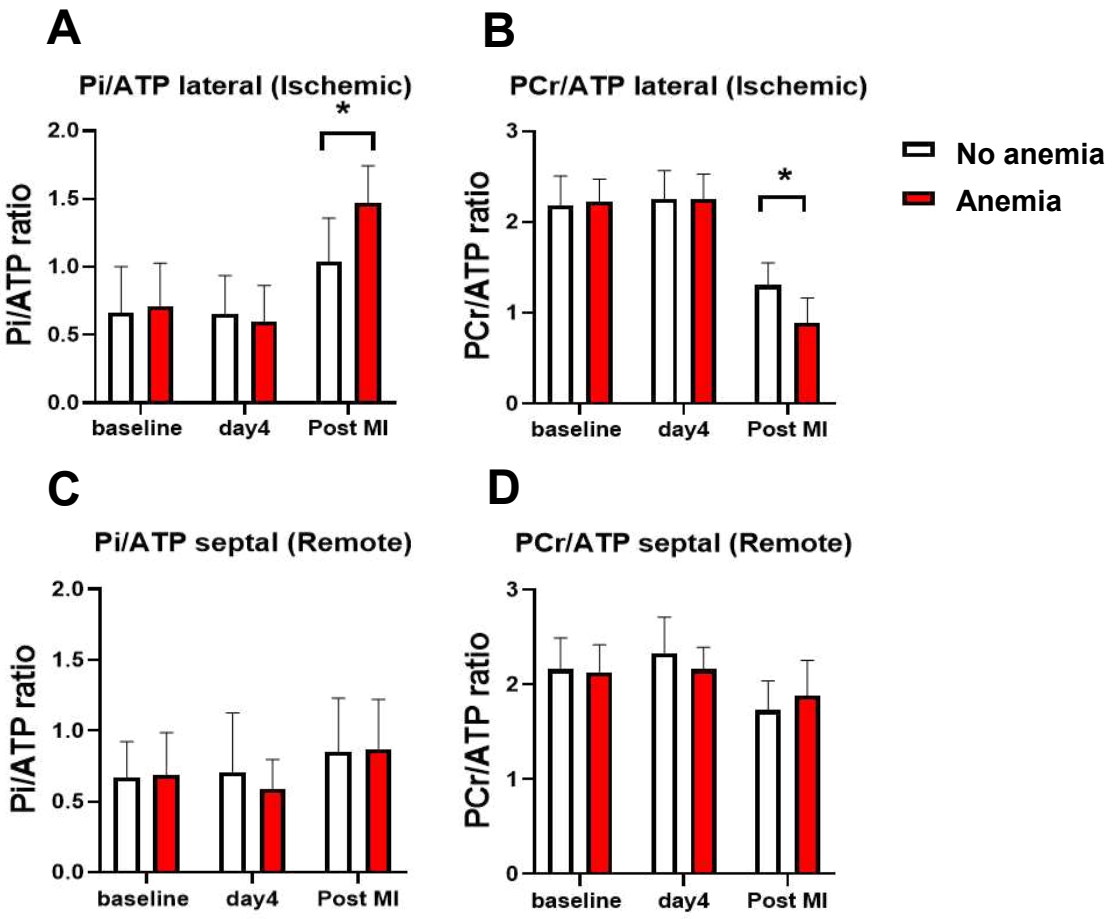

Figure 10: Altered cardiac energetics in anemic mice after AMI. Pi/ATP and PCr/ATP ratios were averaged at lateral (ischemic, A & B) and septal (remote, C & D) region of heart in anemic (red bar) and non-anemic (white bar) mice at basal, three days after anemia and 24 h post-AMI. Values are shown as means (SD). *, p≤0.05. One-Way ANOVA and Bonferroni's post-hoc test was used compare groups.

In addition to cardiac energetics parameters, CMRI measurements enabled the assessment of fractional shortening in the LVs of anemic and non-anemic mice at baseline, after anemia induction and 24 h post-AMI. Regional CMRI measurements revealed that fractional shortening, a parameter displaying the size reduction of the LV during systole, remained unchanged at basal level and after anemia induction at day four (Figure 11 A, B). In the remote region, no significant differences were observed between anemic and non-anemic mice (Figure 11 C). Interestingly, a significant reduction in fractional shortening was observed in the ischemic region of anemic mice after AMI compared to the corresponding region in non-anemic mice (Figure 11 C). These findings indicate that LV contractile function is significantly impaired in the ischemic region of anemic mice following AMI.

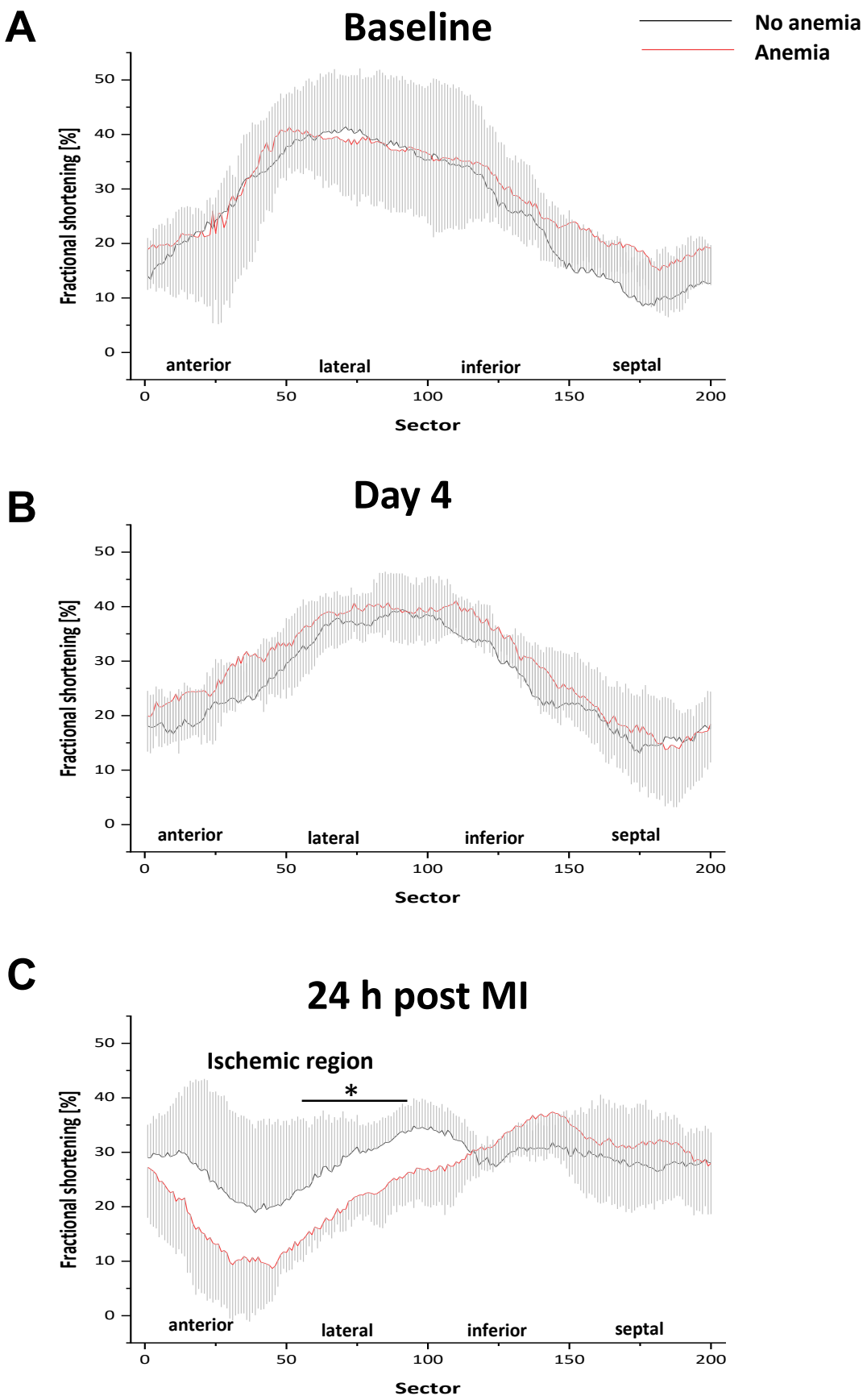

Figure 11: Reduced fractional shortening in anemic mice after AMI. Regional CMRI analyses of cine loops acquired at baseline (A), three days after anemia induction (B) and 24 h post-AMI (C). For statistics of FS, anterior (1–42), lateral (43–100), posterior (101–136), and septal (137–200) sectors were averaged. Data are means ± SD; n = 10 each group *, p≤0.05.

4.1.3 Proteomic analysis

4.1.3.1 Altered OXPHOS and oxidative stress related protein expression in the ischemic region of anemic mice after AMI

CMRI results demonstrated unchanged cardiac energetics in anemic mice without AMI and in the remote region 24 h post-AMI. However, impaired cardiac function in the ischemic region of anemic mice 24 h post-AMI was observed. To investigate the underlying molecular mechanisms, proteomic analysis was conducted to identify alterations in protein expression associated with the observed phenotype. The analysis revealed significant differential regulation of multiple proteins in the ischemic region of anemic mice 24 h post-AMI, as visualized in a volcano plot (Figure 12 A). These differentially regulated proteins were further categorized and presented as a heatmap (Figure 12 B). Compared to the number of mitochondrial proteins altered in the ischemic region, less mitochondrial proteins were differentially expressed in the remote region (Figure 12 B). This suggests that pathways related to energy metabolism and mitochondrial respiration are less affected in the remote myocardium of anemic mice following AMI. Pathway enrichment analysis was subsequently performed on the differentially regulated proteins in both the ischemic and remote regions of anemic mice compared to their non-anemic controls. The results indicated that the top 10 altered pathways in the ischemic region were primarily related to energy metabolism, whereas they remained unchanged in the remote region (Figure 12 C). Interestingly, the proteomic analysis showed increased abundancy of respiratory chain complex subunits for CI and CIII namely NADH ubiquinone oxidoreductase subunit B6 (p=0.02; p-values are calculated based on proteome information) (Ndufb6), NADH ubiquinone oxidoreductase core subunit S7 (p=0.03) (Ndufs7) and ubiquinol-cytochrome c reductase complex (p=0.01) (Uqcr10) in the ischemic region of anemic mice 24 h post-AMI, indicating a potential change in mitochondrial function. Furthermore, succinate dehydrogenase complex assembly factor 2 (p=0.03) (Sdhaf2), a CII assembly factor, was also significantly elevated. Further analysis identified an increase in proteins involved in NAD biosynthesis, a crucial cofactor in the ETS, namely nicotinamide nucleotide adenylyltransferase 3 (p=0.03) (Nmnat3) and kynurenine aminotransferase 3 (p=0.01) (Kyat3) in the ischemic region of anemic mice 24 h post-AMI. Apart from mitochondrial proteins, proteins related to oxidative stress regulation were also differentially expressed. Glutathione peroxidase-1 (Gpx1), a ROS scavenging enzyme, was significantly lower expressed in the ischemic region of anemic mice 24 h post-AMI (p=0.02), hinting at impaired antioxidant capacity in anemia after AMI. Conversely, thioredoxin reductase 2 (p=0.02) (Txnrd2) was significantly increased in the ischemic region of anemic mice after AMI, indicating enhanced antioxidant capacity. In conclusion, these findings highlight significant protein dysregulation in the ischemic region of anemic mice following AMI,

particularly in pathways related to energy metabolism, mitochondrial respiration, and oxidative stress.

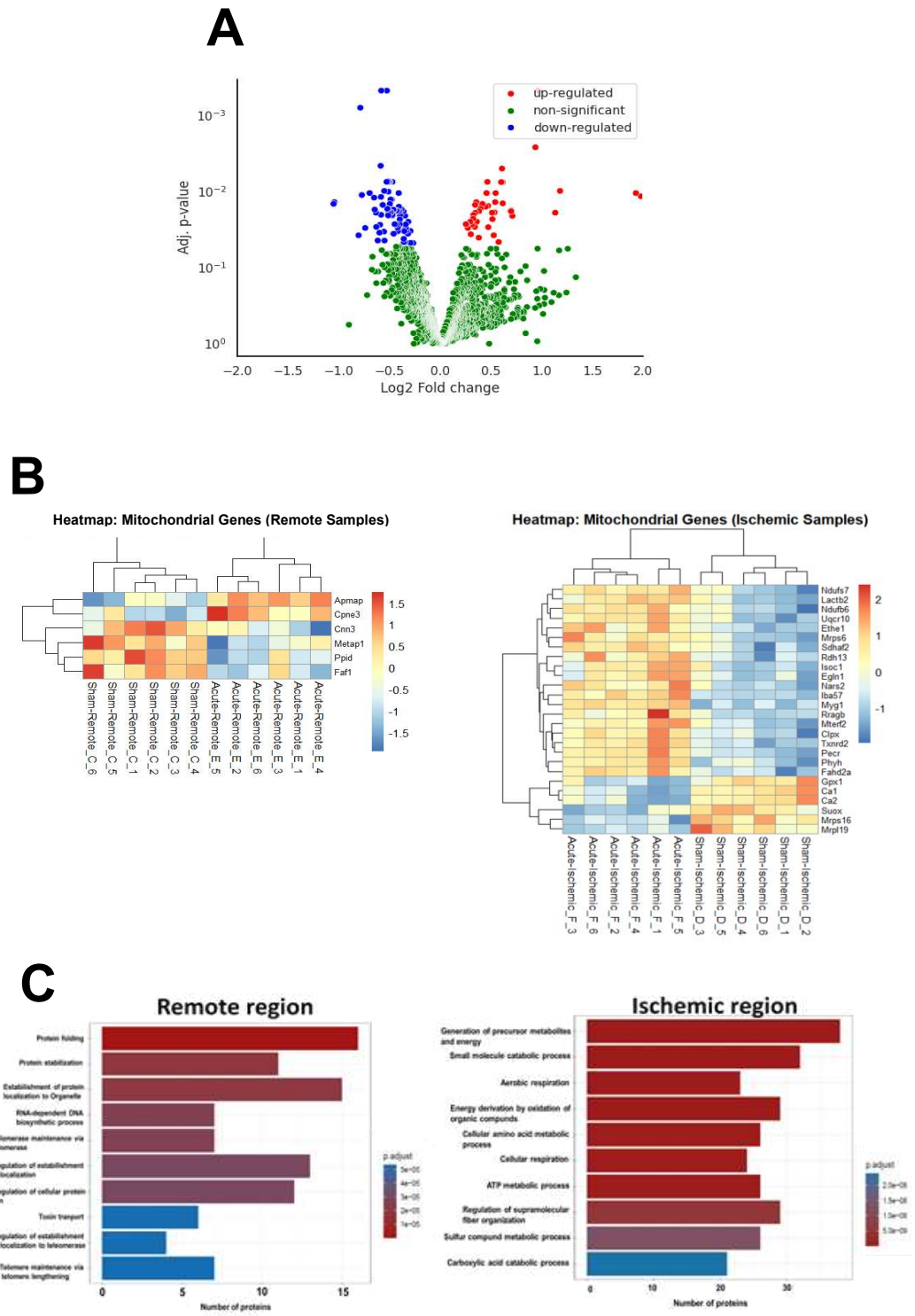

Figure 12: Proteomics analysis of LVs isolated from anemic and non-anemic mice 24 h post-AMI, with focus on significantly altered proteins. (A) Volcano plot of altered proteins depicting the log2 fold change and corresponding -log10 adjusted p-value (fold change <1) in ischemic LVs of anemic and non-anemic mice 24 h post-AMI. (B) Heatmaps depicting the proteomic profile of significantly changed mitochondrial proteins in the remote and ischemic LVs of anemic and non-anemic mice 24 h post-AMI. (C) Proteomics analysis of top biological processes altered in remote and ischemic regions of non-anemic and anemic mice 24 h post-AMI and at basal without AMI in anemic and non-anemic. n=6 per group.

4.1.3.2 Altered mitochondrial dynamics in anemic mice with and without AMI

We used our unbiased proteomic analysis to identify the differentially regulated proteins that are associated with changes in mitochondrial dynamics in anemic and non-anemic mice with and without AMI. We focussed on mitophagy related proteins Bcl-2 interacting protein 3 (BNip3), Prohibitn-2 (Phb2), Mitochondrial E3 ubiquitin protein ligase 1 (Mul1), Optineurin (Optn), Nipsnap Homolog 2 (Nipsnap2), Parkinson disease protein 7 (Park7), BCL2-like 13 (Bcl2l13) and FKBP prolyl isomerase 8 (FKBP8). When comparing non-anemic mice with anemic mice without AMI, significantly increased Nipsnap2 ($p=0.05$) and Park7 ($p=0.05$) expression was observed in anemic mice (Figure 13 E, F). Furthermore, a tendency towards decreased Mul1 abundancy ($p=0.08$) was observed (Figure 13 C). After AMI induction, no significant changes were observed in the remote region of anemic and non-anemic mice after AMI. However, BNip3 was significantly decreased in the ischemic region of anemic mice compared to their non-anemic controls ($p=0.003$) (Figure 13 A). These findings suggest that mitophagy regulation might be altered in anemic mice both before and after AMI, potentially impacting mitochondrial dynamics and function.

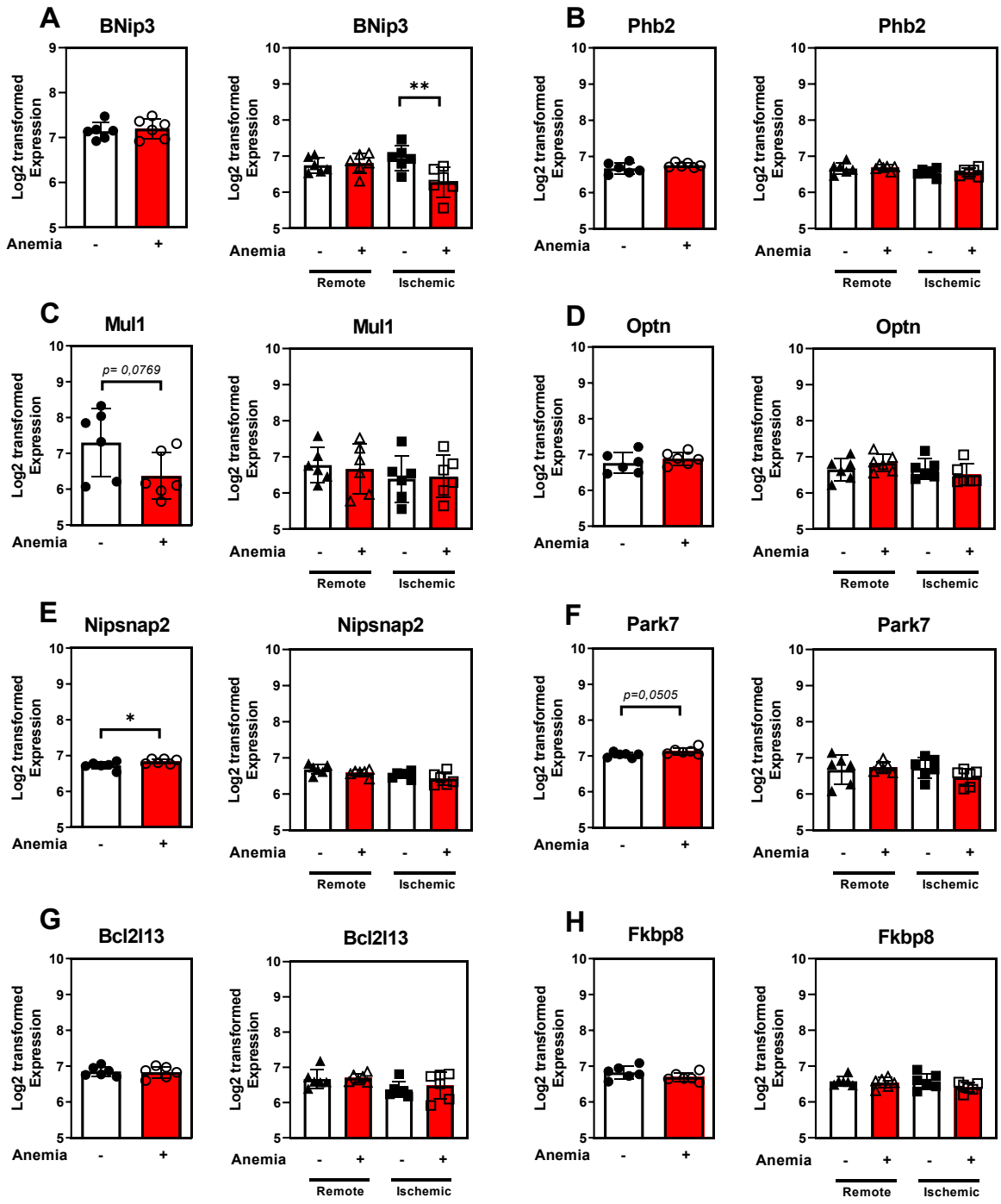

Figure 13: Altered protein expression of mitophagy related proteins in LVs isolated from anemic and non-anemic mice at basal and 24 h post-AMI in remote and ischemic region. Proteomic analysis of proteins associated with mitophagy, namely BNip3 (A), Phb2 (B), Mul1 (C), Optn (D), Nipsnap2 (E), Park7 (F), Bcl2l13 (G) and Fkbp8 (H) in LVs of non-anemic (white bars) and anemic mice (red bars) with and without AMI in remote (triangles) and ischemic (squares) region. Values are shown as the means ± SEM (n=6 per group). *p≤0.05, ** p≤0.01. Student t-test was used to compare between two groups.

To investigate the alterations in mitochondrial fusion related proteins in anemic and non-anemic mice with and without AMI, the expression levels of mitofusin 1 and 2 (Mfn1, Mfn2), OPA1, mitochondrial carrier 2 (Mtch2) and ARF like GTPase 2 (Arl2) were assessed. A significant increase in Arl2 was observed in anemic mice without AMI compared to their non-anemic controls (Figure 14 E), while the other mitochondrial fusion proteins showed no significant differences between anemic and non-anemic mice (Figure 14 A-D). Following AMI induction, neither in the remote nor in the ischemic region of anemic and non-anemic mice significant changes were observed in mitochondrial fusion related proteins (Figure 14 A-E). These observations indicate potentially altered mitochondrial fusion in anemic state, however no differences between anemic and non-anemic mice after AMI induction were observed.

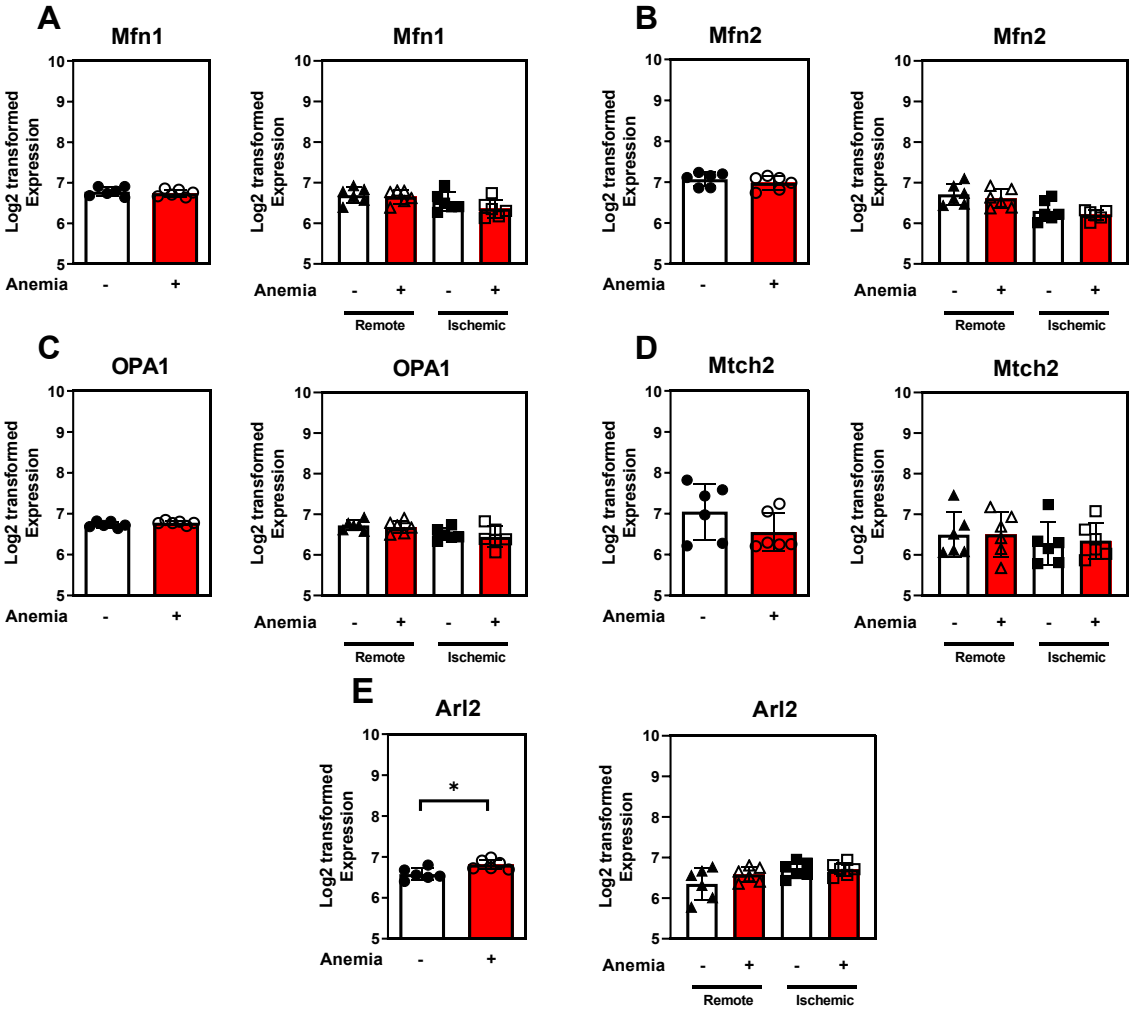

Figure 14: Altered protein expression of mitochondrial fusion related proteins in LVs isolated from anemic and non-anemic mice at basal and unchanged protein expression of mitochondrial fusion related proteins in LVs of anemic and non-anemic mice 24 h post-AMI. Proteomic analysis of proteins associated with mitochondrial fusion, namely Mfn1 (A), Mfn2 (B), OPA1 (C), Mtch2 (D) and Arl2 (E) in LVs of non-anemic (white bars) and anemic mice (red bars) with and without AMI in remote (triangles) and ischemic (squares) region. Values are shown as the means ± SEM (n=6 per group). *p≤0.05. Student t-test was used to compare between two groups.

Additionally, mitochondrial fission was assessed in anemic and non-anemic mice with and without AMI by analysing fission- related proteins, namely mitochondrial 1 (Fis1), OPA3, Dynamin related protein 1 (Drp1), mitochondrial fission process 1 (Mtfn1), solute carrier family 25 member 46 (Slc25a46) and armadillo repeat containing 10 (Armc10). Elevated levels of Drp1 (p=0.02) and Mtfp1 (p=0.03) were observed in anemic mice without AMI compared to non-anemic mice (Figure 15 C, D), whereas no significant differences were observed in Fis1, OPA3, Slc25a46 and Armc10 expression in both groups (Figure 15 A, B, E, F). Following AMI, no significant differences were observed in the remote region of anemic and non-anemic mice (Figure 15 A-F). However, after AMI induction a trend towards increased OPA3 expression in the ischemic region of anemic mice was observed compared to their non-anemic controls (p=0.07) (Figure 15 B). Armc10 expression was significantly reduced in the ischemic region of anemic mice following AMI compared to their non-anemic controls (p=0.02) (Figure 15 F), indicating altered mitochondrial dynamics in anemia following AMI. These findings indicate that mitochondrial fission was altered in anemic mice both before and after AMI, particularly in the ischemic region, highlighting potential dysregulation of mitochondrial homeostasis in anemia.

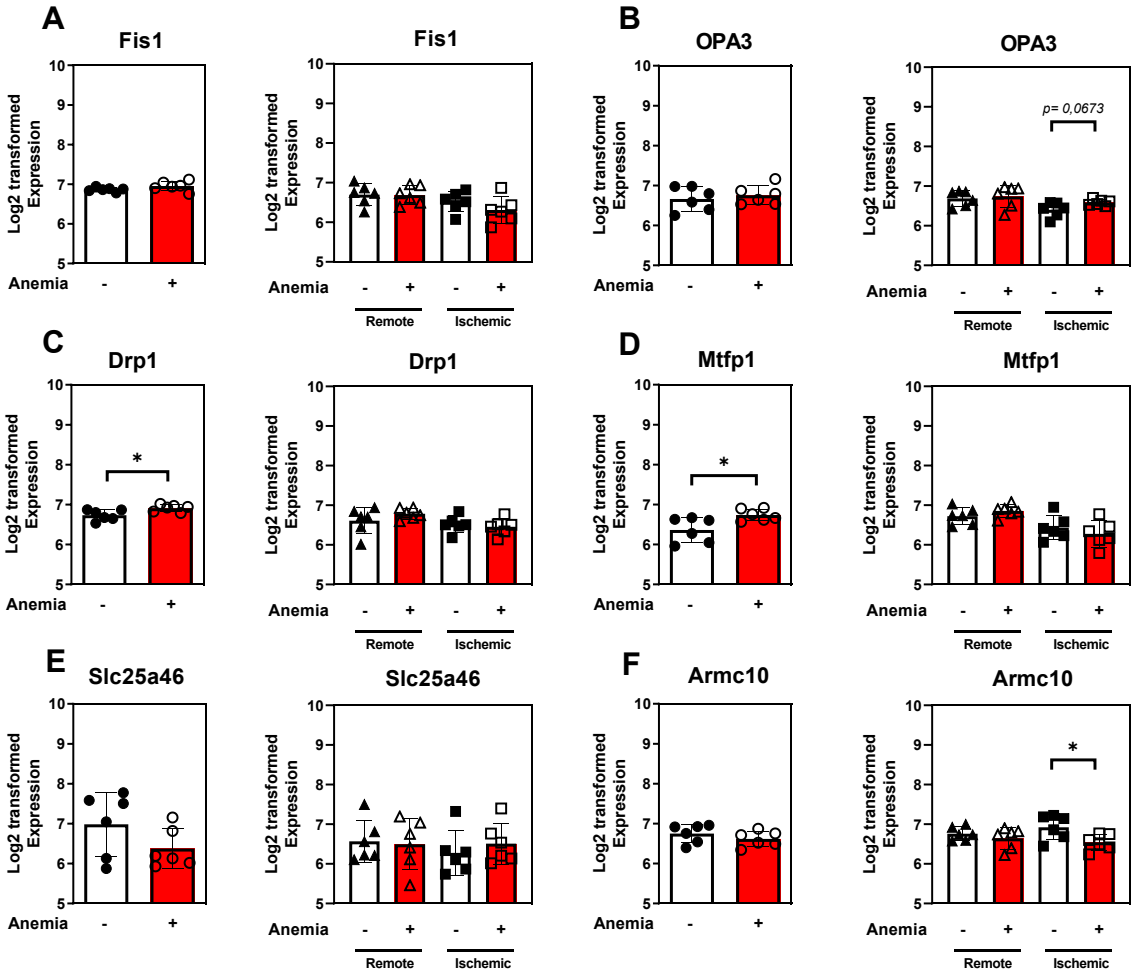

Figure 15: Altered protein expression of mitochondrial fission related proteins in LVs isolated from anemic and non-anemic mice at basal and 24 h post-AMI in remote and ischemic region. Proteomic analysis of proteins associated with mitochondrial fission, namely Fis1 (A), OPA3 (B), Drp1 (C), Mtfp1 (D), Slc25a46 (E) and Armc10 (F) in LVs of non-anemic (white bars) and anemic mice (red bars) with and without AMI in remote (triangles) and ischemic (squares) region. Values are shown as the means ± SEM (n=6 per group). *p≤0.05. Student t-test was used to compare between two groups.

4.1.4 Impaired mitochondrial respiration in anemic mice after AMI

RBCs and their function to transport O_2 to the tissues is crucial for OXPHOS. In anemia, RBC reduction or dysfunction leads to the impairment of gas transport, which might result in impaired delivery of O_2 to the tissues and, subsequently mitochondrial dysfunction. To investigate this, high resolution respirometry measurements using the O2K oxygraph were performed, in which mitochondrial respiration of LV tissues of anemic and non-anemic mice was measured.

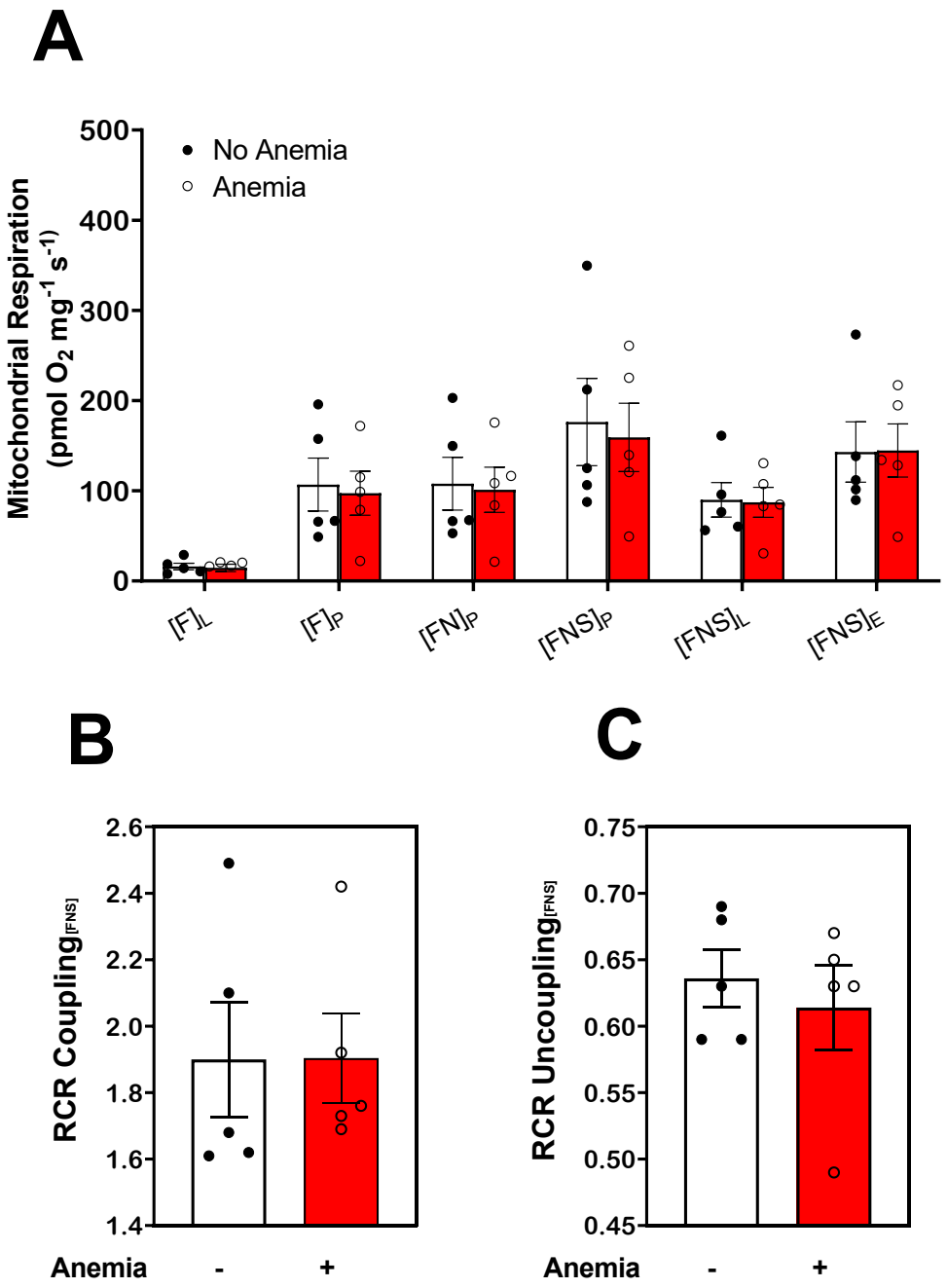

Figure 16: Unchanged myocardial mitochondrial function in LVs of anemic and non-anemic mice. High resolution respirometry analysis of LVs in mice with anemia (red bars) and without anemia (white bars). (A) Mitochondrial OXPHOS capacity was measured in the presence of fatty acids (F), NADH (N)- and succinate (S)-linked substrates and expressed as pmol O2 · mg^{-1} ·s^{-1}. (B-D) Subsequently, RCRs were calculated based on the absolute respiratory values. Values are shown as the means ± SEM. For statistical testing RCRs were log-transformed. Normally distributed data were compared using an unpaired t-test whereas non-normally distributed data were compared using Mann-Whitney test. E: electron transport system capacity, P: oxidative phosphorylation capacity, L: LEAK.

The analysis showed no significant differences in mitochondrial OXPHOS capacity between anemic and non-anemic mice (Figure 16 A), suggesting that mitochondrial function remains unaffected after anemia. Additionally, RCR ratios, calculated based on the raw data, showed no differences between the anemic and non-anemic mice (Figure 16 B, C), indicating preserved coupling efficiency of OXPHOS. These results suggest that mitochondrial function in the LVs of anemic mice remains unchanged.

To further investigate the effect of anemia and AMI on mitochondrial function, respirometry analysis was performed with LVs of anemic and non-anemic mice after AMI. Though not significantly, analysis of the attained data showed that overall mitochondrial OXPHOS was reduced in the anemic and non-anemic ischemic region compared to the remote region (Figure 17 A), likely due to increased necrotic tissue in the ischemic region. RCR Coupling_{FNS} in the remote region of anemic and non-anemic mice post-AMI was unchanged (Figure 17 B). Interestingly, RCR Coupling_{FNS} in the ischemic region of anemic mice was significantly lowered compared to the ischemic region of non-anemic mice (Figure 17 B), suggesting decreased coupling efficiency between the ETS and phosphorylation system. RCR Uncoupling_{FNS} remained unchanged in both ischemic and remote regions between anemic and non-anemic mice (Figure 17 C). Additionally, a trend towards increased LEAK ($[FNS]_L$) was observed in the ischemic region of anemic mice compared to non-anemic controls, indicating increased inner mitochondrial membrane permeability. In conclusion, these results indicate impaired mitochondrial respiration in the ischemic region of anemic mice after AMI, whereas mitochondrial respiration remains unaltered in the remote region.

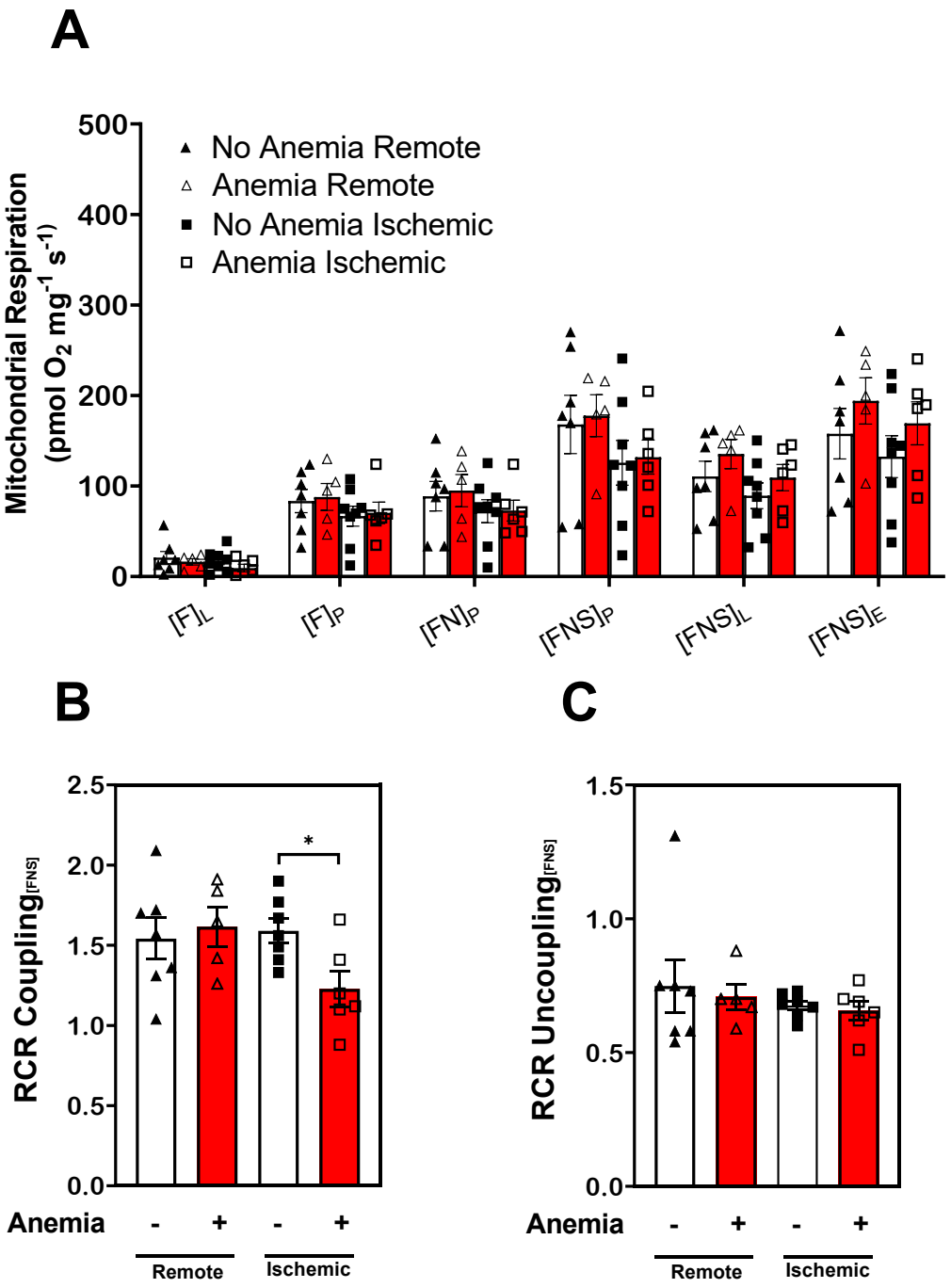

Figure 17: Altered myocardial mitochondrial coupling efficiency in the ischemic region of anemic mice after AMI. High resolution respirometry analysis of the LVs in the remote (triangles) and ischemic (squares) region of the heart 24 h post-AMI in mice with anemia (red bars) and without anemia (white bars). (A) Mitochondrial OXPHOS capacity was measured in the presence of fatty acids (F), NADH (N)- and succinate (S)-linked substrates and expressed as pmol O2 · mg^{-1} ·s^{-1}. (B-C) Subsequently, RCRs were calculated based on the absolute respiratory values. Values are shown as the means ± SEM. For statistical testing RCRs were log-transformed. Normally distributed data were compared using an unpaired t-test whereas non-normally distributed data were compared using Mann-Whitney test. E: electron transport system capacity, P: oxidative phosphorylation capacity, L: LEAK. *p≤0.05.

4.1.5 Altered mitochondrial content in remote and ischemic region of anemic mice after AMI

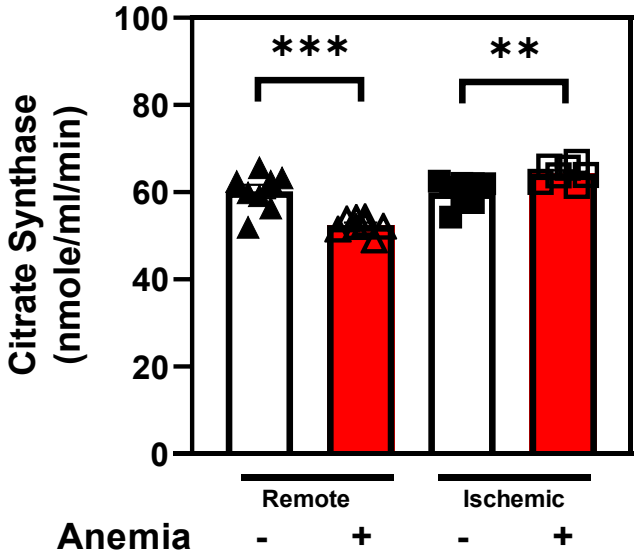

Figure 18: Altered citrate synthase activity in the remote and ischemic region of anemic mice LVs 24 h post-AMI. Mitochondrial content analysis of remote (triangles) and ischemic (squares) region of LVs 24 h post-AMI in mice with anemia (red bars) and without anemia (white bars). Values are shown as the means ± SEM. **p≤0.01, *** p≤0.001. Student t-test was used to compare between two groups.

Mitochondrial density is a crucial factor in determining bioenergetic function. Since the respiratory chain responsible for energy production is embedded within the inner mitochondrial membrane, both its function and the number of mitochondria significantly influence mitochondrial oxidative capacity. Our results revealed impaired mitochondrial respiration in the ischemic region of anemic mice after AMI. To further explore mitochondrial content alterations, we measured CS activity, a marker of mitochondrial density, in the ischemic and remote region of anemic and non-anemic mice after AMI. Our results demonstrated significantly decreased CS activity in the remote region of anemic mice 24 h post-AMI (Figure 18). In the ischemic region of anemic mice 24 h post-AMI, significantly increased CS activity was observed (Figure 18). These observations indicate that mitochondrial number is decreased in the remote region and increased in the ischemic region of anemic mice after AMI.

4.1.6 Unaltered expression of ETS complexes in the ischemic region of anemic mice after AMI

Our proteomic analysis revealed an increase in subunits of CI and CIII, namely Ndufb6, Ndufs7 and Uqcr10. Based on this we examined potential alterations in the expression of ETS complexes I-V. To assess this, western blot analysis was performed in the ischemic region of anemic and non-anemic mice following AMI. The results revealed no significant differences in the expression of CI-V in the ischemic region of anemic and non-anemic mice after AMI (Figure 19 A-G).

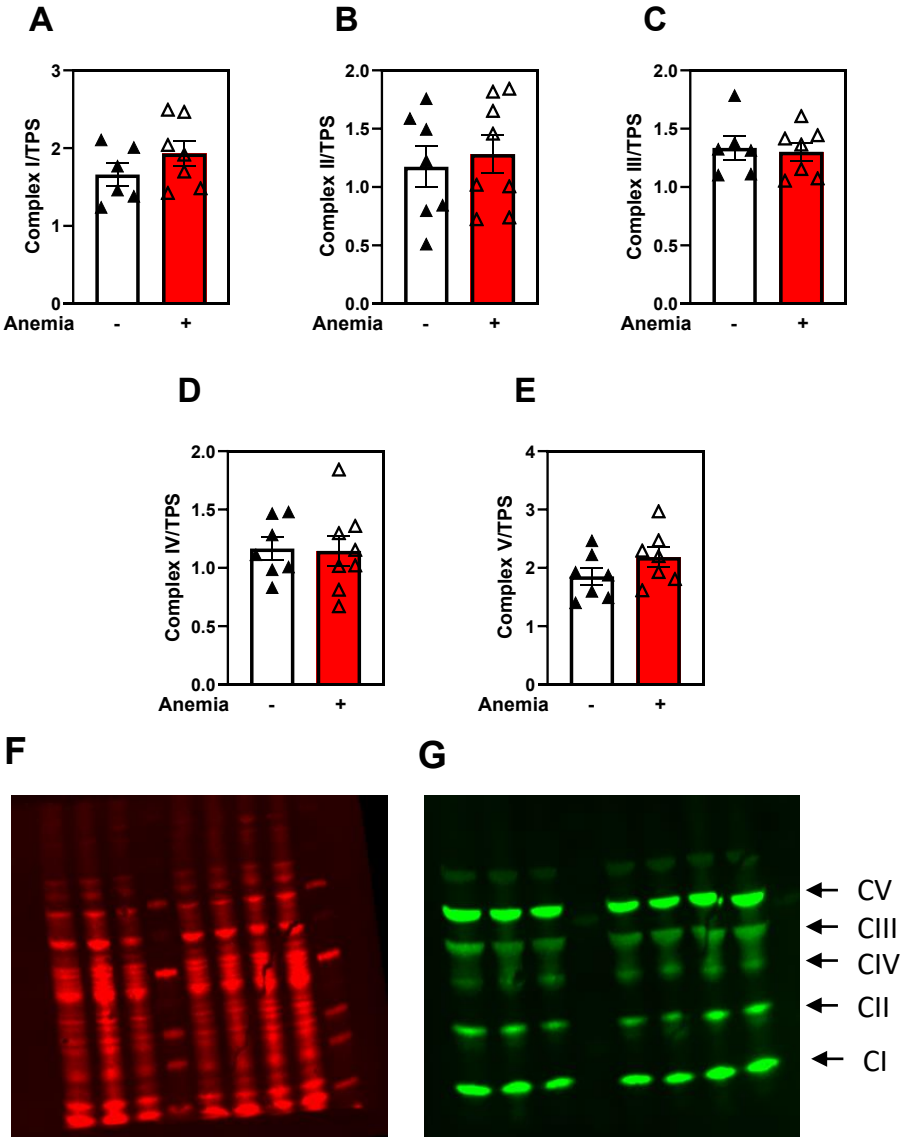

Figure 19: Unchanged expression of ETS complexes in the ischemic region of anemic mice after AMI. After anemia and AMI induction, mice were sacrificed and LV lysates were used to assess protein expression of electron transport system complexes via western blotting (G) in anemic (red bars) and non-anemic (white bars). Protein expression of each complex (A-E) was normalized with total protein staining (F). Values are shown as the means ± SEM. Student t-test was used to compare between two groups.

4.1.7 Altered oxidative stress in anemic mice with and without AMI

4.1.7.1 Altered oxidative stress in anemic mice

Our results revealed decreased contractility and altered cardiac energetics in the ischemic region of anemic mice after AMI. Previous studies have demonstrated that anemia is associated with enhanced ROS levels in the vascular system [127], which might exacerbate pathological outcomes when combined with other morbidities [187]. For this reason, we further wanted to explore whether altered oxidative stress in anemia before and after AMI contribute to the observed phenotype. To assess oxidative stress in anemia, we measured the activity of key redox enzymes and glutathione concentrations in LV tissues of anemic and non-anemic mice.

SOD are metalloenzymes that play a critical role in the antioxidant defence system of cells, by catalyzing the dismutation of O_2^- into O_2 and H_2O_2 [224]. Enzyme activity of SOD in anemic and non-anemic LV samples were measured. The results revealed a significant reduction in SOD acitivity in anemic mice compared to non-anemic mice (Figure 20 A).

Catalase is a ROS-scavenging enzyme that converts two H_2O_2 molecules to oxygen and water, protecting cells from oxidative damage [225]. Catalase activity in anemic and non-anemic LV samples were measured. The analysis revealed no significant differences between anemic and non-anemic mice (Figure 20 B).

As nonenzymatic antioxidant, glutathione plays an important role in detoxification, especially in the cardiovascular system. Through direct or indirect interaction with highly reactive ROS, glutathione maintains redox balance [226]. Glutathione concentrations in LV tissues were significantly reduced in anemic mice compared to non-anemic controls (Figure 20 C), indicating impaired antioxidant capacity.

MPO belongs to the group of peroxidases and is a lysosomal enzyme. It is highly expressed in neutrophils and functions as generator of cytotoxic species, namely HOCl, which is crucial for the immune response against pathogens. However, elevated MPO levels are associated with CVD [227]. MPO activity in LV tissues of anemic and non-anemic mice exhibited a trend toward increased activity in anemic mice ($p= 0.0783$) (Figure 20 D).

In summary, these findings indicate that the antioxidant capacity was significantly altered in anemic mice, as evidenced by reduced SOD activity, diminished glutathione levels and a tendency towards increased MPO activity.

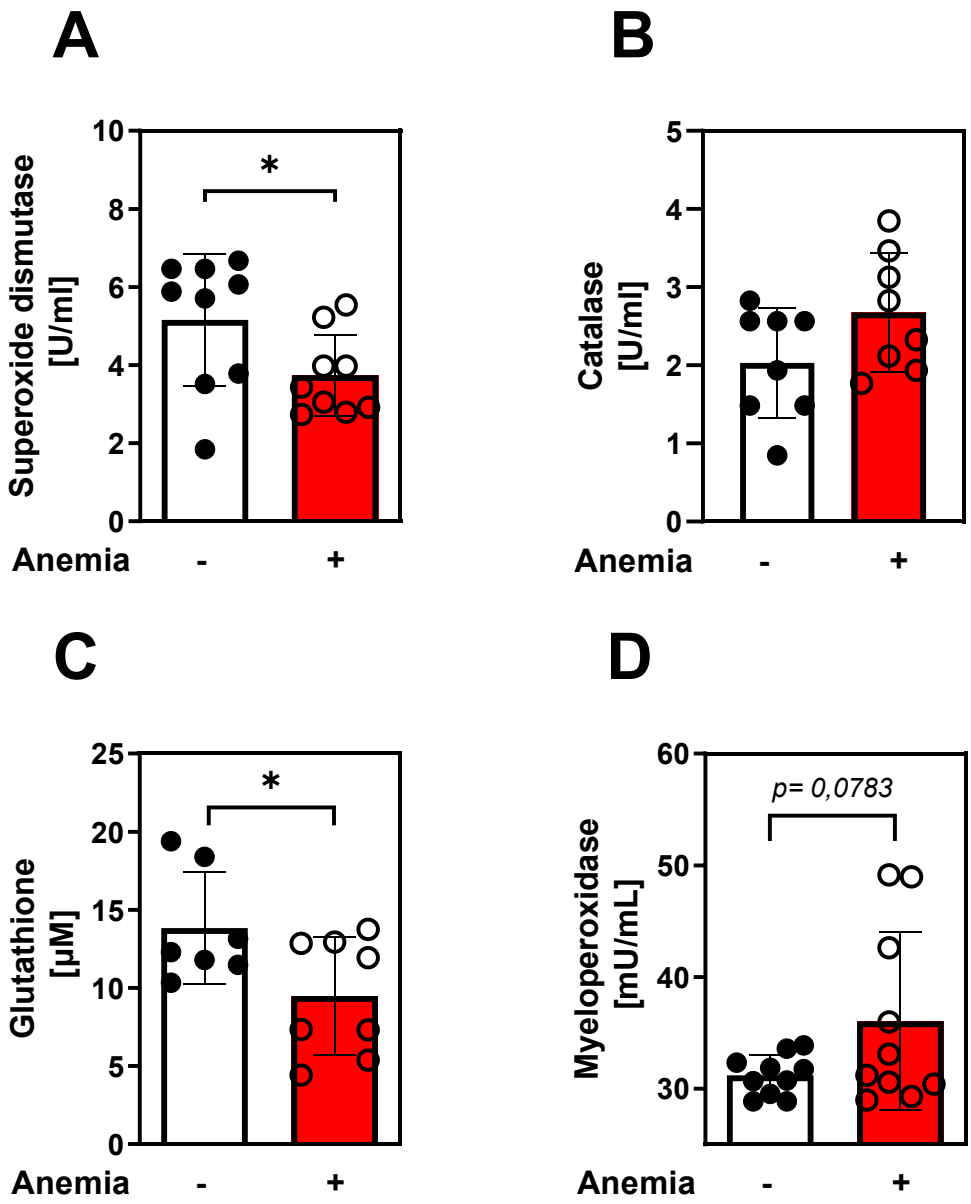

Figure 20: Altered redox balance in LVs of anemic mice. Analysis of redox enzymes, namely Superoxide dismutase (A), Catalase (B) and Myeloperoxidase (D) and redox maintaining reduced Glutathione (GSH) (C), in LVs of anemic mice (red bars) and non-anemic mice (white bars). Values are shown as the means ± SEM (n=8 per group). *p≤0.05. Student t-test was used to compare between two groups

4.1.7.2 Altered redox state in anemic mice after AMI

To investigate redox changes in anemia after AMI, the activity of above mentioned redox enzymes (SOD, catalase and MPO) and GSH were measured in the remote and ischemic region of anemic and non-anemic mice following AMI. Both SOD and catalase activities remained unchanged in anemic and non-anemic mice in remote and ischemic region (Figure 21 A, B). In the remote region of anemic mice after AMI, glutathione concentration was significantly lower compared to their non-anemic controls, whereas in the ischemic region no

significant differences were observed (Figure 21 C). The analysis of the data revealed that in both remote and ischemic regions of anemic mice 24 h post-AMI, MPO activity was significantly increased compared to their non-anemic controls, suggesting increased oxidative stress in LVs of anemic mice after AMI (Figure 21 D). These results suggest that in the remote region of anemic mice, the antioxidant capacity is diminished due to reduced glutathione levels. Furthermore, the results suggest elevated oxidative stress in both remote and ischemic regions of anemic mice after AMI, as oxidative stress promoting enzyme MPO activity was significantly increased.

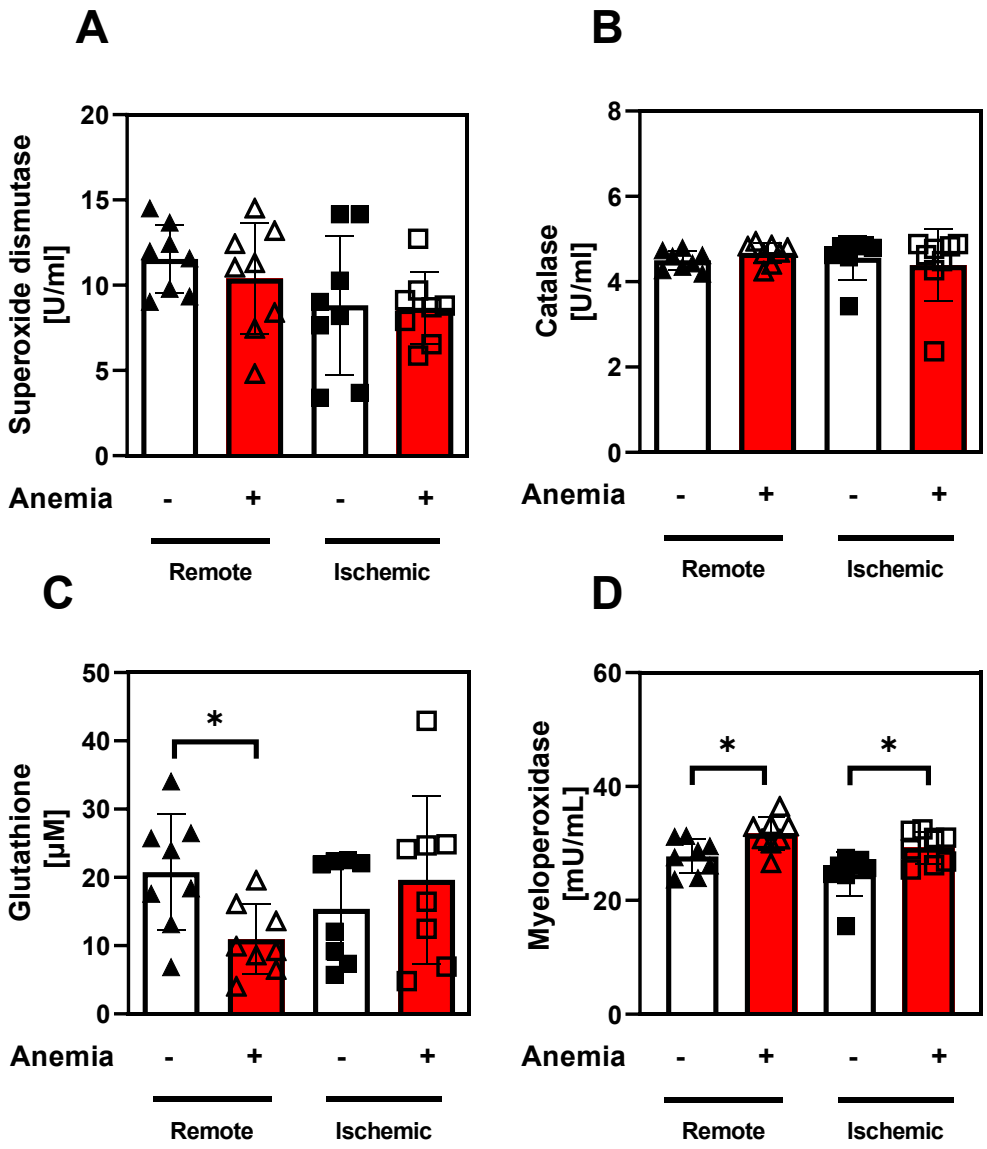

Figure 21: Altered redox balance in LVs of anemic mice 24 h post-AMI. Analysis of redox enzymes, namely Superoxide dismutase (A), Catalase (B) and Myeloperoxidase (D) and redox maintaining tripeptide reduced Glutathione (GSH) (C), in LVs of anemic mice (red bars) and non-anemic mice (white bars) 24 h post-AMI in remote (triangles) and ischemic (squares) region. Values are shown as the means ± SEM (n=8 per group). *p≤0.05. Student t-test was used to compare between two groups.

4.1.8 Regional oxidative damage increase in anemic mice after AMI

Our data demonstrated regional LV dysfunction in anemia after AMI, evidenced by altered PCr/ATP ratio, Pi/ATP ratio, fractional shortening and altered respiration in the ischemic region. Additionally, we showed altered oxidative stress in anemic mice before and after AMI. To further pinpoint the role of ROS, we next evaluated ROS products by analysing 4-HNE levels in LV (ischemic) lysates of anemic and non-anemic mice 24 h post-AMI. 4-HNE is a lipid peroxidation product, which is generated as a result of ROS mediated lipid peroxidation of polyunsaturated fatty acids [228, 229]. Western blot analysis demonstrated significantly higher 4-HNE levels in the ischemic region of anemic mice hearts compared to non-anemic mice hearts (Figure 22 A), indicating increased ROS mediated lipid peroxidation in anemia following AMI.

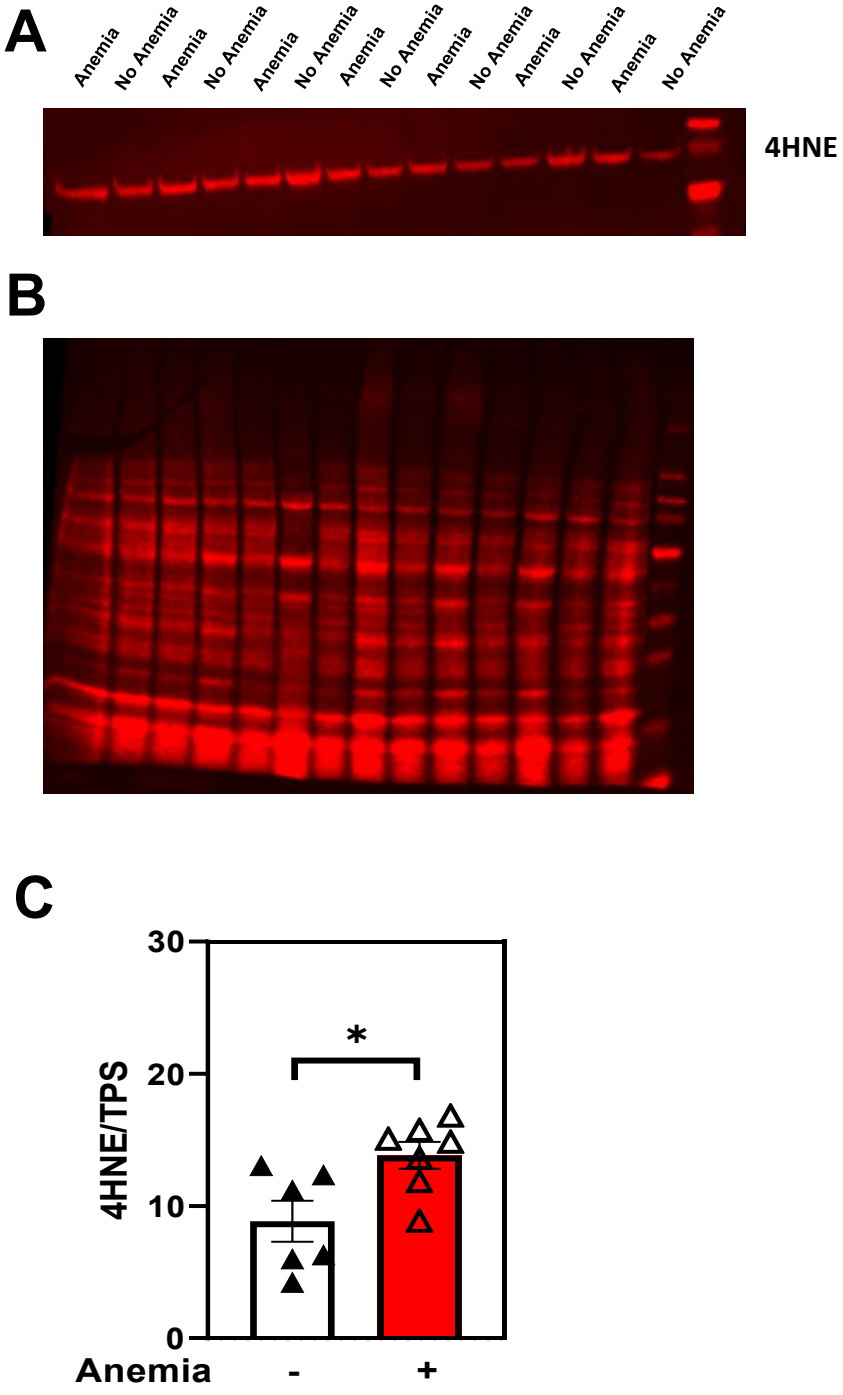

Figure 22: Increased 4-HNE levels in ischemic region of anemic mice after AMI. After anemia and AMI induction, mice were sacrificed and LV lysates were used to assess 4-HNE expression via westernblotting in anemic and non-anemic mice (A). Expression of 4-HNE was normalized via total protein staining (B), and depicted as bar graphs (white bar: no anemia, red bar: anemia) (C). Values are shown as the means ± SEM. *p≤0.05. Student t-test was used to compare between two groups.

4.1.9 Normalized mitochondrial respiration in the ischemic region of anemic mice after NAC supplementation

Our previous findings demonstrated altered oxidative stress in LV tissues of anemic mice with and without AMI. To further evaluate the role of ROS in mediating mitochondrial dysfunction in anemia after AMI, anemic and non-anemic mice were supplemented with NAC for four weeks prior to AMI induction. Respirometry analysis was performed as described before (3.10). Mitochondrial OXPHOS capacity showed no significant differences between anemic and non-anemic mice in remote and ischemic region (Figure 23 A). Interestingly, NAC supplementation preserved RCR Coupling$_{FNS}$ in the ischemic region of anemic mice (Figure 23 B). RCR Uncoupling$_{FNS}$ in remote and ischemic region showed no significant changes between anemic and non-anemic mice (Figure 23 C). These results suggest that ROS scavenging preserved mitochondrial respiration in the ischemic region of anemic mice following AMI.

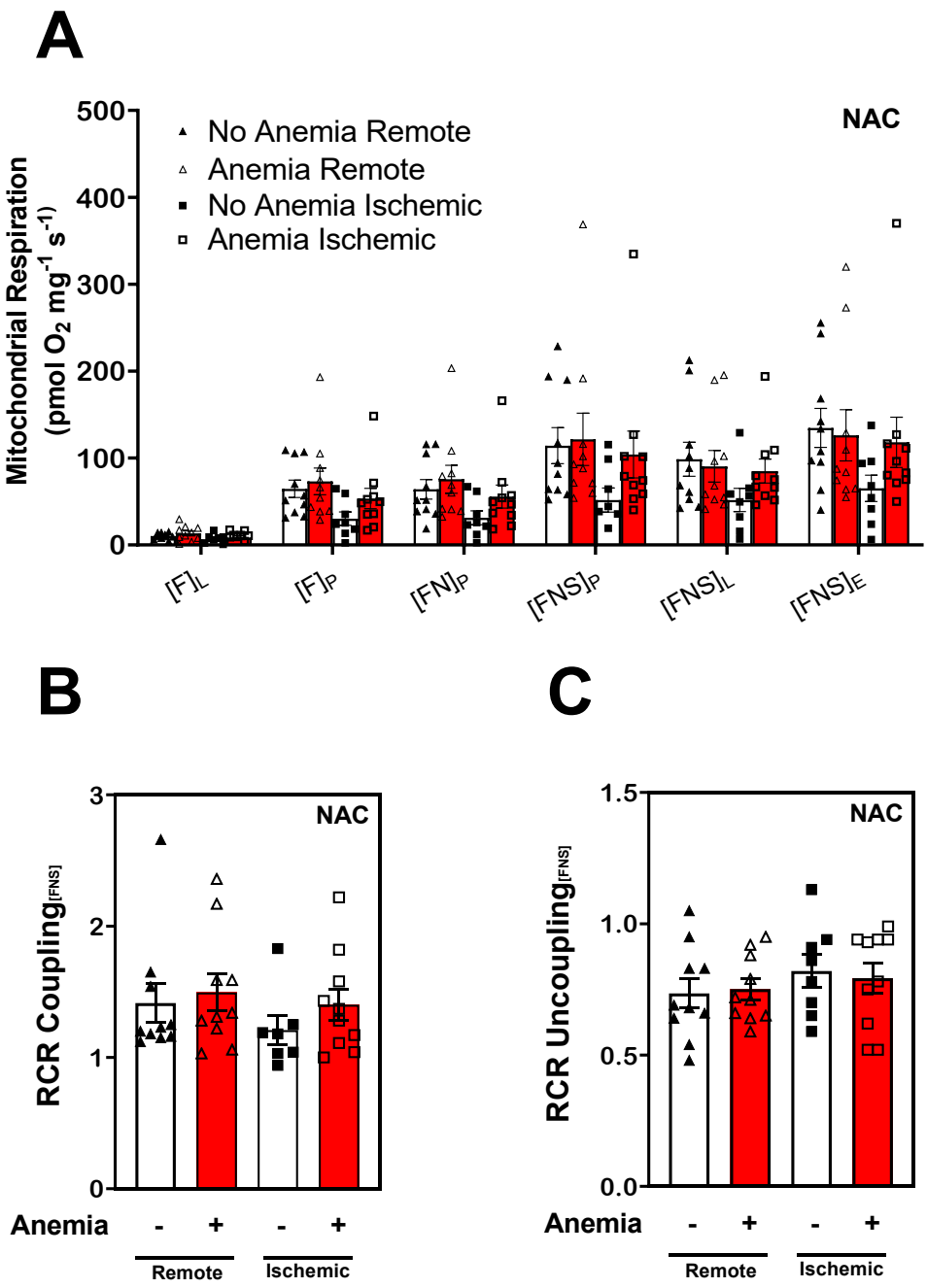

Figure 23: NAC supplementation normalized mitochondrial coupling efficiency in the ischemic region of anemic mice after AMI. Mice were supplemented with NAC for four weeks and anemia was induced. Subsequently, high resolution respirometry was performed in the remote (triangles) and ischemic (squares) region of LVs 24 h post-AMI in mice with anemia (red bars) and without anemia (white bars). (A) Mitochondrial oxidative phosphorylation capacity was measured in the presence of fatty acids (F), NADH (N)- and succinate (S)-linked substrates and expressed as pmol $O^2 \cdot mg^{-1} \cdot s^{-1}$. (B-D) Respiratory control ratios (RCR) were calculated based on the absolute respiratory values. Values are shown as the means ± SEM. For statistical testing RCRs were log-transformed. Normally distributed data were compared using an unpaired t-test whereas non-normally distributed data were compared using Mann-Whitney test. E: electron transport system capacity, P: oxidative phosphorylation capacity, L: LEAK.

4.1.10 Unaltered mitochondrial content after NAC supplementation in remote and ischemic region of anemic mice after AMI

Since our respirometry data of NAC supplemented anemic mice after AMI showed preserved mitochondrial respiration in the ischemic region, we further evaluated potential changes in mitochondrial content after NAC supplementation. Therefore, we measured CS activity in the ischemic and remote regions of anemic and non-anemic mice, supplemented with NAC, 24 h post-AMI. After NAC treatment, no significant differences were observed in CS activity between anemic and non-anemic mice after AMI in both regions (Figure 24). These results conclude that NAC preserved mitochondrial content after AMI in both regions of anemic mice, which were significantly altered without NAC treatment.

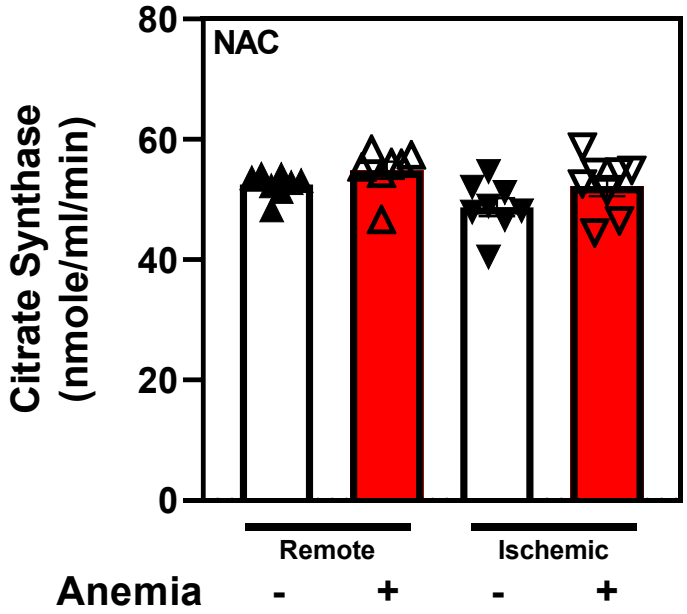

Figure 24: Altered citrate synthase activity in remote and ischemic region of anemic mice after 24 h post-AMI is normalized after NAC treatment. Mice were supplemented with NAC for four weeks and anemia is induced. Mitochondrial content analysis of remote (triangles) and ischemic (squares) region of LVs 24 h post-AMI in mice with anemia (red bars) and without anemia (white bars). Values are shown as the means ± SEM. Student t-test was used to compare between two groups.

4.1.11 Unaltered mitochondrial respiration in mice hearts incubated with anemic CAD patient's RBCs

As our previous studies demonstrated that anemic RBCs impaired vascular function with and without AMI, we examined the role of anemic RBCs on LV energy metabolism after AMI [127, 214]. For this purpose, anemic and non-anemic CAD patient's RBCs were firstly isolated. Subsequently, the isolated RBCs were incubated with wildtype mice hearts in the Langendorff apparatus during 40 min of global ischemia, after which 60 min of reperfusion followed. LVs were isolated and mitochondrial respiration was measured using high resolution respirometry. Respirometry analyses revealed that anemic RBCs did not significantly affect mitochondrial OXPHOS capacity (Figure 25 A). The calculated RCR ratios likewise were not significantly changed between both groups (Figure 25 B, C). These results indicate that RBCs from anemic CAD patients do not affect mitochondrial respiration in healthy mouse hearts subjected to I/R after a short incubation period.

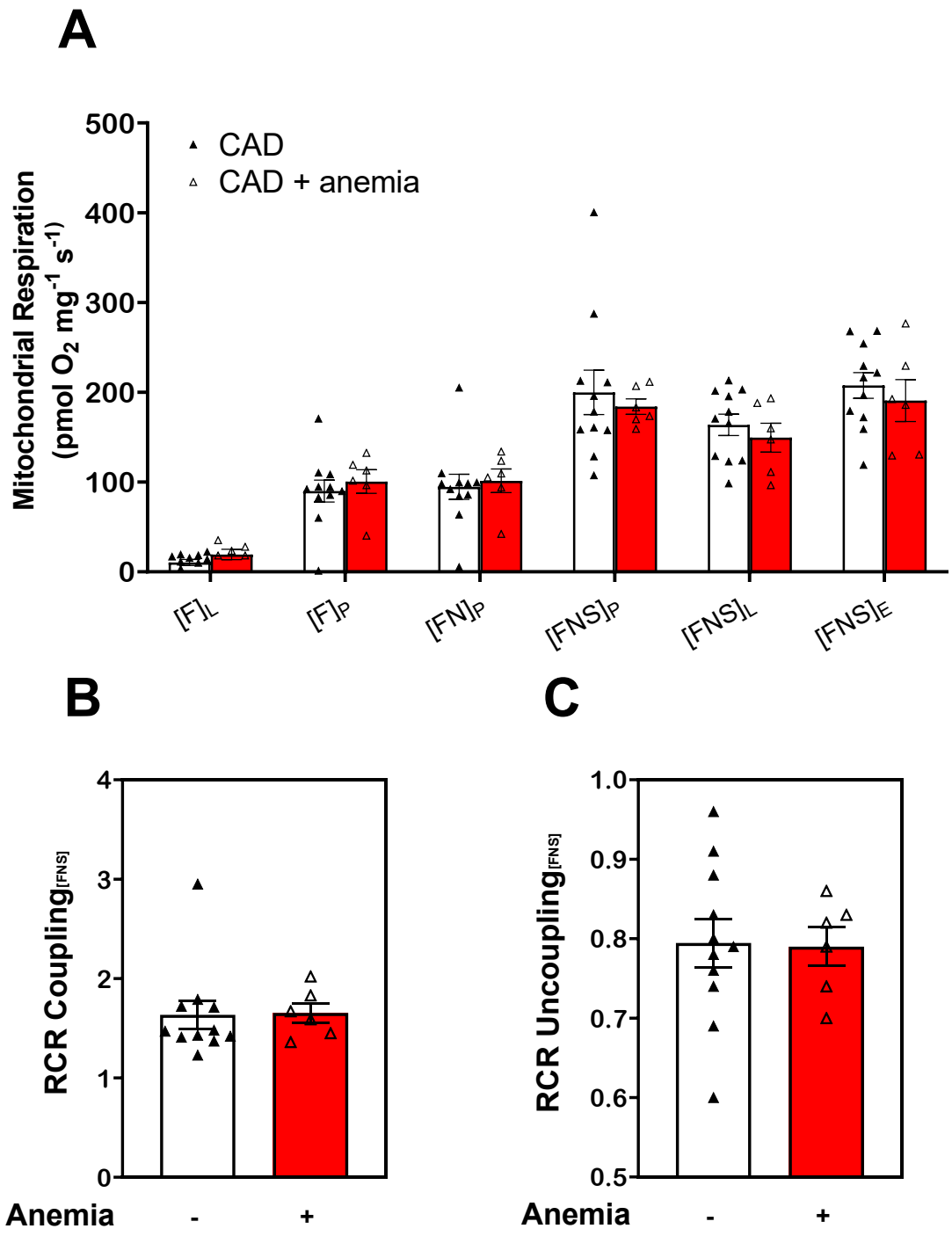

Figure 25: Unchanged myocardial mitochondrial function in LVs of mice exposed to anemic and non-anemic CAD patient's RBCs. High resolution respirometry analysis in LVs of mice, exposed to anemic (red bars) and non-anemic (white bars) CAD patient's RBCs. (A) Mitochondrial OXPHOS capacity was measured in the presence of fatty acids (F), NADH (N)- and succinate (S)-linked substrates and expressed as pmol O2 · mg^{-1} ·s^{-1}. (B-C) Subsequently, respiratory control ratios (RCR) were calculated based on the absolute respiratory values. Values are shown as the means ± SEM. For statistical testing RCRs were log-transformed. Normally distributed data were compared using an unpaired t-test whereas non-normally distributed data were compared using Mann-Whitney test. E: electron transport system capacity, P: oxidative phosphorylation capacity, L: LEAK.

In summary, analysis of blood loss anemia on LV function before and after AMI demonstrated following observations: Echocardiography data revealed adaptive increase in LV function in anemic mice, which was not observed after AMI induction. Following AMI, overall LV function remained unchanged in both anemic and non-anemic mice. CMRI measurements further indicated decreased ATP availability, and also showed impaired LV function in the ischemic region of anemic mice after AMI. To elucidate the underlying pathways for the observed phenotype, we conducted proteomic analysis, which identified differentially regulated proteins associated with energy metabolism and mitochondrial respiration in the ischemic region of anemic mice after AMI. Based on these findings, high resolution respirometry analyses were performed. These data revealed unchanged respiration in anemic mice compared to non-anemic mice. However, impaired mitochondrial respiration in the ischemic region of anemic mice after AMI was observed. To explore whether these alterations were related to ROS levels, we assessed oxidative stress in both anemic and non-anemic mice after AMI. Our data demonstrated impaired redox state in anemic mice without AMI, as well as altered redox state in anemic mice after AMI. In response to these changes, anemic and non-anemic mice were treated with N-acetyl cysteine (NAC), and respirometry analysis was conducted. NAC supplementation preserved the previously impaired mitochondrial respiration in the ischemic region of anemic mice. Mitochondrial density is a crucial factor in determining bioenergetic function. Since the respiratory chain responsible for energy production is embedded within the inner mitochondrial membrane, both its function and the number of mitochondria significantly influence mitochondrial oxidative capacity. For this reason, mitochondrial density, using CS activity measurements were conducted. These data demonstrated altered mitochondrial density in the ischemic and in the remote region of anemic mice after AMI, which were preserved in NAC supplemented anemic mice after AMI. Next, we assessed the expression of CI-CV of the ETS using western blot analysis, and our results revealed no significant differences in CI-CV expression in the ischemic region of anemic mice. Finally, to evaluate a potential mechanism behind the altered mitochondrial respiration in anemia after AMI, we assessed the role of anemic RBCs. For this purpose, we incubated anemic and non-anemic CAD patient's RBCs with wildtype mice hearts *ex vivo*, which were then subjected to global I/R. Afterwards mitochondrial respiration of the LVs was measured using high resolution respirometry, which indicated that anemic CAD patient's RBC did not affect mitochondrial respiration in wildtype mice hearts exposed *ex vivo*.

Taken together, these findings suggest that impaired mitochondrial respiration and energy metabolism in the ischemic region of anemic mice after AMI are likely linked to altered redox states, with NAC supplementation serving to normalize mitochondrial function.

4.2 The effect of RBC eNOS deficiency in anemia on cardiovascular function

Our results demonstrated that anemia leads to regional changes in mitochondrial protein expression and respiration in anemic mice after AMI. In our recent studies we demonstrated that RBC eNOS exhibit cardioprotective especially after AMI [230]. However, RBC eNOS deficiency in anemia has not been studied yet. Therefore, we evaluated the effect of RBC eNOS deficiency in anemia with and without AMI on LV and vascular function. For this purpose, heart function, vascular function and infarct sizes were assessed under anemic conditions and RBC eNOS deficient state. In the following paragraphs the results will be presented.

4.2.1 Dysfunctional RBCs in anemia hamper the hypertension in RBC-eNOS-KO mice

To investigate the effects of anemia on systemic hemodynamics, when eNOS is deficient in RBCs, we assessed hemodynamic parameters in anemic and non-anemic RBC-eNOS-KO mice and their control mice under anesthesia using Millar pressure catheter. RBC-eNOS-KO mice show elevated systolic and diastolic BP compared to their control mice (Figure 26 A, B). However, after anemia induction, RBC-eNOS-KO mice showed similar systolic and diastolic BP as their control group of mice (Figure 26 A, B). No significant differences were observed in the HR of anemic and non-anemic RBC-eNOS-KO mice (Figure 26 C). Similarly, DP showed no significant changes between anemic and non-anemic RBC-eNOS-KO mice (Figure 26 D). Furthermore, dP/dt_{max} and dP/dt_{min} were unchanged in these mouse groups (Figure 26 E, F). These results conclude that basal hypertension phenotype in RBC-eNOS-KO is mitigated after anemia induction.

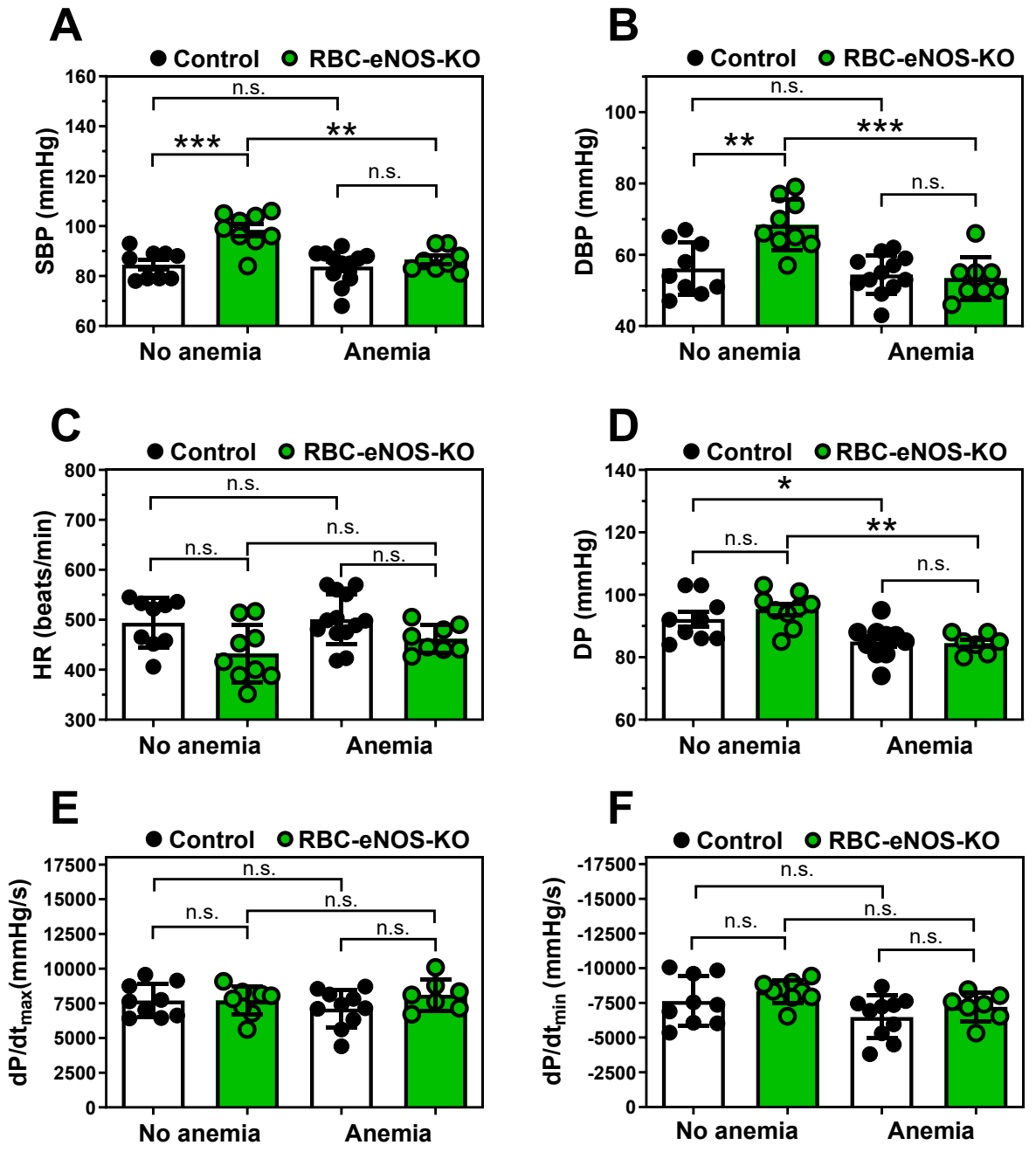

Figure 26: Anemia mitigates hypertension in RBC specific eNOS deficient mice. BP and heart function were assessed using a Millar catheter in control and RBC eNOS deficient mice with and without anemia. (A) Systolic blood pressure (SBP). (B) Diastolic blood pressure (DBP). (C) Heart rate (HR). (D) Left ventricular developed pressure (DP). (E) Maximal rate of left ventricular pressure increase (dP/dtmax) and (F) minimal rate of left ventricular pressure drop (dP/dtmin). All values are presented as mean ± SEM. Multiple groups were compared using one-way analysis of variance (ANOVA) with Tukey's multiple comparison test. *, $p \leq 0.05$; **, $p \leq 0.01$; ***, $p \leq 0.001$; n.s., not significant.

4.2.2 Endothelial function is preserved in anemic RBC-eNOS-KO mice

We further examined the impact of anemia on endothelial function *in vivo* by evaluating FMD responses in anemic and non-anemic RBC-eNOS-KO mice. FMD responses were preserved in RBC-eNOS-KO mice compared to their control littermates, both before and after anemia induction (Figure 27 A, B) indicating that anemia does not affect FMD responses, when eNOS is deficient in RBCs. This finding also further confirms the predominant role of endothelial eNOS in mediating endothelium-dependent relaxation responses.

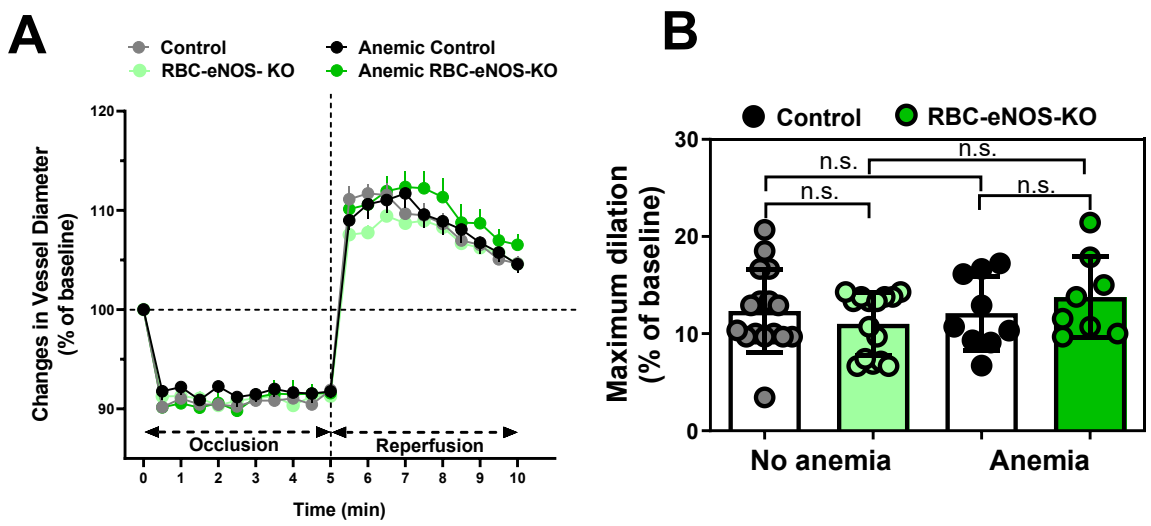

Figure 27: Anemic RBC-specific eNOS-deficient mice show preserved FMD responses. (A) Changes in vessel diameter (% of baseline diameter) in non-anemic controls (grey), RBC eNOS deficient mice (light green), anemic controls (black), and RBC eNOS deficient mice (green). (B) Maximum FMD during the reperfusion phase (6-7 min), averaged and normalized to baseline. The occlusion and release phases of the cuff (reperfusion) are indicated in the respective panels. All values are presented as mean ± SEM. A Student's t-test was used to compare two groups, and multiple groups were compared using one-way analysis of variance (ANOVA) with Tukey's multiple comparison test. n.s., not significant.

To further assess vascular function, we measured endothelium-dependent and -independent relaxation in isolated aortic rings using wire myography. In the presence of indomethacin, anemic RBC-eNOS-KO mice showed relaxation responses comparable to anemic control mice (Figure 28 A). As expected, treatment with the NOS inhibitor L-NAME (100 µM) abolished relaxation in all groups (Figure 28 B), confirming that the responses were NO-dependent. Additionally, relaxation to the exogenous NO donor sodium nitroprusside (SNP) was similar across all groups, indicating that smooth muscle sensitivity to NO was unaffected in RBC eNOS deficient state (Figure 28 C). These results conclude that endothelial function is preserved in RBC eNOS deficient state.

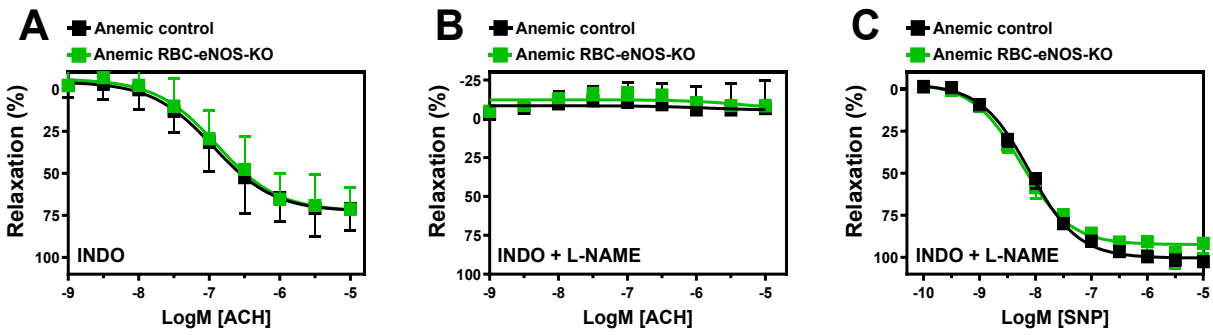

Figure 28: Anemic RBC specific eNOS deficient mice show preserved endothelial-dependent relaxation responses. Aortic rings were isolated from anemic RBC eNOS deficient (green) and respective control mice (black). Aortic segments were pre-contracted with phenylephrine (10 µM), and relaxation responses to acetylcholine (ACh, 1 nM - 10 µM) were measured using a wire myograph. (A) Relaxation in the presence of indomethacin (10 µM, COX inhibitor). (B) Relaxation in the presence of indomethacin and L-NAME (100 µM, NOS inhibitor). (C) Relaxation responses to sodium nitroprusside (SNP, 10 nM - 10 µM) in the presence of indomethacin and L-NAME. All values are presented as mean ± SEM (n = 8-10 per group). CRCs were analyzed by two-way ANOVA and Bonferroni's post hoc test to compare eNOS-deficient mice with their respective control mice

In summary, the absence of eNOS in RBCs does not impact endothelial responses *ex vivo* and *in vivo* under anemic conditions.

4.2.3 Left ventricle (LV) function is preserved in anemic RBC-eNOS-KO mice after AMI

LV function was evaluated by echocardiography at baseline, three days after anemia induction, and 24 h post-AMI in anemic RBC-eNOS-KO and their respective control mice. Key LV functional parameters - including ESV, EDV, CO, SV, HR, and EF - did not differ significantly between anemic RBC-eNOS-KO mice and their anemic control mice (Figure 29 A-E). SV and CO were significantly decreased in both mice groups that underwent AMI, indicating impaired heart function after AMI. In conclusion, these findings indicate that under anemic conditions, eNOS deficiency in RBCs does not influence LV function following AMI in mice.

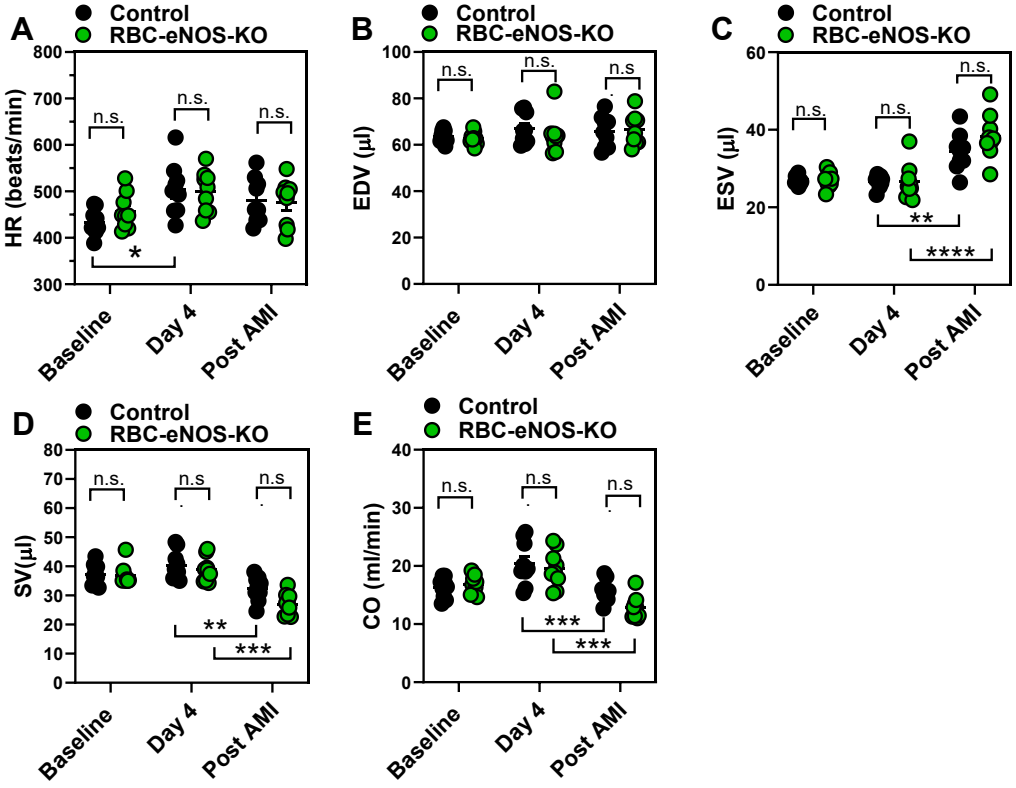

Figure 29: LV dysfunction post-AMI is unchanged in anemic control and RBC eNOS deficient mice. Echocardiographic evaluation of control and RBC eNOS-deficient mice was performed before (Baseline), 3 days after anemia induction (Day 4), and 24 h post-AMI. LV parameters were evaluated, including (A) heart rate (HR), (B) end-diastolic volume (EDV), (C) end-systolic volume (ESV), (D) stroke volume (SV), and (E) cardiac output (CO). All values are presented as mean ± SEM. Multiple groups were compared using two-way analysis of variance (ANOVA) with Tukey's multiple comparison test. **, $p \leq 0.01$; ***, $p \leq 0.001$; ****, $p \leq 0.0001$; n.s., not significant.

4.2.4 Anemic RBC-eNOS-KO mice show increased infarct size after AMI

Infarct sizes were assessed in anemic and non-anemic RBC-eNOS-KO and control mice using TTC stainings. The results demonstrated that infarct size was significantly increased in anemic RBC-eNOS-KO mice compared to anemic control mice (Figure 30 C). These results conclude that deficiency of eNOS in RBCs increases the infarct size in anemic mice after AMI, concluding the cardioprotective role of RBC eNOS under anemic conditions.

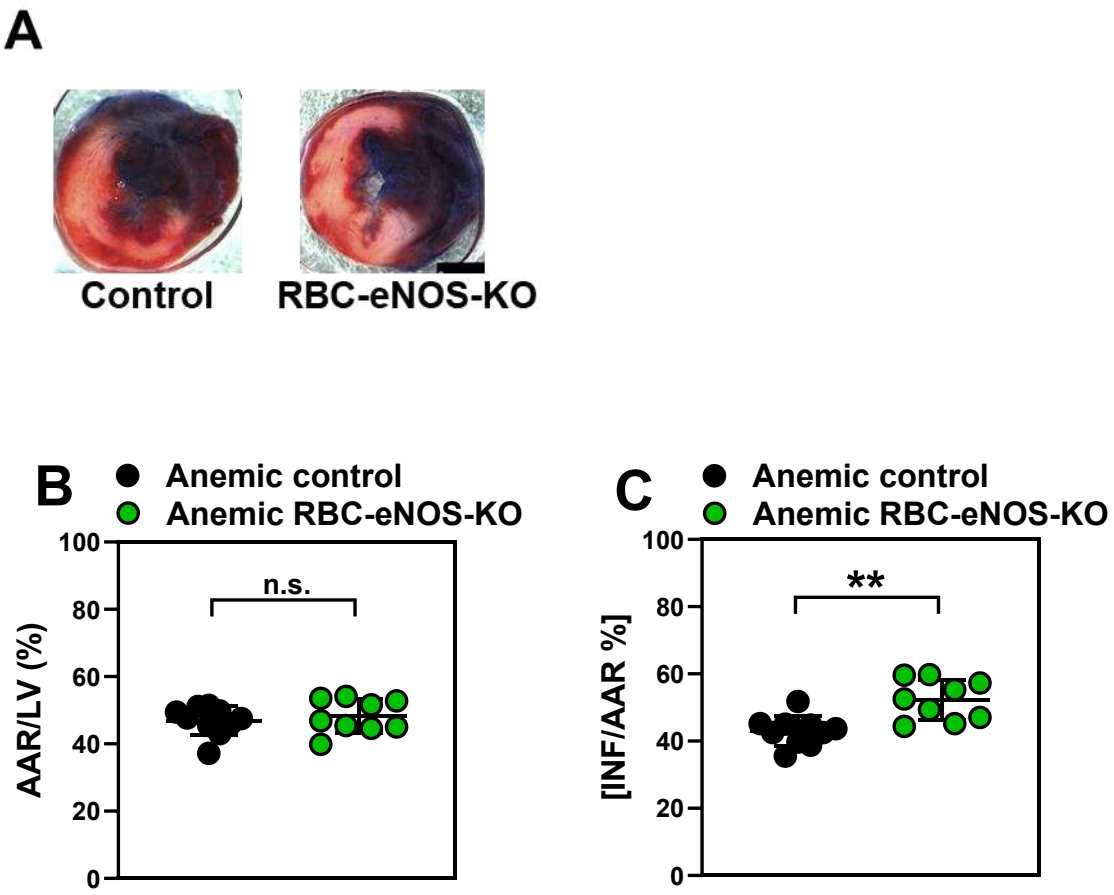

Figure 30: Anemic RBC eNOS deficient mice show an increased infarct size compared to anemic control mice. AMI was induced in RBC eNOS deficient (green circles) and their respective control mice (black circles). (A) Representative heart sections stained with TTC in the indicated animal groups. (B) Quantification of area-at-risk (AAR) relative to the LV. (C) Quantification of infarct area (INF) relative to the area-at-risk (AAR). All values are presented as mean ± SEM. A Student's t-test was used to compare the groups. **, $p \leq 0.01$; n.s., not significant.

Taken together, as we have demonstrated in a previous study, eNOS deficiency in RBCs of non-anemic mice resulted in increased systolic- and diastolic BP compared to mice with RBC eNOS. Anemia induction in RBC eNOS deficient mice led to a mitigated hypertension phenotype, as systolic- and diastolic BP were unchanged in anemic mice compared to control mice with anemia. Vascular function *in vivo* and *ex vivo* in anemic mice deficient of RBC eNOS did not show significant differences compared to anemic mice with RBC eNOS. After AMI induction, LV function was preserved in anemic RBC eNOS deficient mice, indicated by unchanged cardiac parameters compared to the anemic control mice. Measurement of infarct sizes by TTC staining demonstrated enhanced infarct size in RBC-eNOS-KO anemic mice compared to their respective controls, indicating that RBC eNOS limits the infarct size.

5 Discussion

5.1 Blood loss anemia is associated with LV energy imbalance after AMI

Anemia has been identified as a risk factor for the outcome of several CVDs, such as AMI. The presence of anemia in AMI patients increases mortality rate and prolongs the hospital stay [187]. However, concrete mechanisms of how anemia affects AMI are not very well understood. Oxygen delivery is impaired in AMI through blockage of coronary arteries, resulting in the death of CMs. In anemic conditions, impaired oxygen supply to organs occurs through decreased RBCs, Hb or Hct which further reduces oxygen in CMs in AMI patients. When cells lack of oxygen, aerobic respiration is negatively affected. Reduced aerobic respiration might result in less energy production, which in turn influences cardiac function. Even though it is known that energy metabolism plays a crucial role in the pathophysiology of both anemia and AMI, the combined effects of anemia and AMI on cardiac energy metabolism have not been studied yet. The first part of this thesis aims to unravel the effect of anemia on AMI with a focus on energy metabolism. For this purpose, an established blood-loss anemia mouse model was used. To mimic AMI, I/R surgery was performed. Firstly, heart function was assessed *in vivo* using echocardiography and CMRI measurements to elucidate if anemia causes further deterioration on heart function after AMI. Next, proteomic analysis was performed to assess changes in protein expression in the ischemic and remote region of LVs collected from anemic and non-anemic mice after AMI. High resolution respirometry was performed with LV tissues of the ischemic and remote region of anemic and non-anemic mice after AMI to investigate possible changes in mitochondrial function between both groups. Afterwards, the oxidative damage was analysed using colorimetric assays and western blotting to investigate changes in oxidative stress between anemic and non-anemic mice after AMI. To clarify the role of oxidative stress in AMI with anemia, mice were then treated with the ROS scavenger NAC prior to anemia and AMI induction. Subsequently, high resolution respirometry was performed to assess cardiac mitochondrial function. Finally, the effect of RBCs on mitochondrial function in anemia after AMI was investigated. In the following paragraphs, the results will be discussed and finally an outlook is given for future perspectives in this research field based on observed findings in this thesis and based on existing literature.

5.1.1 Blood-loss anemia mouse model

Multiple mouse models of anemia are established to study different types of anemia, such as iron deficiency anemia (IDA) [231], anemia of inflammation [232] and sickle cell anemia [233]. IDA is the most frequent type of anemia in the global population [234], and has been therefore investigated in multiple studies using IDA mouse models [231, 235]. However, hospitalised patients commonly develop HAA. Approximately 40-74% of patients develop HAA during their hospital stay, as a result of frequent blood withdrawal for diagnostic tests and through surgical

interventions [177-179]. CAD patients, e.g. AMI patients, are as well affected, which results in worse outcomes [180-183, 207]. As the hospitalization and thus the blood-loss occurs over a short time period, a blood-loss anemic mouse model was developed, which induces anemia over three consecutive days. The volume of the blood withdrawn is equivalent to 10% of the total body weight of the mice, which might result in the mild loss of plasma proteins, such as vasoactive compounds. Our previous study, however, demonstrated that this blood-loss anemia mouse model does not result in significant protein loss and, therefore, does not lead to complications such as vascular edema and leakage [170]. This mouse model has already been used in combination with I/R surgery by our working group on the topic of endothelial function [214]. The same study elucidated endothelial dysfunction after AMI, which is further aggravated when anemia is present [214]. Since this mouse model is applicable for HAA, well-established and known to induce changes in vascular function post-AMI, we used this mouse model in the present study.

5.1.2 Heart function in anemia post-AMI

In this study, echocardiography measurements and CMRI were performed to assess cardiac function in anemic and non-anemic mice before and 24 h post-AMI. The attained results display increased CO, SV and EF in anemic mice without AMI. These findings are in line with previous studies, which showed that the lack of oxygen supply in anemia mediates compensatory mechanisms, which trigger tachycardia, and increase SV and CO [223, 236], and furthermore confirms the efficiency of the blood-loss anemia mouse model. After AMI induction both, anemic and non-anemic mice showed decreased EF, SV and CO, indicating overall decreased heart function as a result of CM death through ischemia, which is characteristic after MI [237, 238] and confirms successful AMI induction. However, apart from decreased EF in anemic mice after AMI, no significant changes were observed between both groups after AMI. Global heart function was unchanged in anemia after AMI compared to respective non-anemic control mice with AMI, which might be due to the loss of the compensatory changes in the vascular system. To our surprise, CMRI results unveiled that in the ischemic region of anemic mice after AMI fractional shortening, a measure for contractility, was significantly reduced compared to non-anemic mice after AMI. Taken together, global heart function was unchanged after AMI in anemic mice compared to non-anemic mice after AMI. However, in the ischemic region the contractility was decreased, indicating that only the ischemic region of the heart is affected by anemic conditions after AMI.

5.1.3 Cardiac energetics in anemia post-AMI

Due to its continuous contraction, the energy demand in the heart is high. Impairment in energy production could lead to worsened outcome. Hence, cardiac energetics were assessed in mice before and after anemia and AMI induction. Anemic mice without AMI showed no significant

changes in ATP hydrolysis and resynthesis, indicating that anemia alone does not disrupt energy consumption and usage in the heart. This finding is contradictory to a study, which demonstrated decreased ATP levels in iron deficient human embryonic stem cell-derived CMs [239]. Similarly, in numerous other studies decreased cardiac energy was observed in iron deficient states [240-244]. Another study revealed diminished ATP levels in RBCs of individuals with hemolytic anemia [245]. Our CMRI data, however, did not show alterations in ATP hydrolysis and resynthesis in our HAA mimicking anemic mouse model. A possible explanation might be that in blood-loss anemia the compensatory mechanisms to adjust to reduced oxygen delivery to tissues is more effective, regulating ATP availability.

AMI induction in both, anemic and non-anemic mice, resulted in overall elevated ATP hydrolysis and reduced resynthesis in the ischemic region. Increased ATP hydrolysis is driven by the increased demand for energy after AMI. Decreased ATP resynthesis is attributed to the loss of viable CMs in the ischemic region, which lead to decreased respiration and therefore decreased ATP availability [246]. Previous studies have shown that exogenous PCr administration or ATP administration showed beneficial effects after ischemia [247-249], highlighting the effects of AMI on cardiac energetics. After AMI induction, the compensatory mechanism in anemia to stabilize energy availability is diminished, as anemic mice show increased ATP hydrolysis and decreased ATP resynthesis compared to their non-anemic controls after AMI. These results go hand in hand with heart function analysis, which revealed that the compensatory increase in heart function is lost after AMI induction in anemia. This effect is only observed in the ischemic region, whereas in the remote region ATP availability is unchanged, further underlining the regional specific effects of anemia after AMI.

5.1.4 Proteomic analysis in anemia after AMI

5.1.4.1 Mitochondrial respiration linked proteins

As our previous findings showed significant changes in cardiac function and cardiac energetics in the ischemic region of anemic mice after AMI, we analysed the proteome of ischemic and remote LV tissues from anemic and non-anemic mice 24 h post-AMI, to evaluate potential changes in mitochondrial protein expression. In the ischemic region of anemic mice, the top ten altered biological pathways are associated with mitochondria and OXPHOS, whereas in the remote region these pathways seem to be unchanged. The volcano plot unveiled that many proteins are altered in the ischemic region of anemic mice. Among these proteins, a significant number is associated with energy metabolism and mitochondrial dynamics. Interestingly, increased expression of Ndufb6 and Ndufs7, subunits of CI, in the ischemic region of anemic mice after AMI were observed. A previous study demonstrated that Ndufb6 subunit is crucial for complex I activity, using RNA interference in human cell lines [250]. Impaired CI activity or dysfunction is susceptible for ROS generation, harming the cells [251]. As Ndufb6 and Ndufs7

expression are elevated in the ischemic region of anemic mice after AMI, ROS formation may be triggered through increased CI activity. In contrary to our observations, downregulation of Ndufb6 has been observed in different disease states, such as renal cancer [252] and diabetes [253]. Furthermore, in a mouse model of MI, decreased mRNA levels of Ndufb6 were observed [254]. These studies highlight the importance of Ndufb6 and its expression profile in pathologies. Similarly, loss or decreased Ndufs7 expression is associated with different pathologies, e.g. bipolar disorder [255] and tuberculosis [256]. Rhein et al. revealed that Ndufs7 deficiency disrupts the juncture formation between peripheral and membrane arms of CI [257], affecting CI activity. Mitochondrial CI deficiency is associated with CVD development [258]. In a rare anemia type known as fanconi anemia, CI is known to be defect, affecting mitochondrial respiration in affected individuals [259]. It has also been shown that a mutation in Ndufb11, another subunit of CI, leads to the development of X-linked sideroblastic anemia [260]. We speculate that the expression of Ndufb6 and Ndufs7 is upregulated in the ischemic region of anemic mice after AMI as a compensatory response to hypoxia induced by anemia and AMI. However, this upregulation may exacerbate oxidative stress, via reversed ETS, a response to AMI [103], which might be aggravated by anemia. This in turn might result in impaired ATP synthesis and thus contributes to CM- and ultimately cardiac dysfunction and I/R injury. Furthermore, CIII subunit Uqcr10 was significantly higher expressed in the ischemic region of anemic mice after AMI. In contrast, absence of Uqcr10 results in in defective assembly of CIII [261], affecting OXPHOS. As CIII triggers ROS formation [262], defective CIII assembly may increase ROS levels in anemia further deteriorating OXPHOS. CIII plays a crucial role in different CVDs, such as MI [263] and diabetes [264]. With regard on our and previous findings, we assume that CIII activity is affected by the upregulation of Uqcr10, leading to increased ROS production in the ischemic region of anemic mice after AMI. Apart from subunits of the ETS complexes, Sdhaf2, an assembly factor for CII, expression was increased in the ischemic region of anemic mice after AMI compared to their controls. Chen et al. showed that Sdhaf2 enhances CII stabilization, which facilitated mitochondrial respiration through CII activity [265]. Disrupted CII activity was observed in patients with diabetic cardiomyopathy and hypertrophic cardiomyopathy [266], and is associated with ROS [267]. However, our findings demonstrate increased expression of Sdhaf2 in anemia after AMI, which contradicts with previous findings of reduced Sdhaf2 expression in pathologies. We propose, similarly to CI subunit upregulation, that Sdhaf2 expression is increased as a response to less O_2 and viable cells, to maintain mitochondrial respiration in the ischemic region of anemic mice after AMI. NAD biosynthesis related proteins Nmnat3 and Kyat3 were also elevated in the ischemic region of anemic mice. The reduced form of NAD, NADH, is oxidized by CI, fuelling mitochondrial respiration. A study by Hikosaka et al. demonstrated that hemolytic anemia resulted from Nmnat3 deficiency, using a gene-trapped mouse model. This study

demonstrated that Nmnat3 deficiency affected matured RBCs by diminishing their NAD pool. This led to lower ATP concentration and reduced RBC lifespan [268]. The alterations in the protein expression of these proteins might be caused as a result of increased Ndufb6 and Ndufs7. We hypothesize that the overexpression of NAD biosynthesis related proteins Nmnat3 and Kyat3 trigger ROS formation, by fueling CI with their substrate NAD in the ischemic region of anemic mice after AMI.

Taken together, CI, II and III associated proteins were upregulated in the ischemic region of anemic mice after AMI, possibly to compensate the decrease in mitochondrial respiration in anemic state after AMI. However, this eventually caused impairment in mitochondrial respiration through increased CI and CIII activity, resulting in increased oxidative stress. This in turn damages other mitochondrial proteins, which impairs mitochondrial respiration and ATP synthesis, affecting heart function.

5.1.4.2 Mitochondrial dynamics related proteins

Intact mitochondrial dynamics are important for physiological cell function. Impairment in mitochondrial dynamics contribute to the progression of different disease conditions. CVD development is known to be driven by dysfunctional mitochondria [269, 270]. We investigated the expression of various mitochondrial dynamics-related proteins in LV tissues of anemic and non-anemic mice before and after AMI induction. After AMI induction, remote and ischemic regions were analyzed separately.

5.1.4.2.1 Mitophagy in anemia before and after AMI

Proteins related to mitophagy, namely BNip3, Phb2, Mul1, Optn, Nipsnap2, Park7, Bcl2l13 and Fkbp8 were analysed, and the results showed that in anemic mice Nipsnap2 protein expression was significantly higher than in non-anemic mice. A slightly increased Park7 expression and decreased tendency in Mul1 expression were also observed in anemic mice. Several studies have been performed, which described the role of mitophagy in different types of anemia. Hara et al. demonstrated that iron deficiency mediated mitophagy in hepatoma cells, which suppressed the progression liver tumor [271]. A previous study showed that receptor-mediated mitophagy was protective against renal anemia by regulating erythropoietin (EPO) protein [272]. A clinical study proved that dysregulated mitophagy in nucleated erythroid cells led to the pathogenesis of anemia in myelodysplastic syndrome patients [273]. Nipsnap2 accumulation on mitochondrial surfaces triggers mitophagy by recruiting autophagy receptors [274]. Park7 is known to sense ROS in mitochondria, enabling the regulation of mitophagy [275]. Mul1 regulates mitophagy by sensing stress signals in mitochondria [276]. As these proteins are differentially expressed in anemic mice, we assume that mitophagy regulation is altered in anemia. Since Nipsnap2 expression is increased in anemic mice, we believe that mitophagy is increased in anemia, which is line with previous studies that demonstrated that

hypoxia increases mitophagy [277]. We assume that mitophagy might be increased due to decreased oxygen supply and increased ROS in anemia, through which the mitochondria become dysfunctional. Increased mitochondrial stress in dysfunctional mitochondria is then sensed by increased Park7 expression and mitophagy is activated to remove dysfunctional mitochondria. After AMI induction no significant changes were observed in the remote region of anemic and non-anemic mice, indicating unchanged mitophagy. However, in the ischemic region decreased expression of BNip3 was observed in anemic mice. Many studies have shown that mitophagy is heavily affected by ischemia [278, 279]. After AMI, mitophagy is increased, and if suppressed myocardial damage is deteriorated [280-282]. BNip3 has been shown to enhance mitophagy by regulating the crosstalk between mitophagy and apoptosis [283]. In contrast to our results, which indicated that mitophagy is decreased in the ischemic region of anemic mice, studies have reported that BNip3 expression is triggered in hypoxic conditions such as AMI [284].

Based on our findings and existing literature, we assume that anemia alone possesses protective mechanisms such as mitophagy. After AMI induction however this adaptation is lost in the ischemic region, increasing the number of dysfunctional mitochondria.

5.1.4.2.2 Mitochondrial fusion and fission in anemia before and after AMI induction

Mitochondrial fusion associated proteins Mfn1, Mfn2, OPA1, Mtch2 and Arl2 were analysed in the proteome of anemic and non-anemic mice with and without AMI induction. In cardiac setting, Mfn1 and Mfn2 have been identified to play a crucial role. In a rat model of HF Mfn1-ßIIIPKC interaction was inhibited, which led to the improvement of mitochondrial and ultimately cardiac function [285]. Hall et al. demonstrated that ablation of Mfn1 and Mfn2 reduced infarct size and mitochondrial swelling after I/R surgery [286]. Our data showed no significant alterations in Mfn1 and Mfn2 expression in anemia before and after AMI compared to their non-anemic controls. Since Mfn1 and Mfn2 play a key role in AMI, we expected altered expression in anemia after AMI, as the hypoxic conditions are further aggravated. Interestingly, Arl2 expression was increased in anemic mice compared to their controls. Arl2 has been shown to fuel mitochondrial fusion, while deficiency decreases mitochondrial fusion [287]. Hence, increased Arl2 expression in anemia hints on increased mitochondrial fusion. Mitochondrial fusion and its role in anemia has not been elucidated yet, however one study showed that tumor cells showed enlarged mitochondria through increased mitochondrial fusion in prolonged hypoxia [288]. Mitochondrial fusion is not only thought to protect mitochondria from mitophagy but also enables genetic complementation. Genetic complementation through mitochondrial fusion aids to even out the dysfunctionalities of the mitochondria [289]. Therefore, we conclude that in anemia dysfunctional mitochondria are fused to increase their repair rate through genetic complementation. After AMI induction, neither in the ischemic

region nor in the remote region significant changes were observed between anemic and non-anemic mice, indicating that mitochondrial fusion is unaltered in anemia after AMI.

Mitochondrial fission is pivotal for mitochondrial quality control, as fission distinguishes and separates dysfunctional mitochondria from intact mitochondria. Cardiac metabolic homeostasis is balanced by mitochondrial fission and fusion [290], but a heavy shift towards fission contributes to the pathogenesis of several CVDs, including I/R injury [291], pathological hypertrophy [292] and atherosclerosis [293]. However, some studies highlighted the protective property of fission and mitophagy, as dysfunctional mitochondria generate more ROS [294]. Mitochondrial fission proteins, namely Fis1, OPA3, Drp1, Mtfn1, Slc25a46 and Armc10 were analysed in anemic mice before and after AMI. Using Drp1 knockout mouse model, Ishikawa et al. demonstrated that Drp1 deletion resulted in anemia [295]. In our study, blood-loss anemic mice exhibited increased Drp1 and Mtfp1 compared to their non-anemic controls, hinting at increased mitochondrial fission. These results are consistent with the results of mitophagy related proteins, as fission and mitophagy are tightly connected. Mitochondrial fission results from different processes such as loss of Mfns, reduced GTPase activities, reduced ATP production and enhanced ROS levels [296]. Elevated ROS levels are observed in anemic conditions, which possibly increased mitochondrial fission in our experimental group. We assume that through fission, dysfunctional mitochondria are segregated and further removed by mitophagy in anemia. In the ischemic region of anemic mice after AMI induction, Armc10 expression was significantly reduced. Armc10 has shown to induce mitochondrial fission when highly expressed, and to decrease fission when lowly expressed in knockout hepatic cell lines [297]. Hence, our data point towards mitochondrial fission being decreased in the ischemic region of anemic mice after AMI. We propose that the adaptive mechanism, which included increased fission and mitophagy to remove dysfunctional mitochondria, is lost and even further exacerbated after AMI in the ischemic region of anemic mice. This eventually leads to the accumulation of dysfunctional mitochondria and thus increased generation of ROS.

5.1.5 Mitochondrial respiration in anemia before and after AMI

Our CMRI results showed impaired ATP availability in the ischemic region of anemic mice, and our proteomic data suggest alterations in mitochondrial respiration as ETS linked protein expressions were changed. In order to attain an in depth view into mitochondrial function in anemia with and without AMI, respirometry analyses were performed in LV tissues of anemic and non-anemic mice before and after AMI induction. In a rat model of IDA, Fischer et al. assessed mitochondrial respiration in the liver, and demonstrated unchanged respiration [298]. In opposite, a study using iron depletion in CMs showed worsened mitochondrial function in iron deficient state [239]. In another study impaired mitochondrial respiration was observed in Fanconi anemia [299]. Based on these studies we expected altered respiration in our blood-

loss anemic mice tissues. To our surprise, no changes in mitochondrial function were observed. Apart from the contradiction from previous studies, this observation is corresponding to our CMRI and echocardiography data, which showed unchanged ATP availability and adapted heart function. Mitochondrial dysfunction and impaired respiration in AMI has been described previously [300-302]. However, the impact of anemia on mitochondrial function in the context of AMI has not yet been studied. Interestingly, our data shows that after AMI induction, in the ischemic region of anemic mice, RCR Coupling$_{FNS}$ was significantly reduced. RCR Coupling$_{FNS}$ describes how well redox reactions at the ETS are coupled with the phosphorylation of ADP to ATP by ATP synthase. A reduced RCR Coupling$_{FNS}$ indicates either that substrate oxidation at the ETS is impaired or that the proton gradient, which is generated through the activity of CI-IV, cannot be efficiently used by the ATP synthase. This is likely due to the fact that in pathological conditions, in this case anemia following AMI, the inner mitochondrial membrane is often described as leaky and more permeable, allowing protons to diffuse into the mitochondrial matrix and bypass ATP synthase. [303]. In line with this, our data showed a trend towards increased LEAK state in the ischemic region of anemic mice compared to non-anemic mice. This causes the reduction of the proton gradient, which then cannot be used by the ATP synthase for ATP synthesis. As a result, less ATP is produced, which supports our finding of decreased ATP availability in the ischemic region of anemic mice using CMRI. When comparing the mitochondrial respiration in the remote and ischemic region of both, anemic and non-anemic groups, we see an overall decreased respiration the ischemic region, which can be explained by the overall reduction of viable CMs in the ischemic region. Furthermore, we expected adapted increase in CI, II and III linked respiration, which are displayed as $[F]_P$, $[FN]_P$ and $[FNS]_P$, as our proteomics data revealed increased expression in CI, II and III subunits or assembly factors. Despite of worsened RCR Coupling$_{FNS}$, maximal OXPHOS capacity in the presence of substrates feeding electrons to CI, CII and the Q-junction was unaltered in the ischemic region of anemic mice. Since the electrons are passed from CI and II through the Q-junction to CIV, these results indicate that the ETS was unaltered, not contributing to the impaired mitochondrial respiration. Though, we have to take into consideration that the proteomics data only give information about protein expression, not the function.

5.1.6 Oxidative stress in anemia before and after AMI induction

Since our previous results demonstrated impaired mitochondrial respiration in the ischemic region of anemic mice, we investigated oxidative stress in the tissues of our experimental groups. This approach was taken to identify the underlying mechanism in anemia causing exacerbated mitochondrial respiration and thus heart function after AMI. Redox imbalance has been shown to increase oxidative stress, contributing to the progression of CVD [304]. Increased ROS generation and altered antioxidant capacities attribute to redox imbalance

[104]. Antioxidant enzymes SOD and catalase, glutathione concentration and oxidative stress promoting MPO activity were assessed in anemic mice with and without AMI using biochemical assays. Furthermore, ROS level was assessed by determining 4-HNE expression using western blotting. Our working group showed that anemia exhibits increased ROS in aortic lysates and RBCs of chronic blood-loss anemic mice in previous studies [127, 170]. Similarly, we found that in LV tissues of anemic mice redox balance is impaired, as SOD activity and glutathione concentration were decreased. SOD actively scavenges ROS by catalysing the dismutation of $O_2^{\bullet-}$ to H_2O_2 and O_2 [305] and glutathione can be an antioxidant by itself and as a cofactor [306]. Decrease in SOD and glutathione hint at decreased antioxidant capacity. Additionally, a tendency towards increased MPO activity in anemic mice was observed, indicating increased ROS generation as MPO promotes ROS formation by generating HOCl acid using H_2O_2 and chloride [307]. Based on these and previous findings we believe that anemia triggers ROS formation in the LVs, which could further impact cell function by damaging proteins, membranes, DNA etc. After AMI induction, SOD activity was unchanged in remote and ischemic region. Glutathione was significantly decreased in the remote region of anemic mice, whereas in the ischemic region glutathione concentration was unchanged. These results suggest that antioxidant capacity is unchanged in anemia after AMI in the ischemic region. Interestingly, MPO activity was increased in anemia after AMI, in both remote and ischemic regions. Hence, ROS generation is aggravated in anemia after AMI by increased MPO activity, which is in line with our previous study, which elaborated that after AMI, blood-loss anemia is associated with elevated ROS level in endothelial cells [214]. In addition, western blot results revealed increased 4-HNE levels in LV lysates of the ischemic region of anemic mice. 4-HNE is a byproduct of lipid peroxidation, mediated by ROS. The main source of ROS is mitochondrial respiration, but studies have proven that ROS can further impair mitochondrial function by altering mitochondrial components [308, 309]. This observation could explain the previously attained results. We speculate that increased ROS levels in the ischemic region of anemic mice after AMI might affect mitochondrial respiration, eventually leading to diminished ATP levels and therefore reduced contractile function.

5.1.7 Mitochondrial respiration after ROS scavenging in anemia after AMI

After demonstrating that ROS levels are elevated in the ischemic region of anemic mice tissues, we wanted to investigate, whether ROS decreases mitochondrial function. For this purpose, we analysed mitochondrial respiration after treating the mice with NAC, a widely accepted ROS scavenger. NAC scavenging properties are attributed to the antioxidative potential of thiols or through increased glutathione concentration [310]. Our respirometry results show that reduced RCR $Coupling_{FNS}$ is normalized after NAC administration in the ischemic region of anemic mice, further confirming that elevated oxidative stress in anemia deteriorates mitochondrial respiration after AMI. Preserved RCR $Coupling_{FNS}$ indicates, that

the inner mitochondrial membrane is less permeable and leaky compared to non-treated anemic mice tissues, which increases the coupling of the redox reactions at the ETS and the phosphorylation of ADP to ATP by ATP synthase. This observation is consistent with a study on cultured CMs showed that NAC administration improved mitochondrial function. This study evidenced that mitochondrial function was recovered through increased expression of OPA1 [311]. Wright et al. demonstrated that NAC administration, in a mouse model of Huntington's disease, elevated mitochondrial function and improved deficits [312]. We propose that ROS damages the inner mitochondrial membrane, resulting in increased permeability which is prevented by ROS scavenging with NAC.

5.1.8 Mitochondrial content in anemic mice after AMI, with and without NAC treatment

Not only is mitochondrial function critical to bioenergetic function, but also mitochondrial density. For this reason, mitochondrial content in anemic mice after AMI with and without NAC treatment was assessed by measuring CS activity. CS is part of the TCA cycle and thus is expressed in mitochondria. It is commonly used as mitochondrial content marker [313]. Different studies have reported alterations in mitochondrial content in CVDs [314, 315]. Therefore, we were interested in possible changes in mitochondrial content in our experimental groups. We decided to use CS activity measurements as an approach to determine mitochondrial density, as Larsen et. al demonstrated that CS activity showed the strongest association with mitochondrial content [313]. The obtained results showed significantly reduced mitochondrial content in the remote region, but increased mitochondrial content in the ischemic region of anemic mice after AMI. Mitochondrial content is increased in case of high energy demand as a compensatory mechanism. Due to the necrosis of myocardial cells in AMI, energy demand is increased and further aggravated when anemia is present. This explains why we see elevated mitochondrial content in the ischemic region of anemic mice. However, the decrease in mitochondrial content in the remote region cannot be explained and needs further evaluation. The increase in mitochondrial content in the ischemic region in anemic mice is consistent with our previous findings of upregulated CI and CIII subunits and CII assembly proteins and decreased mitochondrial fission and mitophagy related proteins. The respirometry data showed impaired respiration in the ischemic region of anemic mice, indicating that the observed increased mitochondria are not functional but rather dysfunctional. NAC administration preserved altered mitochondrial content in both ischemic and remote regions of anemic mice. Since NAC treatment period started before anemia and AMI induction, we believe that mitochondrial damage through ROS was inhibited. This eventually hampered oxidative damage, which did not lead to adaptive mechanisms to overcome worsened mitochondrial and thus heart function.

We furthermore assessed protein expression of the ETS complexes in the ischemic region of anemic and non-anemic mice after AMI. We hypothesized based on the increased mitochondrial content and increased expression of CI, II and III related proteins, that ETS CI, II and III are upregulated in the ischemic region of anemic mice. To our surprise, in contradiction to our findings, no significant alterations in ETS complex expression were observed. However, it's important to note that the proteomic analysis only revealed reduced expression of two out of 45 CI subunits, one out of 11 CIII subunits and one CII assembly protein. These alterations may not affect the overall expression levels of the ETS complexes, which could explain the lack of observable changes. In previous studies, various biochemical markers for mitochondrial content have been used, such as mtDNA copy number, cardiolipin content and more. Larsen et. al compared these markers with the gold standard to assess mitochondrial density: electron microscopy. However, this study measured mitochondrial content in skeletal muscle of healthy patients and not in heart tissues and in disease [313]. Therefore, it is still unknown which method is more suited for heart tissues in disease. For this reason, it is difficult to judge which method and the resulting results are more accurate in this study.

5.1.9 Effect of anemic RBCs on mitochondrial respiration

Our working group has shown that anemic RBCs are dysfunctional and are associated with increased ROS, membrane instability and reduced NO pool [170]. We furthermore demonstrated that cardioprotective properties of RBCs are lost in anemia after AMI, by *ex vivo* isolated perfused heart experiments [145]. Kuhn et al. proposed that non-canonical functions of RBCs, such as NO metabolism, oxidative stress, blood rheology and viscosity could impact CVD outcome [152]. Therefore, we wanted to investigate the effect of anemic RBCs on mitochondrial function in LVs of wild type mice *ex vivo*. Our data shows that anemic RBCs did not alter mitochondrial function in wild type mice hearts *ex vivo*. Based on our previous findings on dysfunctional RBCs in anemia and other literature, we expected that anemic RBCs have an effect on mitochondrial function in CMs. Moreover, this thesis demonstrated that the absence of eNOS in anemic RBCs led to impaired vascular healing, as evidenced by increased infarct size. Given that vascular healing is dependent on mitochondrial function, we expected that mitochondrial respiration would be altered in CMs incubated with anemic RBCs. A possible explanation for our observation is that the incubation time of the RBCs with the mice hearts was too short to trigger changes in mitochondrial respiration. Another reason may be that anemic RBCs alone do not impair mitochondrial respiration in CMs but together with other cell types changes might occur.

5.2 The role of RBC eNOS in anemia before and after AMI

Anemia is commonly observed in patients with CVD, including both acute and chronic coronary syndromes as well as heart failure. Approximately 30% of patients presenting with STEMI either have anemia at admission or develop it during hospitalization a condition that has been linked to poor clinical outcomes [181, 316]. Numerous studies have established that anemia, either independently or in conjunction with other comorbidities, contributes to a worse prognosis in AMI [211]. These findings suggest that dysfunctional RBCs in anemic conditions play a role in exacerbating CVD severity. Our previous study demonstrated that anemia triggers a compensatory upregulation of eNOS and enhances FMD, aiming to maintain adequate peripheral tissue perfusion despite reduced oxygen-carrying capacity [170]. Concurrently, anemia is associated with RBC dysfunction indicated by reduced NO bioavailability, increased ROS production, compromised membrane integrity, and elevated NO scavenging by free plasma Hb [170]. In the same study, we also demonstrated that anemia negatively affects cardiac function even though infarct size was unchanged [170]. Previous investigations have reported that RBCs from AMI patients lose their cardioprotective properties during I/R injury in *ex vivo* models [145]. However, the impact of anemia on vascular and cardiac function under conditions of eNOS deficiency in RBCs remains unclear. This study aimed to unravel the effects of RBC eNOS in anemia on cardiac- and vascular function with and without AMI. To reach our aim, we used a RBC-eNOS-KO mouse model, in which anemia was induced. Hemodynamics were assessed using Millar catheter measurements. Vascular function *in vivo* and *ex vivo* were analysed by FMD measurements and wire myography. To further elucidate the role of RBC eNOS in anemia after AMI, cardiac function was assessed using echocardiography in anemic and non-anemic RBC-eNOS-KO mice 24 h after AMI. Finally, infarct sizes in these mice were measured using TTC staining. In the following paragraphs the results will be discussed using existing literature.

5.2.1 Cardiac function in anemia and RBC eNOS deficiency

Endothelial eNOS function is pivotal for vascular tone regulation, as it produces NO, an important modulator in the vascular system. Previous studies have demonstrated that eNOS deficiency led to endothelial dysfunction and thus hypertension, with a greater risk to thrombosis, atherosclerosis and stroke [317, 318]. Leo et al. investigated the impact of targeted eNOS deletion in ECs and RBCs on vascular- and cardiac function in mice. This study observed abolished vascular function in EC specific eNOS deficient mice, whereas RBC eNOS deficiency did not alter vascular function. However, both EC- and RBC eNOS deficiency resulted in hypertensive phenotypes [157]. This finding is in line with our observation, that non-anemic mice without RBC eNOS exhibited increased BP. Interestingly, we observed that anemic RBC eNOS deficient mice showed normalized systolic and diastolic BP. Volumetric viscosity changes and/or other increased vasodilatory mechanisms in anemia are likely the

reason for this observation. Based on our previous study, which demonstrated increased eNOS expression in anemia [170], the mitigated phenotype in anemic RBC eNOS deficient mice may be due to compensatory increase in eNOS in other cell types, such as ECs and CMs which further need to be investigated.

5.2.2 Vascular function in anemia and RBC eNOS deficiency

A global deletion of eNOS leads to impaired vascular function, demonstrated by previous studies [319]. Cell-specific eNOS deletion in ECs was shown to impair endothelial function. The same study observed no significant changes in vascular function when RBC eNOS is deficient [157]. This finding corresponds to our results, which showed no alterations in endothelial function *in vivo* and *ex vivo* in non-anemic RBC eNOS deficient mice. As our hemodynamics measurements revealed mitigated hypertension in anemic RBC eNOS deficient mice, we expected differences in vascular function. Vascular function was unchanged in anemic RBC eNOS deficient mice indicating that vascular endothelial eNOS plays a fundamental role in vessel tone regulation rather than RBC eNOS.

5.2.3 The effect of RBC eNOS deficiency on cardiac function and infarct size in anemia after AMI

To unravel the effect of RBC eNOS in anemia after AMI, echocardiography measurements were performed. Mice that underwent AMI surgery, independent of RBC eNOS expression, exhibited decreased cardiac performance, evidenced by decreased SV and CO and increased ESV. Similarly, previous studies stated that AMI resulted in increased ESV [320], decreased SV [321] and CO [322], revealing decreased contractile function. However, no significant changes in HR, ESV, EDV, SV and CO between anemic mice with and without RBC eNOS were observed, indicating that RBC eNOS deficiency in anemia after AMI does not affect cardiac function. Based on these findings, we expected unchanged infarct size in anemic mice deficient of RBC eNOS. Nevertheless, infarct size evaluation demonstrated enhanced infarct size in anemic RBC eNOS deficient mice compared to their anemic control mice. These results align with our previous study, which elucidated the importance of RBC eNOS in AMI, underlining the cardioprotective properties of RBC eNOS, by increased infarct size in RBC eNOS deficient state [230]. These findings indicate that RBC eNOS confers protection in anemia after AMI, although a direct impact on cardiac function remains unproven. Further research should be conducted to investigate the mechanism of how cardiac function in anemic RBC eNOS deficient state after AMI is preserved, even though infarct size is increased.

The findings of this study conclude that RBCs in anemia mitigate the increase in blood pressure in RBC eNOS deficient mice. Furthermore, this study demonstrated the cardioprotective role of RBC eNOS in anemia after AMI, as infarct sizes were significantly increased in RBC eNOS deficient state under anemic conditions.

6 Clinical relevance

Previous studies highlighted the importance of anemia in different comorbidities such as heart failure, LV hypertrophy, chronic kidney disease, diabetes mellitus and atherosclerosis, by showing that anemia exerted worsened outcomes [188, 191-193]. This study demonstrated that the presence of anemia in AMI worsens regional LV function and impairs mitochondrial respiration in the ischemic region, underlining the adverse effect of anemia in AMI. The key findings suggest to consider PCr/ATP and Pi/ATP ratio assessment to evaluate regional energy demand and usage in LVs of STEMI patients and subsequently their overall prognosis. As these can be easily assessed by non-invasive CMRI imaging, the assessment can be implemented to improve therapeutic strategies in STEMI patients with anemia [323].

This study also demonstrates that despite unchanged respirometry, blood loss anemia results in compensatory upregulation of mitochondrial related proteins. This finding highlights the importance of treating anemia even without onset of CVDs. Another important finding of the study is the upregulation of MPO, especially after AMI, in anemic mice. Preliminary data of our working group showed that inhibition of MPO in aortic segments of anemic mice improved endothelial function e*x vivo*. A recent clinical trial study showed that MPO inhibitors are proven to improve heart function in heart failure patients [324]. However, the beneficial effects of MPO inhibitors after AMI need to be further investigated in the context of anemia.

Furthermore, our findings indicate that oxidative stress in anemia is the primary contributor to these changes, as the detrimental effects of anemia were mitigated with NAC supplementation. NAC treatment has previously been shown to enhance mitochondrial function in a mouse model of Huntington’s disease [297] and in a rat model of I/R injury [301]. Clinically, NAC is widely used to treat paracetamol overdose, and diseases related to oxidative stress and inflammation [302]. Furthermore, a clinical study including diabetic patients demonstrated that NAC treatment decreased major adverse cardiovascular events [303].

In this study, NAC administration improved mitochondrial function and mitochondrial density, which may have improved mitochondrial respiration in the ischemic region under anemic conditions. Therefore, this study further underlines the advantageous effects of NAC on mitochondrial dysfunction in anemia after AMI, and proposes NAC as therapeutic approach for ROS induced mitochondrial dysfunction in anemia after AMI. NAC is a well-accepted supplement in clinical practice with minimal side effects, thus the findings of this study could be readily implemented for anemic patients with AMI. Given NAC's established safety profile and widespread clinical use, the findings of this study suggest its integration into the treatment of anemic patients with AMI.

The activity of eNOS is crucial for a functional cardiovascular system (CVS). Uncoupling of eNOS or other dysfunctionalities induce endothelial dysfunction by limiting NO bioavailability [169]. Indirect modulation of eNOS is currently used in clinical practice. In clinical trials, supplementation of L-arginine, the substrate of eNOS, ameliorated symptoms associated with CVDs [325]. We have previously shown that RBC eNOS exhibits cardioprotective properties in AMI [230]. This study further highlighted the importance of RBC eNOS in anemia after AMI, as infarct sizes were increased when RBC eNOS was deficient. Based on these findings, we propose RBC eNOS as therapeutic target in anemia after AMI. L-arginine supplementation might increase RBC eNOS in anemia, which eventually recovers the cardioprotective properties, improving the outcome after AMI.

7 Conclusions and future perspectives

The leading cause of mortality worldwide is AMI, and in combination with other comorbidities, the outcome is worsened. Anemia has been shown to result in poor prognosis when present in AMI. However, the underlying mechanisms of how anemia affects AMI outcome remain unknown. Therefore, this study aimed to unravel the underlying effect of anemia on cardiac metabolism after AMI. This study demonstrates that anemia is associated with an adaptive enhancement in global LV function, which is lost after AMI, indicating a pathological impact of anemia on LV function. CMRI data revealed a decreased cardiac energetic state (PCr/ATP) specifically in the ischemic region of anemic mice compared to control mice. In line with these findings, the ischemic region of anemic mice showed reduced contractility, reflecting regional LV dysfunction. This also aligns with our respirometry data, which shows impaired mitochondrial respiration in the ischemic region anemic mice after AMI, even though we observed compensatory increase in CI, CII and CIII subunits and assembly proteins. In the ischemic region we also observed increased MPO activity and 4-HNE levels, concluding the potential role of ROS in mediating regional LV dysfunction in anemia after AMI. Notably, ROS scavenging with NAC preserved mitochondrial respiration in the ischemic region, further supporting the role of ROS in LV dysfunction in anemia after AMI. Overall, the findings of this study suggest that targeting cardiac metabolism and mitochondrial respiration could serve as a potential therapeutic strategy for anemic patients post-AMI. Furthermore, this study highlights the potential of NAC as a promising therapeutic approach to mitigate adverse outcomes in this population. Future research should investigate mitochondrial morphology in CMs in anemia, both with and without AMI, as impaired oxygen supply may affect mitochondrial structure. Additionally, the role of dysfunctional anemic RBCs in mitochondrial respiration warrants further exploration. Expanding knowledge in this field could facilitate the development of novel therapeutic approaches for managing anemia in the context of AMI.

Functional eNOS is crucial for a healthy CVS, and dysfunctionalities or absence have been shown to negatively impact the CVS. Different cell-specific eNOS play different roles in vascular and cardiac function. However, the role of cell-specific eNOS, such as RBC eNOS, in anemia with and without AMI may affect the CVS differently. For this reason, this study aimed to investigate the role of RBC eNOS in anemia with and without AMI. The results of this study demonstrate that RBC eNOS deficiency in anemia does not affect vascular endothelial function. Interestingly, this study showed mitigated hypertension in RBC eNOS deficient anemic mice. In addition, we showed that RBC eNOS has cardioprotective properties in anemia after AMI, without directly impairing cardiac function. Nevertheless, it is not fully understood yet how anemia mitigated increased BP when RBC eNOS is deficient. In future, eNOS expression and activity should be evaluated in heart and vascular tissue, to gain a

deeper insight into the mechanisms of cell-specific eNOS. Additionally, hemodilution in RBC eNOS deficient anemic mice should be evaluated, to possibly explain the observed mitigated hypertension phenotype. Advancing our understanding in this field may enable the development of new therapeutic strategies including RBC eNOS in CVDs such as AMI and anemia.

8 References

1. Rehman, I. and A. Rehman, *Anatomy, Thorax, Heart*, in *StatPearls*. 2024: Treasure Island (FL).
2. Litvinukova, M., et al., *Cells of the adult human heart.* Nature, 2020. **588**(7838): p. 466-472.
3. Emond, M., et al., *Long-term survival of medically treated patients in the Coronary Artery Surgery Study (CASS) Registry.* Circulation, 1994. **90**(6): p. 2645-57.
4. Hammermeister, K.E., T.A. DeRouen, and H.T. Dodge, *Variables predictive of survival in patients with coronary disease. Selection by univariate and multivariate analyses from the clinical, electrocardiographic, exercise, arteriographic, and quantitative angiographic evaluations.* Circulation, 1979. **59**(3): p. 421-30.
5. White, H.D., et al., *Left ventricular end-systolic volume as the major determinant of survival after recovery from myocardial infarction.* Circulation, 1987. **76**(1): p. 44-51.
6. Herlitz, J., et al., *Long term prognosis after CABG in relation to preoperative left ventricular ejection fraction.* Int J Cardiol, 2000. **72**(2): p. 163-71; discussion 173-4.
7. Yamaguchi, A., et al., *Left ventricular end-systolic volume index in patients with ischemic cardiomyopathy predicts postoperative ventricular function.* Ann Thorac Surg, 1995. **60**(4): p. 1059-62.
8. Bigger, J.T., Jr., et al., *The relationships among ventricular arrhythmias, left ventricular dysfunction, and mortality in the 2 years after myocardial infarction.* Circulation, 1984. **69**(2): p. 250-8.
9. Moss, A.J., et al., *Improved survival with an implanted defibrillator in patients with coronary disease at high risk for ventricular arrhythmia. Multicenter Automatic Defibrillator Implantation Trial Investigators.* N Engl J Med, 1996. **335**(26): p. 1933-40.
10. Moss, A.J., et al., *Prophylactic implantation of a defibrillator in patients with myocardial infarction and reduced ejection fraction.* N Engl J Med, 2002. **346**(12): p. 877-83.
11. Horii, T., et al., *Left ventricle volume affects the result of mitral valve surgery for idiopathic dilated cardiomyopathy to treat congestive heart failure.* Ann Thorac Surg, 2006. **82**(4): p. 1349-54; discussion 1354-5.
12. Tafreshi, R.I., A. Shahmohammadi, and P.N. Davari, *Predictors of left ventricular performance after valve replacement in children and adolescents with chronic aortic regurgitation.* Pediatr Cardiol, 2005. **26**(4): p. 331-7.
13. Pinto, F.J., *Echocardiography in left ventricular dysfunction.* Ital Heart J, 2004. **5 Suppl 6**: p. 41S-47S.
14. Investigators, S., et al., *Effect of enalapril on mortality and the development of heart failure in asymptomatic patients with reduced left ventricular ejection fractions.* N Engl J Med, 1992. **327**(10): p. 685-91.
15. Schunkert, H., et al., *Left-ventricular dysfunction.* Lancet, 1998. **351**(9099): p. 372.
16. Lazzeroni, D., O. Rimoldi, and P.G. Camici, *From Left Ventricular Hypertrophy to Dysfunction and Failure.* Circ J, 2016. **80**(3): p. 555-64.
17. Chockalingam, A., et al., *Acute left ventricular dysfunction in the critically ill.* Chest, 2010. **138**(1): p. 198-207.
18. Domanski, M.J. and M.E. Farkouh, *Optimal Treatment of Patients With Left Ventricular Dysfunction and Severe Coronary Artery Disease.* Circulation, 2018. **138**(19): p. 2079-2080.
19. Mechanic, O.J., M. Gavin, and S.A. Grossman, *Acute Myocardial Infarction*, in *StatPearls*. 2024: Treasure Island (FL).
20. Salari, N., et al., *The global prevalence of myocardial infarction: a systematic review and meta-analysis.* BMC Cardiovasc Disord, 2023. **23**(1): p. 206.
21. Alaour, B., F. Liew, and T.E. Kaier, *Cardiac Troponin - diagnostic problems and impact on cardiovascular disease.* Ann Med, 2018. **50**(8): p. 655-665.
22. Barberi, C. and K.E. van den Hondel, *The use of cardiac troponin T (cTnT) in the postmortem diagnosis of acute myocardial infarction and sudden cardiac death: A systematic review.* Forensic Sci Int, 2018. **292**: p. 27-38.

23. Nascimento, B.R., et al., *Implementing myocardial infarction systems of care in low/middle-income countries.* Heart, 2019. **105**(1): p. 20-26.
24. Daga, L.C., U. Kaul, and A. Mansoor, *Approach to STEMI and NSTEMI.* J Assoc Physicians India, 2011. **59 Suppl**: p. 19-25.
25. Reed, G.W., J.E. Rossi, and C.P. Cannon, *Acute myocardial infarction.* Lancet, 2017. **389**(10065): p. 197-210.
26. Dugani, S.B., et al., *Risk Factors for Premature Myocardial Infarction: A Systematic Review and Meta-analysis of 77 Studies.* Mayo Clin Proc Innov Qual Outcomes, 2021. **5**(4): p. 783-794.
27. Bruyninckx, R., et al., *Signs and symptoms in diagnosing acute myocardial infarction and acute coronary syndrome: a diagnostic meta-analysis.* Br J Gen Pract, 2008. **58**(547): p. 105-11.
28. Ozaki, Y., et al., *CVIT expert consensus document on primary percutaneous coronary intervention (PCI) for acute myocardial infarction (AMI) update 2022.* Cardiovasc Interv Ther, 2022. **37**(1): p. 1-34.
29. Mefford, M.T., et al., *Sex-Specific Trends in Acute Myocardial Infarction Within an Integrated Healthcare Network, 2000 Through 2014.* Circulation, 2020. **141**(7): p. 509-519.
30. Simonsson, M., et al., *Temporal trends in bleeding events in acute myocardial infarction: insights from the SWEDEHEART registry.* Eur Heart J, 2020. **41**(7): p. 833-843.
31. Saito, Y., et al., *Treatment strategies of acute myocardial infarction: updates on revascularization, pharmacological therapy, and beyond.* J Cardiol, 2023. **81**(2): p. 168-178.
32. Lavie, C.J., B.J. Gersh, and J.H. Chesebro, *Reperfusion in acute myocardial infarction.* Mayo Clin Proc, 1990. **65**(4): p. 549-64.
33. Choi, J.H. and J. Pile-Spellman, *Reperfusion Changes After Stroke and Practical Approaches for Neuroprotection.* Neuroimaging Clin N Am, 2018. **28**(4): p. 663-682.
34. Baechli, C., et al., *Association of comorbidities with clinical outcomes in patients after acute myocardial infarction.* Int J Cardiol Heart Vasc, 2020. **29**: p. 100558.
35. Zghebi, S.S., et al., *Comorbidity clusters and in-hospital outcomes in patients admitted with acute myocardial infarction in the USA: A national population-based study.* PLoS One, 2023. **18**(10): p. e0293314.
36. Yadegarfar, M.E., et al., *Association of treatments for acute myocardial infarction and survival for seven common comorbidity states: a nationwide cohort study.* BMC Med, 2020. **18**(1): p. 231.
37. Doenst, T., T.D. Nguyen, and E.D. Abel, *Cardiac metabolism in heart failure: implications beyond ATP production.* Circ Res, 2013. **113**(6): p. 709-24.
38. Gibbs, C.L., *Cardiac energetics.* Physiol Rev, 1978. **58**(1): p. 174-254.
39. Suga, H., *Ventricular energetics.* Physiol Rev, 1990. **70**(2): p. 247-77.
40. Yaniv, Y., et al., *Matching ATP supply and demand in mammalian heart: in vivo, in vitro, and in silico perspectives.* Ann N Y Acad Sci, 2010. **1188**: p. 133-42.
41. Nguyen, B.Y., et al., *Mitochondrial function in the heart: the insight into mechanisms and therapeutic potentials.* Br J Pharmacol, 2019. **176**(22): p. 4302-4318.
42. Kolwicz, S.C., Jr., S. Purohit, and R. Tian, *Cardiac metabolism and its interactions with contraction, growth, and survival of cardiomyocytes.* Circ Res, 2013. **113**(5): p. 603-16.
43. Murphy, E., et al., *Mitochondrial Function, Biology, and Role in Disease: A Scientific Statement From the American Heart Association.* Circ Res, 2016. **118**(12): p. 1960-91.
44. Gandoy-Fieiras, N., J.R. Gonzalez-Juanatey, and S. Eiras, *Myocardium Metabolism in Physiological and Pathophysiological States: Implications of Epicardial Adipose Tissue and Potential Therapeutic Targets.* Int J Mol Sci, 2020. **21**(7).
45. Neubauer, S., *The failing heart--an engine out of fuel.* N Engl J Med, 2007. **356**(11): p. 1140-51.
46. Siasos, G., et al., *Mitochondria and cardiovascular diseases-from pathophysiology to treatment.* Ann Transl Med, 2018. **6**(12): p. 256.

47. Garbern, J.C. and R.T. Lee, *Mitochondria and metabolic transitions in cardiomyocytes: lessons from development for stem cell-derived cardiomyocytes.* Stem Cell Res Ther, 2021. **12**(1): p. 177.
48. Zuccolotto Dos Reis, F.H., *Mitochondria and the heart.* Eur Heart J, 2024. **45**(22): p. 1963-1964.
49. Kadow, Z.A. and J.F. Martin, *Distinguishing Cardiomyocyte Division From Binucleation.* Circ Res, 2018. **123**(9): p. 1012-1014.
50. Quiros, P.M., A. Mottis, and J. Auwerx, *Mitonuclear communication in homeostasis and stress.* Nat Rev Mol Cell Biol, 2016. **17**(4): p. 213-26.
51. Duchen, M.R., *Mitochondria and calcium: from cell signalling to cell death.* J Physiol, 2000. **529 Pt 1**(Pt 1): p. 57-68.
52. Susin, S.A., et al., *Molecular characterization of mitochondrial apoptosis-inducing factor.* Nature, 1999. **397**(6718): p. 441-6.
53. Osellame, L.D., T.S. Blacker, and M.R. Duchen, *Cellular and molecular mechanisms of mitochondrial function.* Best Pract Res Clin Endocrinol Metab, 2012. **26**(6): p. 711-23.
54. Duchen, M.R., *Ca(2+)-dependent changes in the mitochondrial energetics in single dissociated mouse sensory neurons.* Biochem J, 1992. **283 (Pt 1)**(Pt 1): p. 41-50.
55. Jouaville, L.S., et al., *Regulation of mitochondrial ATP synthesis by calcium: evidence for a long-term metabolic priming.* Proc Natl Acad Sci U S A, 1999. **96**(24): p. 13807-12.
56. Starkov, A.A., *The role of mitochondria in reactive oxygen species metabolism and signaling.* Ann N Y Acad Sci, 2008. **1147**: p. 37-52.
57. Mohamed Yusoff, A.A., *Role of mitochondrial DNA mutations in brain tumors: A mini-review.* J Cancer Res Ther, 2015. **11**(3): p. 535-44.
58. Al Ojaimi, M., A. Salah, and A.W. El-Hattab, *Mitochondrial Fission and Fusion: Molecular Mechanisms, Biological Functions, and Related Disorders.* Membranes (Basel), 2022. **12**(9).
59. Malka, F., et al., *Separate fusion of outer and inner mitochondrial membranes.* EMBO Rep, 2005. **6**(9): p. 853-9.
60. Song, M., et al., *Abrogating Mitochondrial Dynamics in Mouse Hearts Accelerates Mitochondrial Senescence.* Cell Metab, 2017. **26**(6): p. 872-883 e5.
61. Ichishita, R., et al., *An RNAi screen for mitochondrial proteins required to maintain the morphology of the organelle in Caenorhabditis elegans.* J Biochem, 2008. **143**(4): p. 449-54.
62. Kanazawa, T., et al., *The C. elegans Opa1 homologue EAT-3 is essential for resistance to free radicals.* PLoS Genet, 2008. **4**(2): p. e1000022.
63. Liu, Y.J., et al., *Mitochondrial fission and fusion: A dynamic role in aging and potential target for age-related disease.* Mech Ageing Dev, 2020. **186**: p. 111212.
64. Scott, I. and R.J. Youle, *Mitochondrial fission and fusion.* Essays Biochem, 2010. **47**: p. 85-98.
65. Qian, W., et al., *Mitochondrial hyperfusion induced by loss of the fission protein Drp1 causes ATM-dependent G2/M arrest and aneuploidy through DNA replication stress.* J Cell Sci, 2012. **125**(Pt 23): p. 5745-57.
66. Ding, W.X. and X.M. Yin, *Mitophagy: mechanisms, pathophysiological roles, and analysis.* Biol Chem, 2012. **393**(7): p. 547-64.
67. Gustafsson, A.B. and G.W. Dorn, 2nd, *Evolving and Expanding the Roles of Mitophagy as a Homeostatic and Pathogenic Process.* Physiol Rev, 2019. **99**(1): p. 853-892.
68. Cadenas, E. and K.J. Davies, *Mitochondrial free radical generation, oxidative stress, and aging.* Free Radic Biol Med, 2000. **29**(3-4): p. 222-30.
69. Mui, D. and Y. Zhang, *Mitochondrial scenario: roles of mitochondrial dynamics in acute myocardial ischemia/reperfusion injury.* J Recept Signal Transduct Res, 2021. **41**(1): p. 1-5.
70. Piamsiri, C., et al., *Chronic mitochondrial dynamic-targeted therapy alleviates left ventricular dysfunction by reducing multiple programmed cell death in post-myocardial infarction rats.* Eur J Pharmacol, 2024. **977**: p. 176736.
71. Yang, J., et al., *Mitochondrial Dysfunction in Cardiovascular Diseases: Potential Targets for Treatment.* Front Cell Dev Biol, 2022. **10**: p. 841523.

72. Dunn, J. and M.H. Grider, *Physiology, Adenosine Triphosphate*, in *StatPearls*. 2024: Treasure Island (FL).
73. Bonora, M., et al., *ATP synthesis and storage.* Purinergic Signal, 2012. **8**(3): p. 343-57.
74. Chandel, N.S., *Glycolysis.* Cold Spring Harb Perspect Biol, 2021. **13**(5).
75. Martinez-Reyes, I. and N.S. Chandel, *Mitochondrial TCA cycle metabolites control physiology and disease.* Nat Commun, 2020. **11**(1): p. 102.
76. Arnold, P.K. and L.W.S. Finley, *Regulation and function of the mammalian tricarboxylic acid cycle.* J Biol Chem, 2023. **299**(2): p. 102838.
77. Ahmad, M., A. Wolberg, and C.I. Kahwaji, *Biochemistry, Electron Transport Chain*, in *StatPearls*. 2024: Treasure Island (FL).
78. Sharma, L.K., J. Lu, and Y. Bai, *Mitochondrial respiratory complex I: structure, function and implication in human diseases.* Curr Med Chem, 2009. **16**(10): p. 1266-77.
79. Henriques, B.J., et al., *Electron transfer flavoprotein and its role in mitochondrial energy metabolism in health and disease.* Gene, 2021. **776**: p. 145407.
80. Neupane, P., et al., *ATP Synthase: Structure, Function and Inhibition.* Biomol Concepts, 2019. **10**(1): p. 1-10.
81. Talley, J.T. and S.S. Mohiuddin, *Biochemistry, Fatty Acid Oxidation*, in *StatPearls*. 2024: Treasure Island (FL).
82. Schwenk, R.W., et al., *Fatty acid transport across the cell membrane: regulation by fatty acid transporters.* Prostaglandins Leukot Essent Fatty Acids, 2010. **82**(4-6): p. 149-54.
83. Ma, Y., et al., *Fatty acid oxidation: An emerging facet of metabolic transformation in cancer.* Cancer Lett, 2018. **435**: p. 92-100.
84. Harmuth, T., et al., *Mitochondrial Morphology, Function and Homeostasis Are Impaired by Expression of an N-terminal Calpain Cleavage Fragment of Ataxin-3.* Front Mol Neurosci, 2018. **11**: p. 368.
85. Crabtree, A., et al., *Defining Mitochondrial Cristae Morphology Changes Induced by Aging in Brown Adipose Tissue.* Adv Biol (Weinh), 2024. **8**(1): p. e2300186.
86. Wallace, D.C., *A mitochondrial paradigm of metabolic and degenerative diseases, aging, and cancer: a dawn for evolutionary medicine.* Annu Rev Genet, 2005. **39**: p. 359-407.
87. Boesch, P., et al., *DNA repair in organelles: Pathways, organization, regulation, relevance in disease and aging.* Biochim Biophys Acta, 2011. **1813**(1): p. 186-200.
88. Liu, M., et al., *Mitochondrial dysfunction in heart failure and its therapeutic implications.* Front Cardiovasc Med, 2022. **9**: p. 945142.
89. Zhou, B. and R. Tian, *Mitochondrial dysfunction in pathophysiology of heart failure.* J Clin Invest, 2018. **128**(9): p. 3716-3726.
90. Lake, N.J., et al., *Leigh syndrome: One disorder, more than 75 monogenic causes.* Ann Neurol, 2016. **79**(2): p. 190-203.
91. Van Goethem, G., et al., *Mutation of POLG is associated with progressive external ophthalmoplegia characterized by mtDNA deletions.* Nat Genet, 2001. **28**(3): p. 211-2.
92. Goto, Y., I. Nonaka, and S. Horai, *A mutation in the tRNA(Leu)(UUR) gene associated with the MELAS subgroup of mitochondrial encephalomyopathies.* Nature, 1990. **348**(6302): p. 651-3.
93. Frazier, A.E., D.R. Thorburn, and A.G. Compton, *Mitochondrial energy generation disorders: genes, mechanisms, and clues to pathology.* J Biol Chem, 2019. **294**(14): p. 5386-5395.
94. Wang, Y., et al., *Accelerated expansion of pathogenic mitochondrial DNA heteroplasmies in Huntington's disease.* Proc Natl Acad Sci U S A, 2021. **118**(30).
95. Baker, M.J., et al., *Mitochondrial biology and dysfunction in secondary mitochondrial disease.* Open Biol, 2022. **12**(12): p. 220274.
96. Niyazov, D.M., S.G. Kahler, and R.E. Frye, *Primary Mitochondrial Disease and Secondary Mitochondrial Dysfunction: Importance of Distinction for Diagnosis and Treatment.* Mol Syndromol, 2016. **7**(3): p. 122-37.
97. Rahman, J. and S. Rahman, *Mitochondrial medicine in the omics era.* Lancet, 2018. **391**(10139): p. 2560-2574.

98. Cadenas, S., *ROS and redox signaling in myocardial ischemia-reperfusion injury and cardioprotection.* Free Radic Biol Med, 2018. **117**: p. 76-89.
99. Boveris, A., E. Cadenas, and A.O. Stoppani, *Role of ubiquinone in the mitochondrial generation of hydrogen peroxide.* Biochem J, 1976. **156**(2): p. 435-44.
100. Efremov, R.G. and L.A. Sazanov, *Respiratory complex I: 'steam engine' of the cell?* Curr Opin Struct Biol, 2011. **21**(4): p. 532-40.
101. Iwata, S., et al., *Complete structure of the 11-subunit bovine mitochondrial cytochrome bc1 complex.* Science, 1998. **281**(5373): p. 64-71.
102. Peoples, J.N., et al., *Mitochondrial dysfunction and oxidative stress in heart disease.* Exp Mol Med, 2019. **51**(12): p. 1-13.
103. Chouchani, E.T., et al., *Ischaemic accumulation of succinate controls reperfusion injury through mitochondrial ROS.* Nature, 2014. **515**(7527): p. 431-435.
104. Ray, P.D., B.W. Huang, and Y. Tsuji, *Reactive oxygen species (ROS) homeostasis and redox regulation in cellular signaling.* Cell Signal, 2012. **24**(5): p. 981-90.
105. Jakubczyk, K., et al., *Reactive oxygen species - sources, functions, oxidative damage.* Pol Merkur Lekarski, 2020. **48**(284): p. 124-127.
106. Brieger, K., et al., *Reactive oxygen species: from health to disease.* Swiss Med Wkly, 2012. **142**: p. w13659.
107. de Almeida, A., et al., *ROS: Basic Concepts, Sources, Cellular Signaling, and its Implications in Aging Pathways.* Oxid Med Cell Longev, 2022. **2022**: p. 1225578.
108. Sies, H. and D.P. Jones, *Reactive oxygen species (ROS) as pleiotropic physiological signalling agents.* Nat Rev Mol Cell Biol, 2020. **21**(7): p. 363-383.
109. Day, R.M. and Y.J. Suzuki, *Cell proliferation, reactive oxygen and cellular glutathione.* Dose Response, 2006. **3**(3): p. 425-42.
110. Bigarella, C.L., R. Liang, and S. Ghaffari, *Stem cells and the impact of ROS signaling.* Development, 2014. **141**(22): p. 4206-18.
111. Jomova, K., et al., *Reactive oxygen species, toxicity, oxidative stress, and antioxidants: chronic diseases and aging.* Arch Toxicol, 2023. **97**(10): p. 2499-2574.
112. Hurd, T.R., M. DeGennaro, and R. Lehmann, *Redox regulation of cell migration and adhesion.* Trends Cell Biol, 2012. **22**(2): p. 107-15.
113. Moris, D., et al., *The role of reactive oxygen species in the pathophysiology of cardiovascular diseases and the clinical significance of myocardial redox.* Ann Transl Med, 2017. **5**(16): p. 326.
114. Li, C., et al., *A reactive oxygen species-responsive antioxidant nanotherapy for the treatment of drug-induced tissue and organ injury.* Biomater Sci, 2020. **8**(24): p. 7117-7131.
115. Mittal, M., et al., *Reactive oxygen species in inflammation and tissue injury.* Antioxid Redox Signal, 2014. **20**(7): p. 1126-67.
116. Kim, H., J. Yun, and S.M. Kwon, *Therapeutic Strategies for Oxidative Stress-Related Cardiovascular Diseases: Removal of Excess Reactive Oxygen Species in Adult Stem Cells.* Oxid Med Cell Longev, 2016. **2016**: p. 2483163.
117. Taverne, Y.J., et al., *Reactive oxygen species and the cardiovascular system.* Oxid Med Cell Longev, 2013. **2013**: p. 862423.
118. Juan, C.A., et al., *The Chemistry of Reactive Oxygen Species (ROS) Revisited: Outlining Their Role in Biological Macromolecules (DNA, Lipids and Proteins) and Induced Pathologies.* Int J Mol Sci, 2021. **22**(9).
119. Dizdaroglu, M., et al., *Chemical nature of in vivo DNA base damage in hydrogen peroxide-treated mammalian cells.* Arch Biochem Biophys, 1991. **285**(2): p. 388-90.
120. Halliwell, B., *Oxidants and human disease: some new concepts.* FASEB J, 1987. **1**(5): p. 358-64.
121. Birben, E., et al., *Oxidative stress and antioxidant defense.* World Allergy Organ J, 2012. **5**(1): p. 9-19.

122. Di Mascio, P., M.E. Murphy, and H. Sies, *Antioxidant defense systems: the role of carotenoids, tocopherols, and thiols.* Am J Clin Nutr, 1991. **53**(1 Suppl): p. 194S-200S.
123. Gongora, M.C., et al., *Role of extracellular superoxide dismutase in hypertension.* Hypertension, 2006. **48**(3): p. 473-81.
124. Jeeva, J.S., et al., *Enzymatic antioxidants and its role in oral diseases.* J Pharm Bioallied Sci, 2015. **7**(Suppl 2): p. S331-3.
125. Traber, M.G. and J.F. Stevens, *Vitamins C and E: beneficial effects from a mechanistic perspective.* Free Radic Biol Med, 2011. **51**(5): p. 1000-13.
126. Kisaoglu, A., et al., *Tissue damage and oxidant/antioxidant balance.* Eurasian J Med, 2013. **45**(1): p. 47-9.
127. Chennupati, R., et al., *Chronic anemia is associated with systemic endothelial dysfunction.* Front Cardiovasc Med, 2023. **10**: p. 1099069.
128. Panth, N., K.R. Paudel, and K. Parajuli, *Reactive Oxygen Species: A Key Hallmark of Cardiovascular Disease.* Adv Med, 2016. **2016**: p. 9152732.
129. Panday, A., et al., *NADPH oxidases: an overview from structure to innate immunity-associated pathologies.* Cell Mol Immunol, 2015. **12**(1): p. 5-23.
130. Handy, D.E. and J. Loscalzo, *Redox regulation of mitochondrial function.* Antioxid Redox Signal, 2012. **16**(11): p. 1323-67.
131. Kuroda, J., et al., *NADPH oxidase 4 (Nox4) is a major source of oxidative stress in the failing heart.* Proc Natl Acad Sci U S A, 2010. **107**(35): p. 15565-70.
132. Poznyak, A.V., et al., *Overview of OxLDL and Its Impact on Cardiovascular Health: Focus on Atherosclerosis.* Front Pharmacol, 2020. **11**: p. 613780.
133. Kevin, L.G., et al., *Ischemic preconditioning alters real-time measure of O2 radicals in intact hearts with ischemia and reperfusion.* Am J Physiol Heart Circ Physiol, 2003. **284**(2): p. H566-74.
134. Braunersreuther, V. and V. Jaquet, *Reactive oxygen species in myocardial reperfusion injury: from physiopathology to therapeutic approaches.* Curr Pharm Biotechnol, 2012. **13**(1): p. 97-114.
135. Zweier, J.L., et al., *Measurement and characterization of postischemic free radical generation in the isolated perfused heart.* J Biol Chem, 1989. **264**(32): p. 18890-5.
136. Di Lisa, F. and P. Bernardi, *Modulation of Mitochondrial Permeability Transition in Ischemia-Reperfusion Injury of the Heart. Advantages and Limitations.* Curr Med Chem, 2015. **22**(20): p. 2480-7.
137. Garcia-Dorado, D., et al., *The end-effectors of preconditioning protection against myocardial cell death secondary to ischemia-reperfusion.* Cardiovasc Res, 2006. **70**(2): p. 274-85.
138. Halestrap, A.P., S.J. Clarke, and S.A. Javadov, *Mitochondrial permeability transition pore opening during myocardial reperfusion--a target for cardioprotection.* Cardiovasc Res, 2004. **61**(3): p. 372-85.
139. Ruiz-Meana, M., et al., *Role of sarcoplasmic reticulum in mitochondrial permeability transition and cardiomyocyte death during reperfusion.* Am J Physiol Heart Circ Physiol, 2009. **297**(4): p. H1281-9.
140. Solaini, G. and D.A. Harris, *Biochemical dysfunction in heart mitochondria exposed to ischaemia and reperfusion.* Biochem J, 2005. **390**(Pt 2): p. 377-94.
141. Yoo, J.H., et al., *Oxidative status in iron-deficiency anemia.* J Clin Lab Anal, 2009. **23**(5): p. 319-23.
142. Fibach, E. and E. Rachmilewitz, *The role of oxidative stress in hemolytic anemia.* Curr Mol Med, 2008. **8**(7): p. 609-19.
143. Nagababu, E., et al., *Iron-deficiency anaemia enhances red blood cell oxidative stress.* Free Radic Res, 2008. **42**(9): p. 824-9.
144. Fujii, J., et al., *Oxidative stress as a potential causal factor for autoimmune hemolytic anemia and systemic lupus erythematosus.* World J Nephrol, 2015. **4**(2): p. 213-22.

145. Wischmann, P., et al., *Red Blood Cell-Mediated Cardioprotection Is Impaired in ST-Segment Elevation Myocardial Infarction Patients With Anemia.* JACC Basic Transl Sci, 2023. **8**(10): p. 1392-1394.
146. Barbalato, L. and L.S. Pillarisetty, *Histology, Red Blood Cell*, in *StatPearls*. 2024: Treasure Island (FL).
147. Zhang, X., et al., *Red blood cells in biology and translational medicine: natural vehicle inspires new biomedical applications.* Theranostics, 2024. **14**(1): p. 220-248.
148. Satchwell, T.J., *Generation of red blood cells from stem cells: Achievements, opportunities and perspectives for malaria research.* Front Cell Infect Microbiol, 2022. **12**: p. 1039520.
149. Diez-Silva, M., et al., *Shape and Biomechanical Characteristics of Human Red Blood Cells in Health and Disease.* MRS Bull, 2010. **35**(5): p. 382-388.
150. Ahmed, M.H., M.S. Ghatge, and M.K. Safo, *Hemoglobin: Structure, Function and Allostery.* Subcell Biochem, 2020. **94**: p. 345-382.
151. Marengo-Rowe, A.J., *Structure-function relations of human hemoglobins.* Proc (Bayl Univ Med Cent), 2006. **19**(3): p. 239-45.
152. Kuhn, V., et al., *Red Blood Cell Function and Dysfunction: Redox Regulation, Nitric Oxide Metabolism, Anemia.* Antioxid Redox Signal, 2017. **26**(13): p. 718-742.
153. Cortese-Krott, M.M., *The Reactive Species Interactome in Red Blood Cells: Oxidants, Antioxidants, and Molecular Targets.* Antioxidants (Basel), 2023. **12**(9).
154. Islami, M.M., *Dapsone-induced Methemoglobinemia Case Report.* J Microsc Ultrastruct, 2024. **12**(3): p. 159-161.
155. Balaji, S.N. and V. Trivedi, *Extracellular Methemoglobin Mediated Early ROS Spike Triggers Osmotic Fragility and RBC Destruction: An Insight into the Enhanced Hemolysis During Malaria.* Indian J Clin Biochem, 2012. **27**(2): p. 178-85.
156. Moller, M.N., et al., *Oxidants and Antioxidants in the Redox Biochemistry of Human Red Blood Cells.* ACS Omega, 2023. **8**(1): p. 147-168.
157. Leo, F., et al., *Red Blood Cell and Endothelial eNOS Independently Regulate Circulating Nitric Oxide Metabolites and Blood Pressure.* Circulation, 2021. **144**(11): p. 870-889.
158. Gladwin, M.T., J.H. Crawford, and R.P. Patel, *The biochemistry of nitric oxide, nitrite, and hemoglobin: role in blood flow regulation.* Free Radic Biol Med, 2004. **36**(6): p. 707-17.
159. Forstermann, U. and W.C. Sessa, *Nitric oxide synthases: regulation and function.* Eur Heart J, 2012. **33**(7): p. 829-37, 837a-837d.
160. Esplugues, J.V., *NO as a signalling molecule in the nervous system.* Br J Pharmacol, 2002. **135**(5): p. 1079-95.
161. Kone, B.C., et al., *Protein interactions with nitric oxide synthases: controlling the right time, the right place, and the right amount of nitric oxide.* Am J Physiol Renal Physiol, 2003. **285**(2): p. F178-90.
162. Sharma, J.N., A. Al-Omran, and S.S. Parvathy, *Role of nitric oxide in inflammatory diseases.* Inflammopharmacology, 2007. **15**(6): p. 252-9.
163. Cinelli, M.A., et al., *Inducible nitric oxide synthase: Regulation, structure, and inhibition.* Med Res Rev, 2020. **40**(1): p. 158-189.
164. Wood, K.C., et al., *Circulating blood endothelial nitric oxide synthase contributes to the regulation of systemic blood pressure and nitrite homeostasis.* Arterioscler Thromb Vasc Biol, 2013. **33**(8): p. 1861-71.
165. Forstermann, U. and T. Munzel, *Endothelial nitric oxide synthase in vascular disease: from marvel to menace.* Circulation, 2006. **113**(13): p. 1708-14.
166. Chen, J.Y., et al., *Nitric oxide bioavailability dysfunction involves in atherosclerosis.* Biomed Pharmacother, 2018. **97**: p. 423-428.
167. Gallo, G., M. Volpe, and C. Savoia, *Endothelial Dysfunction in Hypertension: Current Concepts and Clinical Implications.* Front Med (Lausanne), 2021. **8**: p. 798958.
168. Umar, S. and A. van der Laarse, *Nitric oxide and nitric oxide synthase isoforms in the normal, hypertrophic, and failing heart.* Mol Cell Biochem, 2010. **333**(1-2): p. 191-201.

169. Yang, Y.M., et al., *eNOS uncoupling and endothelial dysfunction in aged vessels.* Am J Physiol Heart Circ Physiol, 2009. **297**(5): p. H1829-36.
170. Wischmann, P., et al., *Anaemia is associated with severe RBC dysfunction and a reduced circulating NO pool: vascular and cardiac eNOS are crucial for the adaptation to anaemia.* Basic Res Cardiol, 2020. **115**(4): p. 43.
171. Turner, J., M. Parsi, and M. Badireddy, *Anemia*, in *StatPearls*. 2024: Treasure Island (FL).
172. Bliss, S., *Anemia and Oxygen Delivery.* Vet Clin North Am Small Anim Pract, 2015. **45**(5): p. 917-30.
173. Cappellini, M.D. and I. Motta, *Anemia in Clinical Practice-Definition and Classification: Does Hemoglobin Change With Aging?* Semin Hematol, 2015. **52**(4): p. 261-9.
174. Weckmann, G., et al., *Association of Anemia with Clinical Symptoms Commonly Attributed to Anemia-Analysis of Two Population-Based Cohorts.* J Clin Med, 2023. **12**(3).
175. Chaparro, C.M. and P.S. Suchdev, *Anemia epidemiology, pathophysiology, and etiology in low- and middle-income countries.* Ann N Y Acad Sci, 2019. **1450**(1): p. 15-31.
176. Levi, M., *Twenty-five million liters of blood into the sewer.* J Thromb Haemost, 2014. **12**(10): p. 1592.
177. Koch, C.G., et al., *Hospital-acquired anemia: prevalence, outcomes, and healthcare implications.* J Hosp Med, 2013. **8**(9): p. 506-12.
178. Thavendiranathan, P., et al., *Do blood tests cause anemia in hospitalized patients? The effect of diagnostic phlebotomy on hemoglobin and hematocrit levels.* J Gen Intern Med, 2005. **20**(6): p. 520-4.
179. Makam, A.N., et al., *Incidence, Predictors, and Outcomes of Hospital-Acquired Anemia.* J Hosp Med, 2017. **12**(5): p. 317-322.
180. Vaglio, J., et al., *Relation of anemia at discharge to survival after acute coronary syndromes.* Am J Cardiol, 2005. **96**(4): p. 496-9.
181. Salisbury, A.C., et al., *Incidence, correlates, and outcomes of acute, hospital-acquired anemia in patients with acute myocardial infarction.* Circ Cardiovasc Qual Outcomes, 2010. **3**(4): p. 337-46.
182. Wu, W.C., et al., *Blood transfusion in elderly patients with acute myocardial infarction.* N Engl J Med, 2001. **345**(17): p. 1230-6.
183. Langston, R.D., et al., *Renal insufficiency and anemia are independent risk factors for death among patients with acute myocardial infarction.* Kidney Int, 2003. **64**(4): p. 1398-405.
184. Hamaguchi, S., et al., *Anemia is an independent predictor of long-term adverse outcomes in patients hospitalized with heart failure in Japan. A report from the Japanese Cardiac Registry of Heart Failure in Cardiology (JCARE-CARD).* Circ J, 2009. **73**(10): p. 1901-8.
185. Tremblay, D., et al., *Mild anemia as a single independent predictor of mortality in patients with COVID-19.* EJHaem, 2021. **2**(3): p. 319-326.
186. Lee, W.H., et al., *Anemia as an Independent Predictor of Adverse Cardiac Outcomes in Patients with Atrial Fibrillation.* Int J Med Sci, 2015. **12**(8): p. 618-24.
187. Goel, H., et al., *Anemia in Cardiovascular Disease: Marker of Disease Severity or Disease-modifying Therapeutic Target?* Curr Atheroscler Rep, 2021. **23**(10): p. 61.
188. Sarnak, M.J., et al., *Anemia as a risk factor for cardiovascular disease in The Atherosclerosis Risk in Communities (ARIC) study.* J Am Coll Cardiol, 2002. **40**(1): p. 27-33.
189. Walker, A.M., et al., *Anemia as a predictor of cardiovascular events in patients with elevated serum creatinine.* J Am Soc Nephrol, 2006. **17**(8): p. 2293-8.
190. Lanser, L., et al., *Anemia of Chronic Disease in Patients With Cardiovascular Disease.* Front Cardiovasc Med, 2021. **8**: p. 666638.
191. Groenveld, H.F., et al., *Anemia and mortality in heart failure patients a systematic review and meta-analysis.* J Am Coll Cardiol, 2008. **52**(10): p. 818-27.
192. Weiner, D.E., et al., *Effects of anemia and left ventricular hypertrophy on cardiovascular disease in patients with chronic kidney disease.* J Am Soc Nephrol, 2005. **16**(6): p. 1803-10.

193. Mehdi, U. and R.D. Toto, *Anemia, diabetes, and chronic kidney disease.* Diabetes Care, 2009. **32**(7): p. 1320-6.
194. Metra, M., et al., *Anemia and heart failure: a cause of progression or only a consequence?* Heart Int, 2007. **3**(1): p. 1.
195. Schunkert, H. and H.W. Hense, *A heart price to pay for anaemia.* Nephrol Dial Transplant, 2001. **16**(3): p. 445-8.
196. Pereira, A.A. and M.J. Sarnak, *Anemia as a risk factor for cardiovascular disease.* Kidney Int Suppl, 2003(87): p. S32-9.
197. Gibbons, G.H. and V.J. Dzau, *The emerging concept of vascular remodeling.* N Engl J Med, 1994. **330**(20): p. 1431-8.
198. London, G.M. and P.S. Parfrey, *Cardiac disease in chronic uremia: pathogenesis.* Adv Ren Replace Ther, 1997. **4**(3): p. 194-211.
199. Levin, A., et al., *Prevalent left ventricular hypertrophy in the predialysis population: identifying opportunities for intervention.* Am J Kidney Dis, 1996. **27**(3): p. 347-54.
200. Hong, Y.J., et al., *Relation between anemia and vulnerable coronary plaque components in patients with acute coronary syndrome: virtual histology-intravascular ultrasound analysis.* J Korean Med Sci, 2012. **27**(4): p. 370-6.
201. da Silveira, A.D., et al., *Association of anemia with clinical outcomes in stable coronary artery disease.* Coron Artery Dis, 2008. **19**(1): p. 21-6.
202. Aronson, D., et al., *Changes in haemoglobin levels during hospital course and long-term outcome after acute myocardial infarction.* Eur Heart J, 2007. **28**(11): p. 1289-96.
203. Hasin, T., et al., *Prevalence and prognostic significance of transient, persistent, and new-onset anemia after acute myocardial infarction.* Am J Cardiol, 2009. **104**(4): p. 486-91.
204. Jhand, A.S., et al., *Impact of anemia on outcomes and resource utilization in patients with myocardial infarction: A national database analysis.* Int J Cardiol, 2024. **408**: p. 132111.
205. Patel, U.D., et al., *Impact of anemia on physical function and survival among patients with coronary artery disease.* Clin Cardiol, 2008. **31**(11): p. 546-50.
206. Fariba, F., M. Moradi, and M.A. Seifrabie, *The prevalence of anemia in the patients who survived and died due to myocardial infarction (MI).* J Med Life, 2015. **8**(Spec Iss 4): p. 159-162.
207. Padda, J., et al., *Acute Anemia and Myocardial Infarction.* Cureus, 2021. **13**(8): p. e17096.
208. Levy, P.S., R.L. Quigley, and S.A. Gould, *Acute dilutional anemia and critical left anterior descending coronary artery stenosis impairs end organ oxygen delivery.* J Trauma, 1996. **41**(3): p. 416-23.
209. Naito, Y., et al., *Adaptive response of the heart to long-term anemia induced by iron deficiency.* Am J Physiol Heart Circ Physiol, 2009. **296**(3): p. H585-93.
210. Dauerman, H.L., et al., *Bleeding complications in patients with anemia and acute myocardial infarction.* Am J Cardiol, 2005. **96**(10): p. 1379-83.
211. Moghaddam, N., et al., *Association of Anemia With Outcomes Among ST-Segment-Elevation Myocardial Infarction Patients Receiving Primary Percutaneous Coronary Intervention.* Circ Cardiovasc Interv, 2018. **11**(12): p. e007175.
212. Westenbrink, B.D., et al., *Anemia predicts thromboembolic events, bleeding complications and mortality in patients with atrial fibrillation: insights from the RE-LY trial.* J Thromb Haemost, 2015. **13**(5): p. 699-707.
213. Bindra, K., et al., *Abnormal haemoglobin levels in acute coronary syndromes.* QJM, 2006. **99**(12): p. 851-62.
214. Solga, I., et al., *Distinct effects of acute and chronic blood loss anemia on vascular function after acute myocardial infarction.* bioRxiv, 2024: p. 2024.09.24.614629.
215. Mahendiran, T., et al., *Prognosis of Patients with Chronic and Hospital-Acquired Anaemia After Acute Coronary Syndromes.* J Cardiovasc Transl Res, 2020. **13**(4): p. 618-628.
216. Sun, S.Y., *N-acetylcysteine, reactive oxygen species and beyond.* Cancer Biol Ther, 2010. **9**(2): p. 109-10.

217. Flogel, U., et al., *In vivo monitoring of inflammation after cardiac and cerebral ischemia by fluorine magnetic resonance imaging.* Circulation, 2008. **118**(2): p. 140-8.
218. Kulak, N.A., et al., *Minimal, encapsulated proteomic-sample processing applied to copy-number estimation in eukaryotic cells.* Nat Methods, 2014. **11**(3): p. 319-24.
219. Pesta, D. and E. Gnaiger, *High-resolution respirometry: OXPHOS protocols for human cells and permeabilized fibers from small biopsies of human muscle.* Methods Mol Biol, 2012. **810**: p. 25-58.
220. Huang, L., et al., *Targeting citrate as a novel therapeutic strategy in cancer treatment.* Biochim Biophys Acta Rev Cancer, 2020. **1873**(1): p. 188332.
221. Muessig, J.M., et al., *A Model of Blood Component-Heart Interaction in Cardiac Ischemia-Reperfusion Injury using a Langendorff-Based Ex Vivo Assay.* J Cardiovasc Pharmacol Ther, 2020. **25**(2): p. 164-173.
222. Schuler, D., et al., *Measurement of endothelium-dependent vasodilation in mice--brief report.* Arterioscler Thromb Vasc Biol, 2014. **34**(12): p. 2651-7.
223. Silverberg, D.S., D. Wexler, and A. Iaina, *The role of anemia in the progression of congestive heart failure. Is there a place for erythropoietin and intravenous iron?* J Nephrol, 2004. **17**(6): p. 749-61.
224. Wang, Y., et al., *Superoxide dismutases: Dual roles in controlling ROS damage and regulating ROS signaling.* J Cell Biol, 2018. **217**(6): p. 1915-1928.
225. Nandi, A., et al., *Role of Catalase in Oxidative Stress- and Age-Associated Degenerative Diseases.* Oxid Med Cell Longev, 2019. **2019**: p. 9613090.
226. Deponte, M., *Glutathione catalysis and the reaction mechanisms of glutathione-dependent enzymes.* Biochim Biophys Acta, 2013. **1830**(5): p. 3217-66.
227. Ramachandra, C.J.A., et al., *Myeloperoxidase As a Multifaceted Target for Cardiovascular Protection.* Antioxid Redox Signal, 2020. **32**(15): p. 1135-1149.
228. Roy, B., K. Sundar, and S.S. Palaniyandi, *4-hydroxy-2-nonenal decreases coronary endothelial cell migration: Potentiation by aldehyde dehydrogenase 2 inhibition.* Vascul Pharmacol, 2020. **131**: p. 106762.
229. Ayala, A., M.F. Munoz, and S. Arguelles, *Lipid peroxidation: production, metabolism, and signaling mechanisms of malondialdehyde and 4-hydroxy-2-nonenal.* Oxid Med Cell Longev, 2014. **2014**: p. 360438.
230. Cortese-Krott, M.M., et al., *Red blood cell eNOS is cardioprotective in acute myocardial infarction.* Redox Biol, 2022. **54**: p. 102370.
231. Schwartz, A.J., et al., *A genetic mouse model of severe iron deficiency anemia reveals tissue-specific transcriptional stress responses and cardiac remodeling.* J Biol Chem, 2019. **294**(41): p. 14991-15002.
232. Rivera, S. and T. Ganz, *Animal models of anemia of inflammation.* Semin Hematol, 2009. **46**(4): p. 351-7.
233. Bakeer, N., et al., *Sickle cell anemia mice develop a unique cardiomyopathy with restrictive physiology.* Proc Natl Acad Sci U S A, 2016. **113**(35): p. E5182-91.
234. Badireddy, M. and K.M. Baradhi, *Chronic Anemia*, in *StatPearls*. 2024: Treasure Island (FL).
235. Chung, Y.J., et al., *Iron-deficiency anemia reduces cardiac contraction by downregulating RyR2 channels and suppressing SERCA pump activity.* JCI Insight, 2019. **4**(7).
236. Mozos, I., *Mechanisms linking red blood cell disorders and cardiovascular diseases.* Biomed Res Int, 2015. **2015**: p. 682054.
237. Chew, D.S., et al., *Change in Left Ventricular Ejection Fraction Following First Myocardial Infarction and Outcome.* JACC Clin Electrophysiol, 2018. **4**(5): p. 672-682.
238. Wohlfahrt, P., et al., *Trajectories and determinants of left ventricular ejection fraction after the first myocardial infarction in the current era of primary coronary interventions.* Front Cardiovasc Med, 2022. **9**: p. 1051995.
239. Hoes, M.F., et al., *Iron deficiency impairs contractility of human cardiomyocytes through decreased mitochondrial function.* Eur J Heart Fail, 2018. **20**(5): p. 910-919.

240. Charles-Edwards, G., et al., *Effect of Iron Isomaltoside on Skeletal Muscle Energetics in Patients With Chronic Heart Failure and Iron Deficiency.* Circulation, 2019. **139**(21): p. 2386-2398.
241. Dong, F., et al., *Dietary iron deficiency induces ventricular dilation, mitochondrial ultrastructural aberrations and cytochrome c release: involvement of nitric oxide synthase and protein tyrosine nitration.* Clin Sci (Lond), 2005. **109**(3): p. 277-86.
242. Haddad, S., et al., *Iron-regulatory proteins secure iron availability in cardiomyocytes to prevent heart failure.* Eur Heart J, 2017. **38**(5): p. 362-372.
243. Melenovsky, V., et al., *Skeletal Muscle Abnormalities and Iron Deficiency in Chronic Heart Failure(An Exercise (31)P Magnetic Resonance Spectroscopy Study of Calf Muscle).* Circ Heart Fail, 2018. **11**(9): p. e004800.
244. Papalia, F., et al., *Cardiac energetics in patients with chronic heart failure and iron deficiency: an in-vivo (31) P magnetic resonance spectroscopy study.* Eur J Heart Fail, 2022. **24**(4): p. 716-723.
245. Mills, G.C., W.C. Levin, and J.B. Alperin, *Hemolytic anemia associated with low erythrocyte ATP.* Blood, 1968. **32**(1): p. 15-32.
246. Bagur, R., et al., *The impact of cardiac ischemia/reperfusion on the mitochondria-cytoskeleton interactions.* Biochim Biophys Acta, 2016. **1862**(6): p. 1159-71.
247. Sharov, V.G., et al., *Protection of ischemic myocardium by exogenous phosphocreatine. I. Morphologic and phosphorus 31-nuclear magnetic resonance studies.* J Thorac Cardiovasc Surg, 1987. **94**(5): p. 749-61.
248. Lian, Z.X., et al., *ATP-induced cardioprotection against myocardial ischemia/reperfusion injury is mediated through the RISK pathway.* Exp Ther Med, 2016. **12**(4): p. 2063-2068.
249. Wang, C.X., et al., *The Protective Effect of Cx43 Protein-Mediated Phosphocreatine on Myocardial Ischemia/Reperfusion Injury.* Cardiol Res Pract, 2021. **2021**: p. 8838151.
250. Loublier, S., et al., *The NDUFB6 subunit of the mitochondrial respiratory chain complex I is required for electron transfer activity: a proof of principle study on stable and controlled RNA interference in human cell lines.* Biochem Biophys Res Commun, 2011. **414**(2): p. 367-72.
251. Sharma, L.K., et al., *Mitochondrial respiratory complex I dysfunction promotes tumorigenesis through ROS alteration and AKT activation.* Hum Mol Genet, 2011. **20**(23): p. 4605-16.
252. Narimatsu, T., et al., *Downregulation of NDUFB6 due to 9p24.1-p13.3 loss is implicated in metastatic clear cell renal cell carcinoma.* Cancer Med, 2015. **4**(1): p. 112-24.
253. Mootha, V.K., et al., *PGC-1alpha-responsive genes involved in oxidative phosphorylation are coordinately downregulated in human diabetes.* Nat Genet, 2003. **34**(3): p. 267-73.
254. Xu, Z., et al., *TMT-based proteomics reveals methylprotodioscin alleviates oxidative stress and inflammation via COX6C in myocardial infraction.* Biomed Pharmacother, 2024. **180**: p. 117489.
255. Sun, X., et al., *Downregulation in components of the mitochondrial electron transport chain in the postmortem frontal cortex of subjects with bipolar disorder.* J Psychiatry Neurosci, 2006. **31**(3): p. 189-96.
256. Smulan, L.J., et al., *Sirtuin 3 Downregulation in Mycobacterium tuberculosis-Infected Macrophages Reprograms Mitochondrial Metabolism and Promotes Cell Death.* mBio, 2021. **12**(1).
257. Rhein, V.F., et al., *NDUFAF5 Hydroxylates NDUFS7 at an Early Stage in the Assembly of Human Complex I.* J Biol Chem, 2016. **291**(28): p. 14851-60.
258. Forte, M., et al., *Mitochondrial complex I deficiency and cardiovascular diseases: current evidence and future directions.* J Mol Med (Berl), 2019. **97**(5): p. 579-591.
259. Cappelli, E., et al., *Mitochondrial respiratory complex I defects in Fanconi anemia.* Trends Mol Med, 2013. **19**(9): p. 513-4.
260. Lichtenstein, D.A., et al., *A recurring mutation in the respiratory complex 1 protein NDUFB11 is responsible for a novel form of X-linked sideroblastic anemia.* Blood, 2016. **128**(15): p. 1913-1917.

261. Robinson, D.R.L., et al., *Applying Sodium Carbonate Extraction Mass Spectrometry to Investigate Defects in the Mitochondrial Respiratory Chain.* Front Cell Dev Biol, 2022. **10**: p. 786268.
262. Bleier, L. and S. Drose, *Superoxide generation by complex III: from mechanistic rationales to functional consequences.* Biochim Biophys Acta, 2013. **1827**(11-12): p. 1320-31.
263. Heather, L.C., et al., *Critical role of complex III in the early metabolic changes following myocardial infarction.* Cardiovasc Res, 2010. **85**(1): p. 127-36.
264. Lang, A.L., et al., *A Defect in Mitochondrial Complex III but Not in Complexes I or IV Causes Early beta-Cell Dysfunction and Hyperglycemia in Mice.* Diabetes, 2023. **72**(9): p. 1262-1276.
265. Chen, C.L., et al., *SDHAF2 facilitates mitochondrial respiration through stabilizing succinate dehydrogenase and cytochrome c oxidase assemblies.* Mitochondrion, 2024. **79**: p. 101952.
266. Wang, X., et al., *Publisher Correction: Cardiac disruption of SDHAF4-mediated mitochondrial complex II assembly promotes dilated cardiomyopathy.* Nat Commun, 2022. **13**(1): p. 4690.
267. Drose, S., *Differential effects of complex II on mitochondrial ROS production and their relation to cardioprotective pre- and postconditioning.* Biochim Biophys Acta, 2013. **1827**(5): p. 578-87.
268. Hikosaka, K., et al., *Deficiency of nicotinamide mononucleotide adenylyltransferase 3 (nmnat3) causes hemolytic anemia by altering the glycolytic flow in mature erythrocytes.* J Biol Chem, 2014. **289**(21): p. 14796-811.
269. Beg, M.A., et al., *Targeting mitochondrial dynamics and redox regulation in cardiovascular diseases.* Trends Pharmacol Sci, 2024. **45**(4): p. 290-303.
270. Forte, M., et al., *The role of mitochondrial dynamics in cardiovascular diseases.* Br J Pharmacol, 2021. **178**(10): p. 2060-2076.
271. Hara, Y., et al., *Iron loss triggers mitophagy through induction of mitochondrial ferritin.* EMBO Rep, 2020. **21**(11): p. e50202.
272. Geng, G., et al., *Receptor-mediated mitophagy regulates EPO production and protects against renal anemia.* Elife, 2021. **10**.
273. Jiang, H., et al., *Impaired Mitophagy of Nucleated Erythroid Cells Leads to Anemia in Patients with Myelodysplastic Syndromes.* Oxid Med Cell Longev, 2018. **2018**: p. 6328051.
274. Princely Abudu, Y., et al., *NIPSNAP1 and NIPSNAP2 Act as "Eat Me" Signals for Mitophagy.* Dev Cell, 2019. **49**(4): p. 509-525 e12.
275. Wang, B., et al., *Essential control of mitochondrial morphology and function by chaperone-mediated autophagy through degradation of PARK7.* Autophagy, 2016. **12**(8): p. 1215-28.
276. Cilenti, L., et al., *Mitochondrial MUL1 E3 ubiquitin ligase regulates Hypoxia Inducible Factor (HIF-1alpha) and metabolic reprogramming by modulating the UBXN7 cofactor protein.* Sci Rep, 2020. **10**(1): p. 1609.
277. Zhang, W., et al., *Hypoxic mitophagy regulates mitochondrial quality and platelet activation and determines severity of I/R heart injury.* Elife, 2016. **5**.
278. Turkieh, A., et al., *Mitophagy Regulation Following Myocardial Infarction.* Cells, 2022. **11**(2).
279. Xu, C., et al., *Mitophagy-regulated mitochondrial health strongly protects the heart against cardiac dysfunction after acute myocardial infarction.* J Cell Mol Med, 2022. **26**(4): p. 1315-1326.
280. Kanamori, H., et al., *The role of autophagy emerging in postinfarction cardiac remodelling.* Cardiovasc Res, 2011. **91**(2): p. 330-9.
281. Maejima, Y., et al., *Mst1 inhibits autophagy by promoting the interaction between Beclin1 and Bcl-2.* Nat Med, 2013. **19**(11): p. 1478-88.
282. Hoshino, A., et al., *p53-TIGAR axis attenuates mitophagy to exacerbate cardiac damage after ischemia.* J Mol Cell Cardiol, 2012. **52**(1): p. 175-84.
283. Pattingre, S., et al., *Bcl-2 antiapoptotic proteins inhibit Beclin 1-dependent autophagy.* Cell, 2005. **122**(6): p. 927-39.
284. Vijayalingam, S., et al., *Overexpression of BH3-Only Protein BNIP3 Leads to Enhanced Tumor Growth.* Genes Cancer, 2010. **1**(9): p. 964-71.

285. Ferreira, J.C.B., et al., *A selective inhibitor of mitofusin 1-betaIIPKC association improves heart failure outcome in rats.* Nat Commun, 2019. **10**(1): p. 329.
286. Hall, A.R., et al., *Correction: Hearts deficient in both Mfn1 and Mfn2 are protected against acute myocardial infarction.* Cell Death Dis, 2021. **12**(7): p. 660.
287. Newman, L.E., et al., *The ARL2 GTPase regulates mitochondrial fusion from the intermembrane space.* Cell Logist, 2017. **7**(3): p. e1340104.
288. Chiche, J., et al., *Hypoxic enlarged mitochondria protect cancer cells from apoptotic stimuli.* J Cell Physiol, 2010. **222**(3): p. 648-57.
289. Yang, L., et al., *Mitochondrial fusion provides an 'initial metabolic complementation' controlled by mtDNA.* Cell Mol Life Sci, 2015. **72**(13): p. 2585-98.
290. Ikeda, Y., et al., *Endogenous Drp1 mediates mitochondrial autophagy and protects the heart against energy stress.* Circ Res, 2015. **116**(2): p. 264-78.
291. Ong, S.B., et al., *Inhibiting mitochondrial fission protects the heart against ischemia/reperfusion injury.* Circulation, 2010. **121**(18): p. 2012-22.
292. Pennanen, C., et al., *Mitochondrial fission is required for cardiomyocyte hypertrophy mediated by a Ca2+-calcineurin signaling pathway.* J Cell Sci, 2014. **127**(Pt 12): p. 2659-71.
293. Rogers, M.A., et al., *Dynamin-related protein 1 inhibition reduces hepatic PCSK9 secretion.* Cardiovasc Res, 2021. **117**(11): p. 2340-2353.
294. Shimura, D., et al., *Protective mitochondrial fission induced by stress-responsive protein GJA1-20k.* Elife, 2021. **10**.
295. Ishikawa, K., et al., *Pearson syndrome-like anemia induced by accumulation of mutant mtDNA and anemia with imbalanced white blood cell lineages induced by Drp1 deletion in a murine model.* Pharmacol Res, 2022. **185**: p. 106467.
296. Chen, W., H. Zhao, and Y. Li, *Mitochondrial dynamics in health and disease: mechanisms and potential targets.* Signal Transduct Target Ther, 2023. **8**(1): p. 333.
297. Chen, Z., et al., *Global phosphoproteomic analysis reveals ARMC10 as an AMPK substrate that regulates mitochondrial dynamics.* Nat Commun, 2019. **10**(1): p. 104.
298. Fischer, C., et al., *Mitochondrial Respiration in Response to Iron Deficiency Anemia: Comparison of Peripheral Blood Mononuclear Cells and Liver.* Metabolites, 2022. **12**(3).
299. Ravera, S., et al., *Mitochondrial respiratory chain Complex I defects in Fanconi anemia complementation group A.* Biochimie, 2013. **95**(10): p. 1828-37.
300. Ramachandra, C.J.A., et al., *Mitochondria in acute myocardial infarction and cardioprotection.* EBioMedicine, 2020. **57**: p. 102884.
301. Irion, C.I., et al., *Acute Myocardial Infarction Reduces Respiration in Rat Cardiac Fibers, despite Adipose Tissue Mesenchymal Stromal Cell Transplant.* Stem Cells Int, 2020. **2020**: p. 4327965.
302. Wal, P., et al., *Myocardial Infarction as a Consequence of Mitochondrial Dysfunction.* Curr Cardiol Rev, 2023. **19**(6): p. 23-30.
303. Cheng, J., et al., *Mitochondrial Proton Leak Plays a Critical Role in Pathogenesis of Cardiovascular Diseases.* Adv Exp Med Biol, 2017. **982**: p. 359-370.
304. Panda, P., et al., *Biomarkers of Oxidative Stress Tethered to Cardiovascular Diseases.* Oxid Med Cell Longev, 2022. **2022**: p. 9154295.
305. Rosa, A.C., et al., *Superoxide Dismutase Administration: A Review of Proposed Human Uses.* Molecules, 2021. **26**(7).
306. Averill-Bates, D.A., *The antioxidant glutathione.* Vitam Horm, 2023. **121**: p. 109-141.
307. Shaeib, F., et al., *The Impact of Myeloperoxidase and Activated Macrophages on Metaphase II Mouse Oocyte Quality.* PLoS One, 2016. **11**(3): p. e0151160.
308. Guo, C., et al., *Oxidative stress, mitochondrial damage and neurodegenerative diseases.* Neural Regen Res, 2013. **8**(21): p. 2003-14.
309. Bhatti, J.S., G.K. Bhatti, and P.H. Reddy, *Mitochondrial dysfunction and oxidative stress in metabolic disorders - A step towards mitochondria based therapeutic strategies.* Biochim Biophys Acta Mol Basis Dis, 2017. **1863**(5): p. 1066-1077.

310. Halasi, M., et al., *ROS inhibitor N-acetyl-L-cysteine antagonizes the activity of proteasome inhibitors.* Biochem J, 2013. **454**(2): p. 201-8.
311. Zheng, J., et al., *N-acetylcysteine, a small molecule scavenger of reactive oxygen species, alleviates cardiomyocyte damage by regulating OPA1-mediated mitochondrial quality control and apoptosis in response to oxidative stress.* J Thorac Dis, 2024. **16**(8): p. 5323-5336.
312. Wright, D.J., et al., *N-Acetylcysteine improves mitochondrial function and ameliorates behavioral deficits in the R6/1 mouse model of Huntington's disease.* Transl Psychiatry, 2015. **5**(1): p. e492.
313. Larsen, S., et al., *Biomarkers of mitochondrial content in skeletal muscle of healthy young human subjects.* J Physiol, 2012. **590**(14): p. 3349-60.
314. Ashar, F.N., et al., *Association of Mitochondrial DNA Copy Number With Cardiovascular Disease.* JAMA Cardiol, 2017. **2**(11): p. 1247-1255.
315. Sundquist, K., et al., *Role of mitochondrial DNA copy number in incident cardiovascular diseases and the association between cardiovascular disease and type 2 diabetes: A follow-up study on middle-aged women.* Atherosclerosis, 2022. **341**: p. 58-62.
316. Anker, S.D., et al., *Prevalence, incidence, and prognostic value of anaemia in patients after an acute myocardial infarction: data from the OPTIMAAL trial.* Eur Heart J, 2009. **30**(11): p. 1331-9.
317. Eley, L., et al., *eNOS plays essential roles in the developing heart and aorta linked to disruption of Notch signalling.* Dis Model Mech, 2024. **17**(1).
318. Atochin, D.N. and P.L. Huang, *Endothelial nitric oxide synthase transgenic models of endothelial dysfunction.* Pflugers Arch, 2010. **460**(6): p. 965-74.
319. Kanoo, S., et al., *Deletion, but Not Heterozygosity, of eNOS Raises Blood Pressure and Aggravates Nephropathy in BTBR ob/ob Mice.* Nephron, 2024. **148**(9): p. 631-642.
320. Janssens, K., et al., *Post-infarct evolution of ventricular and myocardial function.* Biomech Model Mechanobiol, 2023. **22**(6): p. 1815-1828.
321. Bansal, K., et al., *Anterior Myocardial Infarction*, in *StatPearls*. 2025: Treasure Island (FL).
322. Aymong, E.D., K. Ramanathan, and C.E. Buller, *Pathophysiology of cardiogenic shock complicating acute myocardial infarction.* Med Clin North Am, 2007. **91**(4): p. 701-12; xii.
323. de Wit-Verheggen, V.H.W., et al., *PCr/ATP ratios and mitochondrial function in the heart. A comparative study in humans.* Sci Rep, 2023. **13**(1): p. 8346.
324. Lam, C.S.P., et al., *Myeloperoxidase Inhibition in Heart Failure With Preserved or Mildly Reduced Ejection Fraction: SATELLITE Trial Results.* J Card Fail, 2024. **30**(1): p. 104-110.
325. Boger, R.H., *L-Arginine therapy in cardiovascular pathologies: beneficial or dangerous?* Curr Opin Clin Nutr Metab Care, 2008. **11**(1): p. 55-61.

9 Supplement

Table 2: Patient characteristics of CAD patients with anemia and without anemia. The patient samples were used to perform experiments mentioned in the main figure 24 A-C. IQR: Interquartile range; GFR: Glomerular filtration rate; NA: Not applicable

	No anemia (n=11)	Anemia (n=6)	P-value
Age, years, median (IQR)	80 (45-89)	86 (69-89)	0.2723
Male sex, n (%)	5 (46)	3 (50)	0.8576
Hypertension, n (%)	6 (55)	3 (50)	0.8576
Diabetes mellitus, n (%)	0	0	NA
Active smoking, n (%)	1 (9)	1 (17)	0.6431
GFR, ml/min/1.73m^2, median (IQR)	66 (43-119)	52 (33-61)	0.0779
Hemoglobin, g/dl, median (IQR)	13.2 (12.0-17.0)	10.0 (7.0-11.1)	<0.0001

10 Acknowledgements

Die Danksagung markiert für mich den Abschluss eines wichtigen Kapitels - einer intensiven, lehrreichen und prägenden Zeit meines Lebens. Die Durchführung und Fertigstellung dieser Dissertation wurde durch die Unterstützung zahlreicher Kolleginnen und Kollegen, Betreuer und Institutionen ermöglicht, denen ich hiermit danken möchte.

An erster Stelle danke ich meinem Doktorvater, Prof. Dr. Dr. Christian Jung, für die wertvolle Betreuung dieser Arbeit. Seine wissenschaftliche Expertise, sein Vertrauen in meine Fähigkeiten sowie seine konstruktive Kritik und Unterstützung haben wesentlich zum Gelingen dieser Dissertation beigetragen. Für die stets offene und angenehme Zusammenarbeit bin ich ihm sehr dankbar.

Zudem möchte ich mich herzlich bei meinem Mentor, Prof. Dr. Axel Gödecke, für seine Unterstützung, wertvolles Feedback und seiner Rolle als Gutachter und Mentor bedanken.

Für die Chance, meine Doktorarbeit am CVRL verfassen zu dürfen, danke ich Herrn Univ.-Prof. Dr. Kelm ganz besonders.

Zudem möchte ich meinen herzlichen Dank an Prof. Dr. Gerdes richten, für die Unterstützung im Labor und seine Rolle als Laborleiter.

A special thanks goes to Dr. Chennupati, who supervised me throughout my entire time at the CVRL, both during my Master's thesis and my PhD. Thank you for your valuable feedback, creative ideas, and your constant motivation along my journey as a scientist. Under your guidance, I learned a great deal, both methodologically and in terms of content, in the field of cardiovascular research. You continuously pushed me to give my best – and that helped me grow, both professionally and personally.

Ein großes Dankeschön an Susi und Alex für eure zuverlässige Organisation, für die Sicherheit im Labor und natürlich für eure fachkundigen Meinungen bei offenen Fragen.

Ebenso möchte ich mich bei Steffi bedanken. Danke, dass du die Mausorganisation in unserer Gruppe übernommen hast. Durch deine durchdachte Planung und Expertise war es mir überhaupt erst möglich, meine Experimente umzusetzen. Ich danke dir auch für dein offenes Ohr und deine aufmunternden Worte.

Sarah, danke, dass du mich in dieser Zeit mitbetreut hast. Ich bin dir sehr dankbar, dass du mir nicht nur Methoden beigebracht, sondern sie auch gemeinsam mit mir ausgewertet und diskutiert hast. Danke für deine Hilfsbereitschaft, dein Wissen, das du so selbstverständlich teilst, und ganz allgemein für deine Präsenz bei jeder Herausforderung. Du hast mir so viel geholfen, ohne je etwas dafür zu erwarte. Das ist alles andere als selbstverständlich. Ich kann

es nicht oft genug sagen: Du bist eine fantastische Wissenschaftlerin, und ich schaue zu dir auf. Mito unites!

Natürlich danke ich auch all meinen Freunden im Labor – Chrissi, Cami, Jassi, Hao, Sven, Miri und Ashley – denn durch euch wurde jede Herausforderung leichter. Danke, danke!

Asli, Nati, Lina und Amira – danke für die tolle gemeinsame Zeit im Labor. Ihr wart die besten Studenten! Mit euch war alles einfacher und weniger stressig. Danke fürs Zuhören, Unterstützen und für all die lustigen Momente.

Mein liebstes Isimon, natürlich gilt mein tiefster Dank auch dir. Nur dir verdanke ich es, dass ich überhaupt hier gelandet bin und das werde ich nie vergessen. Hättest du mich damals nicht gefragt, ob ich noch ein Labor für meine Masterarbeit suche, hätte ich diese großartige Zeit im CVRL und all diese wunderbaren Menschen nie kennengelernt. Seit fünf Jahren begleitest du mich nun als Betreuerin, beste Freundin und Senior PhD. Egal ob Höhen oder Tiefen, du warst immer mein Anker im Labor. Wir haben unzählige Stunden miteinander verbracht, Quatsch gemacht, gelacht und gelernt. Für mich bist du die eine Person, der ich alles anvertrauen kann, weil ich weiß, dass du mich nie verurteilen würdest und immer an meiner Seite bleibst. Ich danke dir von Herzen – bestie forever!

Lieber Tishi, danke, dass du in dieser Zeit immer für mich da warst mit offenem Ohr, viel Geduld und Verständnis, auch wenn ich nicht immer einfach war.

Amma, Appa und Anna danke, dass ihr immer an meiner Seite wart, mich unterstützt und motiviert habt. Ihr habt mir diesen Weg ermöglicht, und ich bin euch unendlich dankbar dafür.